Running Head: Isoprene impairs protein S-nitrosylation in poplar

Corresponding author: Jörg-Peter Schnitzler
Email: jp.schnitzler@helmholtz-muenchen.de
Address: Helmholtz Zentrum München, Research Unit Environmental Simulation (EUS) at the Institute of Biochemical Plant Pathology (BIOP), Ingolstädter Landstraße 1, 85764 Neuherberg, Germany
Phone: +49 89 3187 2413
Fax: +49 89 3187 4431

Type of paper: Research Article
Research Area: System Biology, Biochemistry and Metabolism

Modulation of protein S-nitrosylation by isoprene emission in poplar

Elisa Vanzo[1], Juliane Merl-Pham[2], Violeta Velikova[1,3], Andrea Ghirardo[1], Christian Lindermayr[4], Stefanie M. Hauck[2], Jörg Bernhardt[5], Katharina Riedel[5], Jörg Durner[4], Jörg-Peter Schnitzler*[1]

1 Helmholtz Zentrum München, Research Unit Environmental Simulation, Institute of Biochemical Plant Pathology, Ingolstädter Landstraße 1, 85764 Neuherberg, Germany

2 Helmholtz Center München, Research Unit Protein Science, IngolstädterLandstr. 1, D-85764 Neuherberg, Germany

3 Institute of Plant Physiology and Genetics, Bulgarian Academy of Sciences, Acad. G. Bonchev Str. Bl. 21, 1113 Sofia, Bulgaria

4 Helmholtz Zentrum München, Institute of Biochemical Plant Pathology, Ingolstädter Landstr. 1, D-85764 Neuherberg, Germany

5 Institute for Microbiology, Ernst-Moritz-Arndt University, Jahnstrasse 15, 17487 Greifswald, Germany

*Corresponding author: jp-schnitzler@helmholtz-muenchen.de

Summary:

Isoprene emission modulates stress-induced NO production and S-nitrosylation pattern in poplar

Financial source:

The work was financially supported by the European Science Foundation (ESF) Eurocores program 'EuroVOL' within the joint research project 'MOMEVIP'(J.-P.S.) and the Alexander von Humboldt Foundation (V.V.).

Key words: proteomics, isoprene emission, S-nitrosylation, NO emission, ozone, UVB8, thiamine biosynthesis, cell wall lignin, carbon metabolism, protein turnover, NO signaling, volatile organic compounds

Abstract

Researchers have been examining the biological function(s) of isoprene in isoprene-emitting species for two decades. There is overwhelming evidence that leaf-internal isoprene increases the thermo-tolerance of plants and protects them against oxidative stress, thus mitigating a wide range of abiotic stresses. However, the mechanisms of abiotic stress mitigation by isoprene are still under debate. Here we assessed the impact of isoprene on the emission of NO and S-nitroso-proteome of isoprene-emitting (IE) and non-isoprene-emitting (NE) gray poplar (*Populus* × *canescens* (Aiton.) Sm.) after acute ozone fumigation. The short-term oxidative stress induced a rapid and strong emission of NO in NE compared to IE genotypes. Whereas IE and NE plants exhibited under non-stressful conditions only slight differences in their S-nitrosylation pattern, the *in vivo* S-nitroso-proteome of the NE genotype was more susceptible to ozone-induced changes compared to the IE plants. The results suggest that the nitrosative pressure (NO burst) is higher in NE plants, underlining the proposed molecular dialogue between isoprene and the free radical NO. Proteins belonging to the photosynthetic light and dark reactions, the TCA cycle, protein metabolism, and redox regulation exhibited an increased S-nitrosylation in NE samples compared to IE plants upon oxidative stress. Because the post-translational modification of proteins via S-nitrosylation often impacts enzymatic activities, the present data suggest that isoprene indirectly regulates the production of ROS via the control of the S-nitrosylation level of ROS-metabolizing enzymes, thus modulating the extent and velocity at which the ROS and NO signaling molecules are generated within a plant cell.

Introduction

It has been demonstrated that isoprene protects plants against a plethora of abiotic stresses (Singsaas et al., 1997; Behnke et al., 2007; Velikova et al.; 2008, Vickers et al., 2009a). Since the discovery of the positive influence of isoprene emission on plants' photosynthetic processes in the early 1990s (Sharkey and Singsaas, 1995), many efforts have been made to explain the primary mechanism of isoprene functioning. Most attention was given to the hypothesis that

isoprene improves the thermotolerance of the photosynthetic machinery by stabilizing chloroplast (thylakoid) membranes during short, high-temperature episodes (Sharkey and Singsaas, 1995; Loreto and Schnitzler, 2010). Successive studies underlined that isoprene helps maintain high rates of chloroplastic electron transport and CO_2 assimilation during heat stress and accelerates recovery from stress (Singsaas and Sharkey, 2000; Velikova and Loreto, 2005; Velikova et al., 2006; Behnke et al., 2010b; Way et al., 2011).

One mechanistic explanation is that isoprene molecules are dissolved in thylakoid membrane, and prevent membrane lipid denaturation following oxidative stress (Sharkey and Yeh, 2001). It was suggested that isoprene acts directly to stabilize the membrane (Sharkey and Yeh, 2001; Siwko et al., 2007). However, recent experiments with phosphatidylcholine liposomes showed that physiologically relevant intra-membrane concentrations of isoprene do not alter membrane viscosity (Harvey et al., 2015). Nevertheless, Velikova et al. (2011) reported that during high-temperature treatments, isoprene stabilized the macro-organization of the pigment-protein complexes of light-harvesting complex II in the thylakoid grana and the disorganization of macro-assemblies in isoprene-emitting chloroplasts began at higher temperatures compared to their non-emitting counterparts. Moreover, Velikova et al. (2011) showed decreased membrane permeability and more efficient primary photochemistry at PSII in isoprene-emitting plants at high temperatures (40–45 °C). However, how isoprene contributes to this protection is still unknown.

The antioxidant hypothesis is the second mechanistic explanation by which isoprene may directly or indirectly exert its protective effect in plant cells. Plants that were fumigated with isoprene, showed less visible ultra structural (chloroplast) damage and less impairment of photosynthetic processes upon acute ozone fumigation than plants where isoprene was absent (Loreto et al., 2001). In conjunction with this hypothesis leaf levels of H_2O_2 (Loreto and Velikova, 2001; Behnke et al., 2010a), singlet oxygen (Affek and Yakir, 2002; Velikova, et al., 2004), and the free radical nitric oxide (NO) (Velikova et al., 2005) were found to be lower in stressed plants when leaf internal isoprene was present. Taken together, these findings strongly indicate that endogenous isoprene modulates the oxidative and nitrosative load in plant tissue upon abiotic stress. However, the mechanism by which this modulation occurs remains unknown.

The generation of NO and reactive oxygen species (ROS; such as H_2O_2, singlet oxygen) is a general plant response to many environmental stresses (such as acute ozone, drought, salinity,

heavy metals; e.g., Mahalingam et al., 2006; Rodriguez-Serrano et al., 2006; Pasqualini et al., 2008; Corpas et al., 2011; Noctor et al., 2014). Excess generation and accumulation of NO and ROS can cause modifications of cellular macromolecules such as nucleic acids and membrane lipids and proteins, thus leading to malfunctioning of enzymes and organelles, ultimately inducing cell death (Mittler, 2002). Even under optimal conditions, these compounds are continuously produced in primary plant metabolism as side products of the chloroplastic and mitochondrial electron transport chains (Foyer and Noctor, 2003). Cellular levels of ROS and NO are tightly regulated by an efficient antioxidant defense system composed of scavenging enzymes and of a non-enzymatic barrier (Foyer and Noctor, 2003). In this context, isoprene may constitute a part of the non-enzymatic oxidative defense system (Vickers et al., 2009a) and may substitute for other antioxidants (Peñuelas et al., 2005; Behnke at al., 2009).

A more indirect mode of isoprene functioning is also under debate (for a review, see Vickers et al., 2009b). Chloroplasts, the main targets of the proposed isoprene function(s), are a major source of NO (Jasid et al., 2006). It is suggested that endogenous NO in chloroplasts can exert either antioxidant or prooxidant effects on chloroplast macromolecules and influence the integrity of membrane processes (Jasid et al., 2006). NO can prevent in chloroplasts the Fenton reaction by scavenging iron, thus avoiding the formation of hydroxyl radicals (Wink et al., 1995) that can be efficiently quenched by isoprene (Huang et al., 2011). Chloroplasts are also the main site of carbon and nitrogen metabolism and ROS production. Isoprene may modulate directly or indirectly the oxidative and nitrosative state of chloroplasts undergoing stress by modulating NO-related signaling pathways. Due to their lipophilic structure, it is probable that isoprene and NO converge inside plants, but to what extent the molecular dialogue between isoprene and NO can affect NO- and ROS-related signaling is unknown.

NO signaling regulates many plant development processes, such as stomatal closure (Neill et al., 2002), germination (Bethke et al., 2004), flowering (He et al., 2004), senescence (Guo and Crawford, 2005) and hormonal signaling (Simontacchi et al., 2013). NO signaling also plays a well-established role during plant-pathogen responses (Delledone et al., 1998; Durner et al., 1998) and abiotic stress reactions (Corpas et al., 2011). The hypersensitive response (HR) upon pathogen invasion is an example of programmed cell death and shares many similarities with plant's ozone response (Sandermann et al., 1998). In both cases (biotic and abiotic elicitor), the

activation of HR is associated with a burst of NO and ROS occurring in the same time range (Ahlfors et al., 2009).

NO exerts its signaling action by directly altering proteins through post-translational modifications (PTMs; i.e., S-nitrosylation, metal nitrosylation, and tyrosine nitration). S-nitrosylation, the covalent binding of NO to the thiol side of protein-cysteine residues to form nitrosothiols (SNOs) is regarded as the most important PTM of NO signaling in plants (Moreau et al., 2010). The binding and removal of NO is not strictly an enzymatic process and depends strongly on the redox status of the cell (Lindermayr et al., 2009). However, the enzymatic removal of the NO group via de-nitrosylation has been reported (Benhar et al., 2009) ensuring the reversibility of the modification. S-nitrosylation and de-nitrosylation events together form the S-nitrosylation pattern of a cell under physiological conditions, which may strongly change upon stress (e.g., Abat and Deswal, 2009; Ortega-Galisteo et al., 2012). S-nitrosylation of enzymes can either inhibit or activate their function (Astier et al., 2012). It has been suggested that S-nitrosylation is involved in the regulation of ROS level under abiotic stress (Ortega-Galisteo et al., 2012; Lindermayr and Durner, 2015) by targeting the ROS metabolizing enzymes.

The present work assesses the proposed mechanism of isoprene in modulating NO signaling. Because S-nitrosylation, the covalent binding of NO to cysteine moieties, is the main method of NO signaling, we identified targets of S-nitrosylation in isoprene-emitting (IE) and non-isoprene-emitting (NE) gray poplar plants by using the biotin switch assay in conjunction with mass spectrometry. After taking an inventory of putative S-nitrosylated proteins in IE and NE gray poplar plants under non-stressful conditions, we applied short acute ozone stress triggering changes in the NO emission and S-nitroso-proteome depending on the presence of isoprene.

RESULTS AND DISCUSSION

1. Whole proteome analysis highlights some alterations in the protein profile of NE gray poplars under control conditions

LC-MS/MS identification and label-free quantitative analysis of unstressed leaf samples revealed some differences in global protein abundances between IE (WT and EV) and NE (Ra1 and Ra2) genotypes (Figure 1). We identified and quantified 2,025 proteins, among these proteins, 1,388 proteins were identified with ≥ 2 unique peptides and 1,071 proteins of them could be quantified with ≥ 2 unique peptides. Globally, the differences in protein abundance between IE and NE

samples were small (Figure 1) with 97% of the proteins within a logarithmic fold change of ± 1 (Figure 1A). The largest, significant fold changes between IE and NE were observed for the terpenoid cyclase (TC) and, as expected, for the isoprene synthase (ISPS), the target of the RNAi-mediated suppression of the isoprene emission. Moreover, the Rubisco large chain, a 50S ribosomal protein, a ubiquinone biosynthesis protein, and the chloroplast inner membrane import protein Tic22 exhibited a significant lower expression in NE. A higher expression was observed for the basic pentacysteine 4, the EP3-3 chitinase, and the eukaryotic aspartyl protease family protein (Figure 1A).

The orthogonal partial least square (OPLS) was employed to dissect the differences between the IE and NE genotypes (Figure 1B, C, and D). Among 116 discriminant proteins able to discriminate between IE and NE, 31 proteins were higher expressed, and 85 proteins were lower expressed in the NE genotype, compared to IE (Supplemental Table S1).

Proteins with a higher abundance in NE comprised 11 enzymes that are involved in protein degradation (e.g., subtilase, serine protease, ubiquitin family protein) and protein folding (heat shock protein 70, HSP70) . This increase in NE may be indicative of a substantial increase in protein degradation in this genotype. Two other more expressed proteins in NE are related to histones (winged-helix DNA-binding transcription factor, histone superfamily protein). This observation fits with the strong expression of histones in the chloroplast proteome of NE plants (Velikova et al., 2014). NE samples also showed a higher abundance of proteins involved in the stress response. These are the germin-like protein (+0.4) and the EP3-3 chitinase. The germin-like proteins have, besides their action in plant development, a proposed role in the plant defense response (Lane et al., 2002). The expression of these proteins is induced upon various biotic and abiotic stresses, and overexpression of the germin-like proteins enhanced the resistance against powdery mildew in barley (Zimmermann et al., 2006). Similarly, various biotic and abiotic stresses can induce the expression of plant chitinases (Kasprzewska et al., 2003). They catalyze the hydrolysis of β-1,4-bonds in chitin and are classified as PR proteins, e.g., EP3 chitinase from *Daucus carrota* is involved in the programmed cell death (PCD) (Kasprzewska et al., 2003). Interestingly, each line had a specific proteome-pattern, suggesting that genetic transformation process can affect the whole proteome and cause off-targeted effects (Day et al., 2000; Latham et al., 2006).

For the visualization of the proteomic differences between lines and treatments we applied Voronoi treemaps (Figure 2, 4, and 6) as introduced by Bernhardt et al. (2009). The major difference in the protein profiles of NE and IE plants (Figure 2) was the lower abundance of several proteins in the NE genotype mostly involved in the light- and dark-reactions of photosynthesis. By contrast, only one protein related to photosynthesis was more abundant in NE (i.e., ferredoxin reductase). The reduction in protein content comprises subunits of the PSI and PSII complexes (e.g., oxygen-evolving complex, PSII assembly factor, and thylakoid luminal proteins), the cytochrome b_6f complex, the ATP synthase, and the large chain of Rubisco, confirming the proteomic survey of IE and NE poplar chloroplasts (Velikova et al., 2014). It might be speculated that NE plants have a lower demand for components of the photosynthetic apparatus and also for the supply of chlorophyll because several enzymes of the tetrapyrrole biosynthesis pathway that generate essential compounds, such as chlorophyll and heme (Tanaka et al., 2011), are also strongly reduced in concentration in the NE genotype. The lower amount of protein members of the photosynthetic apparatus may influence the physiology of NE poplars under unstressed conditions and upon stress. While initial physiological measurements showed no significant differences in the net CO_2 assimilation rates of both genotypes (Behnke et al., 2007; 2009; 2010a), recent observations reported lower gas exchange (Way et al., 2013) and electron transport rates (Velikova et al., 2015) in the NE genotype compared to the IE genotype.

In accordance to previous observations (Velikova et al., 2014), the down-regulation of antioxidant enzymes in the NE genotype can be confirmed at the cellular proteome level. The down-regulated enzymes are three different APX isoforms, superoxide dismutase (SOD), the glutathione S-transferase F11 (GST), and the monodehydroascorbate reductase (MDHAR) (Figure 2). The level and activity of APX and SOD often correlate, and coordinated increases in either gene expression have been shown to improve tolerance to oxidative stress in cassava (Xu et al., 2014). Due to the lower setting of several antioxidant enzymes in NE plants, the strict control of the ROS production could be de-regulated explaining the higher *in vitro* accumulation of H_2O_2 in NE leaves upon high light and temperature treatment (Behnke et al., 2010a).

Overall, the proteomic characterization of IE and NE cell extracts from unstressed poplars shows that the knock-down of the ISPS enzyme results in a distinct, cellular and chloroplastidic (Velikova et al., 2014) rearrangement of proteins and enzymes involved in photosynthetic processes, glycolysis and TCA cycle, redox regulation and protein translation (Figure 2).

2. Isoprene suppression results in slight modification of the S-nitroso-proteome of gray poplar plants under unstressed conditions

Similar to the overall proteomic survey, a label-free LC-MS/MS approach was applied to quantitatively compare the S-nitroso-proteome of the IE and NE genotypes in control conditions and immediately following the short acute ozone exposure (next section). In total 203 S-nitrosylated proteins were identified (Supplemental Table S2) after biotin-switch and subsequent pull-down.

Globally, IE and NE plants exhibited only minor differences in the S-nitrosylation pattern of unstressed plants (Supplemental Table S4). Five of these discriminant proteins were found to be more S-nitrosylated in NE plants (Supplemental Table S4, Figure 6B). These are Rubisco activase, α-N-arabinofuranosidase (ARA), phosphoribulokinase (PRK), HSP70, and O-acetylserine(thiol)lyase (OAS-TL). By contrast, only one protein, a PSII assembly protein, was less S-nitrosylated in the NE genotype compared to the IE genotype.

Rubisco activase and PRK, two important enzymes in the CO_2 fixation are known targets of several redox-based PTMs (i.e., S-nitrosylation, tyrosine nitration, and glutathionylation; Lindermayr et al., 2005; Lozano-Juste et al., 2011; Tanou et al., 2012) showing that a strong overlap in the signaling pathways of different PTMs exists and that the CBB cycle is strongly redox-regulated (Michelet et al., 2013). Interestingly, Rubisco activase is not only crucial for the maintenance of the high Rubisco activation state (Portis et al., 2003) but also for the photosynthetic light reactions because the knock-down of the Rubisco activase leads to a slower electron transport rate (ETR) and a decrease in the content of PSII components (Cai et al., 2010). Referring to the reduction of ETR and the content of PSII proteins in NE chloroplasts (Velikova et al., 2014), the higher proportion of constitutive S-nitrosylated Rubisco activase and PRK may be functionally related to these alterations. However, no functional characterization of S/de-nitrosylation events on the enzyme activities of the Rubisco activase and PRK has been thus far reported.

The S-nitrosylation of ARA was recently described (Vanzo et al., 2014). ARA hydrolyses the cleavage of terminal arabinofuranosyl residues from the pectin matrix and is involved in secondary cell wall biogenesis in hybrid aspen (*Populus tremula* L. × *P. tremuloides* Michx.) (Aspeborg et al., 2005).

The OAS-TL, catalyzing the last step in the cysteine biosynthesis and sulfur assimilation, has one predicted S-nitrosylation site (Supplemental Table S2), but whether S/de-nitrosylation

impacts enzyme functionality is unknown. Mentionable, Alvarez et al. (2011) demonstrated that tyrosine nitration, another route of NO signaling (Corpas et al., 2009) inhibits the enzymatic activity of OAS-TL.

HSP70 is a prominent target of S-nitrosylation in plants (e.g., Lindermayr et al., 2005; Abat and Deswal, 2009). Heat shock protein (HSP) accumulation in response to heat stress has been reported (Kotak et al., 2007) and there is evidence that NO and H_2O_2 act as signals that promote the gene expression of HSPs under thermal stress (Volkov et al., 2006). Whether the higher degree of S-nitrosylation of HSP70 in NE plants is functionally related to the higher thermal sensitivity (e.g., Behnke et al., 2007; 2010b) of this genotype requires further analysis.

3. Acute ozone fumigation stimulates NO emission and modifies the S-nitroso-proteome of IE and NE gray poplar

3.1. NO emissions of IE and NE gray poplar following acute ozone

Under control conditions, emissions of NO did not differ significantly between NE and IE poplar genotypes, although a tendency in higher emission from NE was observed (Figure 3). Emissions of NO were rapidly induced after the ozone exposure in both genotypes, but NO emissions were much more induced in NE shoots. In both genotypes NO emissions reached maximal rates after approximately 3.5 hours following the ozone treatment. In the NE genotypes the NO emission rates remained high until 7 hours post ozone exposure. In contrast the NO emissions in IE started to decline after the maximum finally reaching almost similar rates as before the ozone treatment. In NE plants NO emission rates also decreased but still showed doubled intensities at the end of the observation period compared to the initial conditions. Such a difference in NO emission between different isoprene emitter types is supported by previous results showing a stronger stimulation of NO emission in *Populus nigra* L. leaves with chemically inhibited isoprene emission exposed to oxidative stress (Velikova et al., 2008). Inverse correlation between isoprene emission and NO production was also observed in ozonized reed (*Phragmites australis* L.) leaves (Velikova et al., 2005). The finding that NE poplar emits significantly higher rates of NO upon ozone fumigation compared to the natural isoprene-emitting genotype (IE) is an indication that isoprene interferes in the signaling pathway activated by NO-ROS interactions.

3.2. Comparison of the IE and NE S-nitroso-proteome reveals the consequences of isoprene suppression in poplar plants following acute ozone

Irrespective to the plant genotypes, ozone induced strong changes in the S-nitroso-proteome. Possible changes in global protein abundance by the ozone treatment have been taken into account. The intensities of the S-nitrosylated proteins were normalized to the corresponding global protein abundances of the control (C) and ozone-treated (O) leaves, respectively.

Principle component analysis (PCA) with these normalized data revealed that the pronounced differences in the abundance of S-nitrosylated proteins between NE and IE appear after ozone treatment, as indicated by a clear separation between ozonated NE and IE samples in the first and second principal components (Supplemental Figure S1A). The functional categorization of the 203 S-nitrosylated proteins revealed a strong dominance of proteins related to photosynthetic processes (21%), followed by protein synthesis, degradation and folding processes (19%) and redox regulation and signaling (8%; Supplemental Figure S1B, Supplemental Table S2).

We again used OPLS to study the S-nitroso-protein patterns of control and ozonated samples in more detail (Figure 5). The separation between treatments and genotypes can be explained by the 63 discriminant S-nitrosylated proteins (out of 203) (Figure 4, Supplemental Table S3).

The general ozone response shared by both genotypes demonstrated a strong ozone-induced increase in the abundance of S-nitrosylated proteins, but the changes in the S-nitroso-proteome of the NE genotype were much more pronounced than in IE. While in IE plants the S-nitrosylation level of 16 proteins (13 up, 3 down) was changed upon acute ozone stress (Supplemental Table S5A, Figure 6C), the S-nitrosylation level of 54 proteins (53 up, 1 down) was altered in the NE genotype upon ozone treatment (Supplemental Table S5B; 6E).

3.3. Target sites of NO action in IE and NE gray poplar

The S-nitroso-proteins, of which the S-nitrosylation abundances significantly differ between the IE and NE genotypes within the ozone-treated plants, are listed in Table 1. These proteins belong to several pathways, such as photosynthesis, the CBB cycle, glycolysis, the TCA cycle, redox metabolism, cell wall metabolism, amino acid degradation, and metal handling (Figure 6F).

3.3.1. Carbon metabolism and photosynthetic proteins in NE

Many enzymes and structural components of carbon metabolism and thus of photosynthesis and catabolizing pathways (glycolysis, TCA cycle) became S-nitrosylated upon ozone (Supplemental

342 Table S3, Figure 5), and for most of the enzymes, the ozone treatment modulated the S-
343 nitrosylation pattern of IE and NE genotypes differentially (Table 1; Figure 6F). Notably, many
344 enzymes of the CBB cycle became more S-nitrosylated in NE compared to IE when acutely
345 stressed by ozone. These enzymes are the sedoheptulose-bisphosphatase (SBPase), Rubisco
346 activase, ribose-5-phosphate isomerase (RPI), PRK, glyceraldehyde-3-phosphate dehydrogenase
347 (GAPDH), TPI, and phosphoglycerate kinase (PGK). The SBPase and the TPI became S-
348 nitrosylated in NE plants upon ozone treatment, whereas the corresponding amount of protein
349 was constitutively down-regulated in NE control plants, emphasizing that many proteins are
350 regulated on several levels. Out of the group of CBB cycle enzymes, only TPI and Rubisco are
351 biochemically characterized, and both appeared to be inhibited by S-nitrosylation (Abat et al.,
352 2008; Abat and Deswal, 2009). The cytosolic GAPDH was reported to be inhibited by S-
353 nitrosylation as well (Holtgrefe et al., 2008; Zaffagnini et al., 2013). However, it is unclear if this
354 is true for the chloroplastidic GAPDH, which shares only low structural similarity with the
355 cytosolic isoenzyme (Shih et al., 1991). In *Arabidopsis* S-nitrosoglutathione reductase knock-out
356 plants, the S-nitrosylated proteins are significantly enriched in chlorophyll metabolism and
357 photosynthesis. These plants consistently show lower chlorophyll levels and altered
358 photosynthetic properties, suggesting that S-nitrosylation is an important regulatory mechanism
359 in these processes (Hu et al., 2015).
360 The TCA cycle enzymes malate dehydrogenase (MDH) and aconitase 1 (ACO1) showed an
361 increase of the S-nitrosylation level upon ozone exposure in NE (Table 1, Figure 6F). Both
362 enzymes become inactivated by S-nitrosylation (Gupta et al., 2012; Ortega-Galisteo et al., 2012).
363 Inactivation of ACO1 by NO leads to an accumulation of citrate, which as a retrograde signal,
364 induces alternative oxidase resulting in a stimulation of the nitrogen and amino acid metabolism
365 (Gupta et al., 2012). The comprehensive metabolomic analyses of the NE and IE genotypes
366 (Way et al. 2013; Kaling et al., 2015) revealed increased concentrations of compounds from the
367 amino acid metabolism, TCA cycle and glycolysis. These findings suggest that the TCA cycle
368 and perhaps glycolysis are constitutively down-regulated in NE plants compared to IE plants and
369 become even more repressed during oxidative/nitrosative stress.
370
371 ***3.3.2. Antioxidant enzymes in NE***
372 Several antioxidant enzymes (i.e., CAT2, APX, thioredoxin-dependent peroxidase 1) also
373 showed more pronounced S-nitrosylation levels in NE compared to IE (Table 1, Figure 6F).

Transgenic plants with reduced protein levels or activities of CAT and APX revealed an accumulation of H_2O_2, an early event in PCD (Dat et al., 2003), and cytosolic APX was found to be S-nitrosylated at the onset of PCD (de Pinto et al., 2013; Yang et al., 2015; Lindermayr and Durner, 2015). The enhanced S-nitrosylation of CAT and APX in the NE genotype upon ozone fumigation may analogically lead to increased H_2O_2 levels compared to IE. Interestingly, chloroplast (Velikova et al., 2014) and whole proteome analyses (Supplemental Table S1) reveal that the protein levels of several antioxidant enzymes are constitutively lower in the NE genotype (e.g., APX, SOD, chloroplastidic peroxiredoxin). By contrast, total ascorbate content was found to be higher in NE plants (Behnke et al., 2009; Way et al., 2013) compared to IE plants. Ascorbate can directly scavenge ROS or act as a reducing substrate for APX (Foyer and Noctor, 2011). It was suggested earlier that the increase of non-volatile antioxidant metabolites in the NE genotype might compensate for the absence of isoprene (Behnke et al., 2009; Way et al, 2013). In view of the present data, we assume that the altered S-nitrosylation status of many ROS-metabolizing enzymes results in a higher oxidative load in plant cells where isoprene is absent. This difference in the cellular redox homeostasis of both genotypes likely exists under physiological (unstressed) conditions, as indicated by higher H_2O_2 levels in the light-exposed chloroplasts of NE leaves (Behnke et al., 2010a).

3.3.3. Cell wall and lignin biosynthesis related proteins in NE

The S-nitrosylation levels of proteins involved in cell wall reconstruction and lignin biosynthesis were also increased by ozone stress in the NE compared to IE genotype (Table 1, Figure 6F). These proteins are the two α-L-arabinofuranosidases proteins (ARA, the fasciclin-like arabinogalactan protein (FLA)) and the cinnamyl alcohol dehydrogenase-like protein (CAD). FLAs are an expanded protein family in plants (Johnson et al., 2003) with implications for processes such as xylem differentiation, cell division, adhesion, and signaling (Seifert and Blaukopf, 2010; Janz et al., 2010). The ARA, a glycosyl hydrolase, is also connected with secondary cell wall formation and cell wall reorganization (Sumiyoshi et al., 2013). Generally, poplar leaves respond to ozone stress with an up-regulation of gene expression and enzyme activities of phenylpropanoid and lignin biosynthetic proteins (Richet et al., 2012), which lead to higher contents of condensed lignin, hydroxycinnamic acids, and flavonoids (Booker and Miller, 1998; Cabané et al., 2004). We recently described the de-nitrosylation of PAL and COMT in WT gray poplar upon ozone exposure (Vanzo et al., 2014) and demonstrated for PAL that *in vitro*

406 PAL activity increased as a result of de-nitrosylation. Because PAL is a key regulatory enzyme
407 controlling the metabolic flux in the phenylpropanoid and down-stream biosynthetic pathways
408 (Booker and Miller, 1998; Cabané et al., 2004), the activities of the other enzymes of the
409 phenolic secondary metabolism, e.g., COMT (Vanzo et al., 2014) or CAD, may also be rapidly
410 regulated by S-nitrosylation. In the NE but not the IE genotype, the CAD protein, catalyzing the
411 final step in the synthesis of monolignols (Di Baccio et al., 2008), was found to be S-nitrosylated
412 after ozone exposure (Table 1). However, whether these differences in S-nitrosylation levels are
413 related to the different constitutive and stress-induced metabolomic differences (Way et al. 2013;
414 Kaling et al. 2015), i.e., of phenolic compounds in NE and IE genotypes, requires additional
415 analysis.
416
417 ***3.3.4. Thiamine biosynthetic proteins in NE***
418 Interestingly two enzymes of the thiamine biosynthetic pathway were identified as putative
419 targets of S-nitrosylation (Supplemental Table S2, Figure 4). These enzymes are the thiamine
420 thiazole synthase (THI) and the thiamine biosynthesis protein, the latter showing an increase in
421 S-nitrosylation in NE genotypes upon ozone. Non-targeted metabolomics indicated that NE
422 leaves have high levels of thiamin monophosphate (Way et al., 2013), a precursor of thiamin
423 biosynthesis. Thiamine pyrophosphate (TPP) is an important coenzyme required for many
424 cellular processes, i.e., the TCA cycle and the MEP pathway (Goyer, 2010), where it acts as a
425 cofactor of 1-deoxy-D-xylulose-5-phosphate synthase (DXS). Chloroplasts of NE genotypes
426 accumulate excessive amounts of dimethylallyl diphosphate (DMADP), the metabolic precursor
427 of isoprene (Ghirardo et al., 2014). DMADP inhibits *in vivo* the activity of DXS (Ghirardo et al.,
428 2014) by competing for the same substrate-binding site with TPP (Banerjee et al., 2013).
429 Whether the differences in stress-induced changes in the S-nitrosylation of thiamine biosynthetic
430 enzymes in NE and IE genotypes are regulatory orchestrated with the differences of the TCA and
431 MEP pathway intermediates and PTMs is, however, unknown.
432
433 ***3.3.5. UV-B photoreceptor in NE***
434 Ozone treatment led to a strong increase in the S-nitrosylation levels of the UV resistance locus 8
435 (UVR8) protein in both genotypes (Table 1, Figure 6A) with more pronounced S-nitrosylation in
436 NE (Supplemental Table S5B, Figure 6E). UVR8 is a receptor protein for UV-B radiation and
437 localized as homodimer in the cytosol (Rizzini et al., 2011). UV-B induces the dimer

438 dissociation, the translocation of the UVR8 monomers into the nucleus and the activation of the
439 transcription factors elongated hypocotyl 5 and MYB12, leading to the expression of a range of
440 genes encoding flavonoid biosynthetic enzymes, DNA repair machineries, and antioxidant
441 proteins (Favory et al., 2009; Heijde and Ulm, 2012). It has been proposed that NO-mediated S-
442 nitrosylation is involved in the nuclear translocation of UVR8 (Tossi et al., 2011), similar to the
443 nuclear translocation of GAPDH undergoing S-nitrosylation (Hara et al., 2005). The present data
444 confirm UVR8 as a target of protein S-nitrosylation (Figure 4, Supplemental Table S2). UV-B
445 exposure and ozone fumigation share many common metabolic and regulatory components, such
446 as the increase in ROS formation and the up-regulation of antioxidants (Rao et al., 1996). One
447 may suggest that the S-nitrosylation of the UVR8 photoreceptor, triggering transcriptional
448 changes favoring the production of ROS-quenching polyphenols (Quideau et al., 2011), may be a
449 general response to oxidative stress. This assumption would indicate a higher amount of phenolic
450 compounds in the NE genotype undergoing conditions of oxidative stress. However, UV-B
451 treatment of the NE genotype resulted in a reduced accumulation of UV-B absorbing compounds
452 compared to IE (Kaling et al., 2015). Additional work is therefore necessary to clarify the
453 importance of UVR8 in the regulation of different regulations of phenolic compound
454 accumulation in NE genotypes compared to the natural situation of isoprene emitters.
455

456 ## Conclusions

457 The present data demonstrate that the isoprene in poplar leaves influences rapid stress-induced
458 changes in NO emission and thus in the pattern of the *in vivo* S-nitroso-proteome. In accordance
459 with the higher NO emission rates in NE, the S-nitroso-proteome of this genotype was more
460 susceptible to ozone-induced changes compared with IE plants. Our results demonstrate that the
461 nitrosative pressure is lower when isoprene is present in leaf cells. The main target sites of NO
462 action in NE poplar are proteins related to the light and dark reactions of photosynthesis, the
463 TCA cycle, protein metabolism, and redox regulation (Figure 7). CAT2, APX, and thioredoxin-
464 dependent peroxidase 1, all being involved in the detoxification of ROS (Mittler, 2002) showed
465 an increase in S-nitrosylation in NE plants upon oxidative stress. These results indicate that
466 isoprene indirectly regulates ROS formation via control of the S-nitrosylation levels of ROS-
467 metabolizing enzymes. There is evidence (Ortega-Galisteo et al., 2012; de Pinto et al., 2013) that
468 S-nitrosylation inhibits the activities of CAT and APX, thus increasing the accumulation of H_2O_2
469 (Dat et al., 2003; Vandenabeele et al., 2004; Davletova et al., 2005) as a prerequisite of the

plant's defense response (Apel and Hirt, 2004; de Pinto et al., 2006). Considering the observed lower constitutive amount of many anti-oxidative enzymes in the NE proteome, the present data indicate that the anti-oxidative defense system in poplar that maintains ROS production under strict control is re-arranged in NE genotypes at the protein level and at the level of protein S-nitrosylation.

Overall, the data strongly support the hypothesis (Vickers et al., 2009b) that unsaturated volatile isoprenoids such as isoprene can alter signaling pathways by modulating to what extent and how rapidly ROS and NO signaling molecules are generated within a cell, thus likely modulating the velocity and extent of the physiological response upon biotic and abiotic stress (Ahlfors et al., 2009; Wang et al., 2013).

Materials and Methods

Plant material and growth conditions

All experiments were performed with the natural hybrid (WT) gray poplar (*Populus* × *canescens* (Aiton.) Sm.; INRA clone 7171-B4; syn. *Populus tremula* × *Populus alba*), a naturally strong isoprene-emitter. Additionally, empty vector control plants (EV) were used. In addition to these two isoprene emitting (IE) lines, two well-characterized isoprene non emitting (NE) lines (35S::*PcISPS*-RNAi lines Ra1 and Ra2; see Behnke *et al*., 2007) were chosen for the experiments. Plantlets were amplified by micropropagation and cultivated (27:24 °C (day/night), 16-h photoperiod, approx. 100 μmol photons m^{-2} s^{-1}) under sterile conditions on half-concentrated MS medium in 1 L glass containers each accommodating 6–7 plantlets each. Every 8–10 weeks, plantlets were transferred to fresh medium. Rooting shoots were transferred to soil substrate (50% v/v Fruhstorfer Einheitserde, 50% v/v silica sand (particle size 1–3 mm)) and grown under a plastic lid to maintain high humidity. Plantlets were adapted to ambient air by gradually opening the lid. After approximately 4 weeks on soil, plants were transferred to bigger pots (2.2 L; 25% v/v Fruhstorfer Einheitserde, 25% v/v silica sand, 50% v/v perlite) and further cultivated in the greenhouse. The soil was initially mixed with a slow release-fertilizer (Triabon (Compo, Münster, Germany) and Osmocote (Scotts Miracle-Gro, Marysville, USA); 1:1, 10 g L^{-1} soil). Climate conditions in the greenhouse were: 22:18 °C (day:night), 16-h photoperiod, supplemental lighting was used (200-240 µmol photons m^{-2} s^{-1}).

Experimental set up and ozone fumigation

The ozone experiment was performed in two sun simulators (for details, see Thiel et al., 1996) in Munich. The sun simulators mimic the spectral irradiance in nature nearly perfectly, simulating natural irradiation. In both chambers (control (C), and ozone (O)), 24 8-week-old plants were placed (6 plants from each genotype; IE: WT, EV; NE: Ra1, Ra2) and acclimated to the prevailing temperature and light conditions (27/18 °C (day/night), approx. 800 µmol photons m^{-2} s^{-1}) for 7 days. The ozone pulse (800 nl L^{-1} for 1 h) was given at 10.00 am. Immediately after fumigation, leaf numbers 9 and 10 (counted from the apex) were frozen in liquid nitrogen for later biochemical and proteomic analyses.

Analysis of NO emissions following acute ozone exposure

Measurements were made at the branch level in a dynamic cuvette system (Vanzo et al., 2014). Whole plants were cut and immediately recut under water, and the branch with 18 leaves was introduced into a gas-tight glass cuvette (38.3 L, 500 µmol m^{-2} s^{-1} PPFD, air temperature 25 °C ± 1 °C, and flux 11.5 l min^{-1}) and exposed to synthetic air made by mixing pure O_2, N_2 and CO_2 from cylinders. Concentrations of the three gases (20%, 80%, 400 µL L^{-1}, respectively) were set with mass flow controllers. Net CO_2 assimilation and transpiration were monitored as differences between cuvette inlet and outlet air by infrared-absorption (Fischer-Rosemount Binos 100 4P, Hasselroth, Germany). When net CO_2 assimilation was stable, ozone fumigation (with 800 nl L^{-1}) was applied for 1 hour. Part of the cuvette outflow was diverted to a NO – NO_2 – NO_3 analyzer (ECO PHYSICS AG, Switzerland, model CLD 88 Y p). The detection limit of this instrument is 50 ppt. The NO emission (Φ_{NO}, nmol mol^{-1}) from the leaves was calculated as described in Velikova et al. (2008). Calculations were made based on the gas diffusion: $\Phi_{NO} = [NO_{cv} \times \Phi_{air}]/S$, where NO_{cv} (nmol mol^{-1}) is the NO concentration in the cuvette, Φ_{air} (mol s-1) is the airflow rate in the cuvette and S is the leaf area in the cuvette (m^2).

Biotin switch assay and LC-MS/MS-based identification and quantification of S-nitrosylated proteins

Six biological replicates per treatment were analyzed from each genotype (IE: WT, EV; NE: Ra1, Ra2). The detection of *in vivo* S-nitrosylated proteins was performed *via* a modified biotin switch assay (Vanzo et al., 2014). Frozen leaf powder was mixed with HENT buffer (100 mM

HEPES-NaOH pH 7.4, 10 mM EDTA, 0.1 mM Neocuproine, 1% (v/v) Triton X-100) in a mixing ratio of leaf powder:buffer 1:5 (w/v). The HENT buffer contained 30 mM NEM and protease inhibitor cocktail tablets (Complete, Roche, Grenzach-Wyhlen, Germany). The homogenate was mixed on a shaker for 30 seconds, incubated on ice for 15 min and centrifuged twice (14,000 g for 10 min). The protein concentration of the supernatant was adjusted to 1 μg $\mu L^{-1}$with HENT buffer. For blocking, four-times the volume (v/v) of HENS (225 mM HEPES-NaOH pH 7.2, 0.9 mM EDTA, 0.1 mM Neocuproine, 2.5% (w/v) SDS)) was freshly prepared, and 30 mM NEM was added to the protein extracts. The samples were incubated at 37°C for 30 minutes. Excess NEM was removed by precipitation with ice-cold acetone, and the protein pellets were re-suspended in 0.5 ml HENS buffer (without NEM) per mg of protein in the starting sample. Biotinylation was achieved by adding biotin-HPDP and SIN (1 mM and 3 mM final concentrations, respectively) with further dark incubation at RT for 1 hour. The controls for false-positive signals (FP) were treated with SIN in the presence of NEM for 25 minutes at 37°C before the biotinylation step (Supplemental Figure S2). After biotinylation, the proteins were precipitated with acetone and subjected to affinity purification of biotinylated proteins by NeutrAvidin agarose, as described elsewhere (Lindermayr et al., 2005). For affinity purification of biotinylated proteins, the precipitated proteins were re-suspended in HENS buffer (100 µL per mg protein in the starting sample) and 2 volumes of neutralization buffer (20 mM HEPES, pH 7.7, 100 mM NaCl, 1 mM EDTA, and 0.5% (v/v) Triton X-100). Biotinylated proteins were incubated for 1 hour at RT with the NeutrAvidin-agarose (30 μL per mg protein). The agarose-matrix was washed extensively with 20 volumes of washing buffer (600 mM NaCl in neutralization buffer) and bound proteins were eluted with 100 mM β-mercaptoethanol in elution buffer (20 mM HEPES, pH 7.7, 100 mM NaCl, 1 mM EDTA) and precipitated with ice-cold acetone.

In-solution digest of S-nitrosylated proteins after NeutrAvidin affinity purification

The pellets from the acetone-precipitation were dissolved in 30 μL of 50 mM ammonium bicarbonate. For protein reduction, 2 μL of 100 mM DTT were added and incubated for 15 min at 60 °C. After cooling to RT, the free cysteine residues were alkylated by adding 2 μL of freshly prepared 300 mM iodoacetamide solution for 30 min. A tryptic digest was performed overnight at 37 °C using 0.5 μg of trypsin (Promega, Mannheim, Germany) per sample. The digestion was stopped by adding trifluoroacetic acid and then stored at -20 °C.

565

566 ***Preparation of whole-cell extracts (WCE) for overall proteomic analyses***

567 From each genotype (IE: WT, EV; NE: Ra1, Ra2), 6 biological replicates per treatment were
568 analyzed. Fifty mg of frozen, homogenized leaf tissue were mixed with 1 mL HENT buffer
569 containing a protease inhibitor cocktail tablet and incubated on ice for 10 min. After
570 centrifugation (14,000 *g*, 10 min), Triton X-100 was removed by passing samples over a
571 Sephadex G-25 column (GE Healthcare, Little Chalfont, UK) using HEN buffer (without Triton
572 X-100). After determination of the protein content by the Bradford assay, aliquots containing 10
573 µg of protein were prepared for LC-MS/MS analysis and subsequent label-free quantification.

574

575 ***Filter-aided proteome preparation (FASP) digest of proteins from WCEs***

576 From each of the WCEs, an aliquot containing 10 μg of protein was digested using a modified
577 FASP procedure (Wisniewski et al., 2009). The proteins were reduced and alkylated using DTT
578 and IAA and then centrifuged through a 30 kDa cut-off filter device (PALL, Port Washington,
579 USA), washed thrice with UA buffer (8 M urea in 0.1 M Tris/HCl pH 8.5) and twice with 50
580 mM AmBic. The proteins were digested for 2 hours at room temperature using 1 μg Lys-C
581 (Wako Chemicals, Neuss, Germany) and for 16 hours at 37°C using 2 μg trypsin (Promega,
582 Mannheim, Germany). The peptides were collected by centrifugation (10 min at 14,000 *g*), and
583 the samples were acidified with 0.5% TFA and stored at -20 °C.

584

585 ***Mass spectrometry***

586 Digested samples (after affinity purification or from WCE) were thawed and centrifuged (14,000
587 *g*) for 5 minutes at 4 °C. The LC-MS/MS analysis was performed as previously described on an
588 Ultimate 3,000 nano-HPLC coupled to a LTQ-OrbitrapXL (Thermo Fischer Scientific, Bremen,
589 Germany) (Hauck et al., 2010). Every sample was automatically injected and loaded onto the
590 trap column at a flow rate of 30 μl min^{-1} in 5% buffer B (98% acetonitrile (ACN)/0.1% formic
591 acid (FA) in HPLC-grade water)) and 95% buffer A (2% ACN/0.1% FA in HPLC-grade water).
592 After 5 minutes, the peptides were eluted from the trap column and separated on the analytical
593 column by a 135-minute gradient from 7% to 32% of acetonitrile in 0.1% formic acid at 300 nl
594 min^{-1} flow rate followed by a short gradient from 32% to 93% acetonitrile for 5 minutes. The
595 gradient was set back between each sample to starting conditions and left to equilibrate for 20
596 minutes. The 10 most abundant peptide ions from the MS pre-scan were fragmented in the linear

ion trap if they showed an intensity of at least 200 counts and if they were at least +2 charged. During fragmentation, a high-resolution (6 x 10^4 full-width half maximum at 400 m/z) MS spectrum was acquired in the Orbitrap with a mass range from 300 to 1,500 Da.

Label-free analysis using Progenesis LC-MS

The acquired spectra were loaded to the Progenesis LC-MS software (v2.5, Nonlinear Dynamics Ltd, Newcastle upon Tyne, UK) for label-free quantification and analyzed as previously described (Hauck et al., 2010; Merl et al., 2012). Features of only one charge or features with more than seven charges were excluded. The raw abundances of the remaining features were normalized to allow for the correction of factors resulting from experimental variation. Rank 1-3 MS/MS spectra were exported as a MASCOT generic file and used for peptide identification with MASCOT (v2.2 and 2.3.02, Matrix Science, London, UK) in the *Populus trichocarpa* protein database (v4; 17,236,452 residues; 45,036 sequences). The search parameters were 10 ppm peptide mass and 0.6 Da MS/MS tolerance, one missed cleavage allowed.

For the identification and quantification of S-nitroso-proteins, N-ethylmaleinimidation and carbamidomethylation were set as variable modifications, as well as methionine oxidation. A MASCOT-integrated decoy database search calculated a false discovery rate (FDR) of 0.17% using a MASCOT ion score cut-off of 30 and a significance threshold of $P < 0.01$.

For the identification and quantification of total proteins in the WCEs of leaves, carbamidomethylation was set as a fixed modification, and methionine oxidation and deamination of asparagine/glutamine as variable modification. A MASCOT-integrated decoy database search calculated a FDR of < 1%. The MASCOT Percolator algorithm was used to distinguish between correct and incorrect spectrum identification (Brosch et al., 2009), with a maximum q value of 0.01. The peptides with a minimum percolator score of 15 were used further.

For each dataset, the peptide assignments were re-imported into the Progenesis LC-MS software. After summing up the abundances of all of the peptides that were allocated to each protein, the identification and quantification results were exported and are given in Supplemental Table S6.

Visualization of proteome data

For proteomics visualization we applied Voronoi treemaps as introduced by Bernhardt et al., (2009). The presented Treemaps subdivide the 2D plane into subsections according to the

hierarchical data structure of gene functional assignments as taken from the corresponding *A. thaliana* orthologs (http://www.arabidopsis.org/tools/bulk/go/index.jsp), which were obtained via the POPGENIE (http://www.popgenie.org) database. For the top level the total area is subdivided into main categories, afterwards the main categories into subcategories and the subcategories into equally sized cells representing significantly changed proteins. According to this classification the "heat shock protein 70" (Fig. 2B), was assigned to the subcategory "protein folding" (Fig. 2A) and this to the category "amino acid and protein synthesis" (Fig. 2A). In the overview images functional classes were encoded by using colors depending on categories. Expression change was encoded by using a blue via grey to orange color gradient with blue for decreased, grey for unchanged and orange for increased expression.

Statistics

The differences in the overall proteome and the S-nitroso-proteome of the IE and NE genotypes between control and ozone-treated samples were analyzed as previously described (Vanzo et al., 2014) using Principal Component Analysis (PCA) and Orthogonal Partial Least Square regression (OPLS) statistical methods from the software packages 'SIMCA-P' (v13.0.0.0, Umetrics, Umeå, Sweden). The results were validated by 'full cross validation' (Erikssonet al., 2006) using a 95% confidence level.

Raw abundances from the label-free analysis of proteome were extracted from the Progenesis LC-MS/MS software (v2.5, Nonlinear Dynamics Ltd). Protein intensities were normalized to the corresponding (averaged) protein abundance in whole-cell extracts (WCE) of the control (C) and ozone-treated (O) leaves. The PCA was performed on normalized, summed S-nitroso-protein intensities (centered and scaled with 1 SD^{-1}), which were pre-processed by logarithmic (base 10) transformation and used as X-variables. Six independent biological replicates were used for each C and O treatment and for IE and NE genotypes, respectively. The size of the analyzed matrix was 2024-by-24 and 206-by-24 for the overall proteome and the S-nitroso-proteome, respectively. The OPLS was performed as PCA by giving as Y-variable a value of 0 to C samples and a value of 1 to O samples. S-nitroso-proteins showing Variable of Importance for the Projection (VIP) greater than 1 and the uncertainty bars of the jack-knifing method smaller than the respective VIP value were defined as discriminant proteins that can separate O from C samples and IE from NE samples. Additionally, discriminant proteins were tested for

660 significance difference ($P < 0.05$) between C and O samples using Student's *t*-test and two-way-
661 ANOVA (SPSS, v22.0, SPSS Inc., Chicago, USA).
662

Supplemental Material

Supplemental Table S1. Proteins, that discriminately separate non–isoprene emitting (NE) from isoprene emitting (IE) gray poplar samples in the OPLS model of the whole proteome.

Supplemental Table S2. Complete list of LC-MS/MS identified S-nitrosylated proteins in isoprene-emitting (IE) and non-isoprene-emitting (NE) gray poplar leaves (control and ozone).

Supplemental Table S3. Proteins, that discriminately separate non–isoprene-emitting (NE) from isoprene-emitting (IE) gray poplar samples in the control (C) and ozone (O) treatment in the OPLS of the S-nitroso proteome.

Supplemental Table S4. Constitutively S-nitrosylated proteins, which are differentially abundant in isoprene-emitting (IE) and non-isoprene-emitting (NE) gray poplar under steady-state conditions (only control samples).

Supplemental Table S5. S-nitrosylated proteins, which are differentially abundant in ozone and control treatments of (A) isoprene-emitting (IE) and (B) non-isoprene-emitting (NE) gray poplar samples.

Supplemental Table S6. Full data set for protein identification of total proteins from whole cell extracts (WCE) and S-nitroso-proteins with corresponding protein abundances after label-free quantification.

Supplemental Figure S1. S-nitrosylated proteins detected in the control and ozone samples of the isoprene emitting and non-isoprene emitting genotypes. A) PCA score plot. B) Functional categorization of the 203 identified S-nitrosylated proteins in IE and NE poplar.

Supplemental Figure S2. Detection of endogenously S-nitrosylated proteins in non-isoprene-emitting (NE) gray poplar. (A) Western blot showing *in vivo* S-nitrosylated proteins including controls for false-positives (FP); (B) Ponceau S staining of total protein.

Acknowledgements

We wish to thank Andreas Albert and Hans Lang for helping with the sun simulator experiment, the ozone fumigation and NO analysis. We also thank Ina Zimmer for technical laboratory assistance.

Author contributions

J.-P.S., C.L., and J.D. conceived the original research plan; C.L. and J.-P.S. supervised the experiments; E.V. and V.V. performed the experiments; J.M.-P., S.M.H., and A.G. provided technical assistance to E.V.; E.V., V.V., J.M.-P., J.B., K.R., and A.G. analyzed the data; E.V. wrote the article with contributions of all co-authors; J.-P.S. supervised and complemented the writing.

Literature cited

Abat JK, Deswal R (2009) Differential modulation of S-nitrosoproteome of *Brassica juncea* by low temperature: change in S-nitrosylation of Rubisco is responsible for the inactivation of its carboxylase activity. Proteomics **9:** 4368-4380

Abat JK, Mattoo AK, Deswal R (2008) S-nitrosylated proteins of a medicinal CAM plant *Kalanchoe pinnata*- ribulose-1,5-bisphosphate carboxylase/oxygenase activity targeted for inhibition. FEBS J **275:** 2862-2872

Affek HP, Yakir D (2002) Protection by isoprene against singlet oxygen in leaves. Plant Physiol **129:** 269-277

Ahlfors R, Brosché M, Kollist H, Kangasjärvi J (2009) Nitric oxide modulates ozone-induced cell death, hormone biosynthesis and gene expression in *Arabidopsis thaliana*. Plant J **58:** 1-12

Alvarez C, Lozano-Juste J, Romero LC, Garcia I, Gotor C, Leon J (2011) Inhibition of Arabidopsis O-acetylserine(thiol)lyase A1 by tyrosine nitration. J Biol Chem **286:** 578-586

Apel K, Hirt H (2004) Reactive oxygen species: Metabolism, oxidative stress, and signal transduction. Annu Rev Plant Biol **55:** 373-399

726 **Aspeborg H, Schrader J, Coutinho PM, Stam M, Kallas Å, Djerbi S, Nilsson P, Denman S,**
727 **Amini B, Sterky F, Master E, Sandberg G, Mellerowicz E, Sundberg B, Henrissat B,**
728 **Teeri TT** (2005) Carbohydrate-active enzymes involved in the secondary cell wall
729 biogenesis in hybrid aspen. Plant Physiol **137:** 983-997
730 **Astier J, Kulik A, Koen E, Besson-Bard A, Bourque S, Jeandroz S, Lamotte O,**
731 **Wendehenne D** (2012) Protein S-nitrosylation: what's going on in plants? Free Radic
732 Biol Med **53:** 1101-1110
733 **Banerjee A, Wu Y, Banerjee R, Li Y, Yan HG, Sharkey TD** (2013) Feedback inhibition of
734 deoxy-D-xylulose-5-phosphate synthase regulates the methylerythritol 4-phosphate
735 pathway. J Biol Chem **288:** 16926-16936
736 **Behnke K, Ehlting B, Teuber M, Bauerfeind M, Louis S, Hänsch R, Polle A, Bohlmann J,**
737 **Schnitzler JP** (2007) Transgenic, non-isoprene emitting poplars don't like it hot. Plant J
738 **51:** 485-499
739 **Behnke K, Kleist E, Uerlings R, Wildt J, Rennenberg H, Schnitzler JP** (2009) RNAi-
740 mediated suppression of isoprene biosynthesis in hybrid poplar impacts ozone tolerance.
741 Tree Physiol **29**: 725-736
742 **Behnke K, Kaiser A, Zimmer I, Brüggemann N, Janz D, Polle A, Hampp R, Hänsch R,**
743 **Popko J, Schmitt-Kopplin P, Ehlting B, Rennenberg H, Barta C, Loreto F,**
744 **Schnitzler JP** (2010a) RNAi-mediated suppression of isoprene emission in poplar
745 transiently impacts phenolic metabolism under high temperature and high light
746 intensities: a transcriptomic and metabolomic analysis. Plant Mol Biol **74:** 61-75
747 **Behnke K, Loivamäki M, Zimmer I, Rennenberg H, Schnitzler JP, Louis S** (2010b) Isoprene
748 emission protects photosynthesis in sunfleck exposed Grey poplar. Photosynth Res **104:**
749 5-17
750 **Benhar M, Forrester MT, Stamler JS** (2009) Protein denitrosylation: enzymatic mechanisms
751 and cellular functions. Nat Rev Mol Cell Biol **10:** 721-732
752 **Bernhardt J, Funke S, Hecker M, Siebourg J (2009)** Visualizing Gene Expression Data via
753 Voronoi Treemaps. Conference paper. Sixth International Symposium on Voronoi
754 Diagrams, ISVD 2009, Copenhagen, Denmark, June 23-26, DOI: 10.1109/ISVD.2009.33
755 **Bethke PC, Gubler F, Jacobsen JV, Jones RL** (2004) Dormancy of Arabidopsis seeds and
756 barley grains can be broken by nitric oxide. Planta **219:** 847-855

Booker FL, Miller JE (1998) Phenylpropanoid metabolism and phenolic composition of soybean [*Glycine max* (L.) Merr.] leaves following exposure to ozone. J Exp Bot **49:** 1191-1202

Brosch M, Yu L, Hubbard T, Choudhary J (2009) Accurate and sensitive peptide identification with Mascot Percolator. J Prot Res **8:** 3176-3181

Cabané M, Pireaux JC, Leger E, Weber E, Dizengremel P, Pollet B, Lapierre C (2004) Condensed lignins are synthesized in poplar leaves exposed to ozone. Plant Physiol **134**: 586-594

Cai B, Zhang A, Yang Z, Lu Q, Wen X, Lu C (2010) Characterization of photosystem II photochemistry in transgenic tobacco plants with lowered Rubisco activase content. J Plant Physiol **167:** 1457-1465

Corpas FJ, Chaki M, Leterrier M, Barroso JB (2009) Protein tyrosine nitration: a new challenge in plants. Plant Signal Behav **4:** 920-923

Corpas FJ, Leterrier M, Valderrama R, Airaki M, Chaki M, Palma JM, Barroso JB (2011) Nitric oxide imbalance provokes a nitrosative response in plants under abiotic stress. Plant Sci **181:** 604-611

Dat JF, Pellinen R, Beeckman T, Van de Cotte B, Langebartels C, Kangasjärvi J, Inze D, Van Breusegem F (2003) Changes in hydrogen peroxide homeostasis trigger an active cell death process in tobacco. Plant J **33:** 621-632

Davletova S, Rizhsky L, Liang HJ, Zhong SQ, Oliver DJ, Coutu J, Shulaev V, Schlauch K, Mittler R (2005) Cytosolic ascorbate peroxidase 1 is a central component of the reactive oxygen gene network of Arabidopsis. Plant Cell **17:** 268-281

Day CD, Lee E, Kobayashi T, Holappa LD, Albert H, Ow DW (2000) Transgene integration into the same chromosome location can produce alleles that express at a predictable level, or alleles that are differentially silenced. Genes Dev **14:** 2869-2880

de Pinto MC, Locato V, Sgobba A, Romero-Puertas MD, Gadaleta C, Delledonne M, De Gara L (2013) S-Nitrosylation of ascorbate peroxidase is part of programmed cell death signaling in tobacco Bright Yellow-2 cells. Plant Physiol **163:** 1766-1775

de Pinto MC, Paradiso A, Leonetti P, De Gara L (2006) Hydrogen peroxide, nitric oxide and cytosolic ascorbate peroxidase at the crossroad between defence and cell death. Plant J**48**: 784-795

788 **Delledonne M, Xia Y, Dixon RA, Lamb C** (1998) Nitric oxide functions as a signal in plant
789 disease resistance. Nature **394:** 585-588
790 **Di Baccio D, Castagna A, Paoletti E, Sebastiani L, Ranier A** (2008) Could the differences in
791 O3 sensitivity between two poplar clones be related to a difference in antioxidant defense
792 and secondary metabolic response to O3 influx? Tree Physiol **28:** 1761-1772
793 **Durner J, Wendehenne D, Klessig DF** (1998) Defense gene induction in tobacco by nitric
794 oxide, cyclic GMP, and cyclic ADP-ribose. Proc Natl Acad Sci USA **95:** 10328-10333
795 **Eriksson L, Johansson E, Kettaneh-Wold N, Trygg J, Wikström C, Wold S** (2006) Multi-
796 and megavariate data analysis. Part I: Basic principles and applications. Umeå, Sweden:
797 Umetrics Academy
798 **Favory JJ, Stec A, Gruber H, et al.** (2009) Interaction of COP1 and UVR8 regulates UV-B-
799 induced photomorphogenesis and stress acclimation in Arabidopsis. Embo J **28:** 591-60
800 **Foyer CH, Noctor G** (2003) Redox sensing and signalling associated with reactive oxygen in
801 chloroplasts, peroxisomes and mitochondria. Physiol Plant **119:** 355-364
802 **Foyer CH, Noctor G** (2011) Ascorbate and glutathione: the heart of the redox hub. Plant
803 Physiol **155:** 2-18
804 **Ghirardo A, Wright LP, Bi Z, Rosenkranz M, Pulido P, Rodríguez-Concepción M,**
805 **Niinemets Ü, Brüggemann N, Gershenzon J, Schnitzler JP** (2014) Metabolic flux
806 analysis of plastidic isoprenoid biosynthesis in poplar leaves emitting and nonemitting
807 isoprene. Plant Physiol **165:** 37-51
808 **Goyer A** (2010) Thiamine in plants: aspects of its metabolism and fucntions. Phytochem **71:**
809 1615-1624
810 **Guo FQ, Crawford NM** (2005) Arabidopsis nitric oxide synthase1 is targeted to mitochondria
811 and protects against oxidative damage and dark-induced senescence. Plant Cell **17:**
812 3436–3450
813 **Gupta KJ, Shah JK, Brotman Y, Jahnke K, Willmitzer L, Kaiser WM, Bauwe H,**
814 **Igamberdiev AU** (2012) Inhibition of aconitase by nitric oxide leads to induction of the
815 alternative oxidase and to a shift of metabolism towards biosynthesis of amino acids. J
816 Exp Bot **63:** 1773-1784
817 **Hara MR, Agrawal N, Kim SF, *et al.*** (2005) S-nitrosylated GAPDH initiates apoptotic cell
818 death by nuclear translocation following Siah1 binding. Nat Cell Biol **7:** 665-674

819 **Harvey CM, Li Z, Tjellsröm H, Blanchard GJ, Sharkey TD** (2015) Concentration of isoprene
820 in artificial and thylakoid membranes. J Bioenerg Biomembr DOI 10.1007/s10863-015-
821 9625-9
822 **Hauck SM, Dietter J, Kramer RL, Hofmaier F, Zipplies JK, et al.** (2010) Deciphering
823 membrane-associated molecular processes in target tissue of autoimmune uveitis by
824 label-free quantitative mass spectrometry. Mol Cell Prot **9:** 2292-2305
825 **He Y, Tang RH, Hao Y, Stevens RD, Cook CW, Ahn SM, Jing L, Yang Z, Chen L, Guo F,**
826 **Fiorani F, Jackson RB, Crawford NM, Pei ZM** (2004) Nitric oxide represses the
827 Arabidopsis floral transition. Science **305:** 1968-1971
828 **Heijde M, Ulm R** (2012) UV-B photoreceptor-mediated signalling in plants. Trends Plant Sci
829 **17:** 230-237
830 **Holtgrefe S, Gohlke J, Starmann J, Druce S, Klocke S, Altmann B, Wojtera J, Lindermayr**
831 **C, Scheibe R** (2008) Regulation of plant cytosolic glyceraldehyde 3-phosphate
832 dehydrogenase isoforms by thiol modifications. Physiol Plant **133:** 211-228
833 **Hu J, Huang X, Chen L, Sun X, Lu C, Zhang L, Wang Y, Zuo J** (2015) Site-specific
834 nitrosoproteomic identification of endogenously S-nitrosylated proteins in Arabidopsis.
835 Plant Physiol **167**: 1731-46
836 **Huang D, Zhang X, Chen ZM, Zhao Y, Shen XL (2011)** The kinetics and mechanism of an
837 aqueous phase isoprene reaction with hydroxyl radical. Atmos Chem Phys **11:** 7399-7415
838 **Janz D, Behnke K, Schnitzler JP, Kanawati B, Schmitt-Kopplin P, Polle A** (2010) Pathway
839 analysis of the transcriptome and metabolome of salt sensitive and tolerant poplar species
840 reveals evolutionary adaption of stress tolerance mechanisms. BMC Plant Biol **10:** 150
841 **Jasid S, Simontacchi M, Bartoli CG, Puntarulo S** (2006) Chloroplasts as a nitric oxide cellular
842 source. Effect of reactive nitrogen species on chloroplastic lipids and proteins Plant
843 Physiol **142:** 1246–1255
844 **Johnson KL, Jones BJ, Bacic A, Schultz CJ** (2003) The fasciclin-like arabinogalactan proteins
845 of arabidopsis. A multigene family of putative cell adhesion molecules. Plant Physiol
846 **133:** 1911-1925
847 **Kaling M, Kanawati B, Ghirardo A, Albert A, Winkler JB, Heller W, Barta C, Loreto F,**
848 **Schmitt-Kopplin P, Schnitzler JP** (2015) UV-B mediated metabolic rearrangements in
849 poplar revealed by non-targeted metabolomics. Plant Cell Environ **38:** 892-904
850 **Kasprzewska A** (2003) Plant chitinases--regulation and function. Cell Mol Biol Lett **8:** 809-824

851 **Kotak S, Larkindale J, Lee U, von Koskull-Doring P, Vierling E, Scharf KD** (2007)
852 Complexity of the heat stress response in plants. Curr Opin Plant Biol **10:** 310-316
853 **Lane BG** (2002) Oxalate, germins, and higher-plant pathogens. IUBMB Life **53:** 67-75
854 **Latham JR, Wilson AK, Steinbrecher RA** (2006) The mutational consequences of plant
855 transformation*.,* J Biomed Biotechnol **25376:** 1-7
856 **Lindermayr C, Durner J** (2015) Interplay of reactive oxygen species and nitric oxide: nitric
857 oxide coordinates reactive oxygen species homeostasis. Plant Physiol **167:** 1209-1210
858 **Lindermayr C, Durner J** (2009) S-Nitrosylation in plants: Pattern and function. J Proteomics
859 **73:** 1-9
860 **Lindermayr C, Saalbach G, Durner J** (2005) Proteomic identification of S-nitrosylated
861 proteins in Arabidopsis. Plant Physiol **137:** 921-930
862 **Loreto F, Mannozzi M, Maris C, Nascetti P, Ferranti F, Pasqualini S** (2001) Ozone
863 quenching properties of isoprene and its antioxidant role in leaves. Plant Physiol **126:**
864 993-1000
865 **Loreto F, Schnitzler JP** (2010) Abiotic stresses and induced BVOCs. Trends Plant Sci **15:** 154-
866 166
867 **Loreto F, Velikova V** (2001) Isoprene produced by leaves protects the photosynthetic apparatus
868 against ozone damage, quenches ozone products, and reduces lipid peroxidation of
869 cellular membranes. Plant Physiol **127:** 1781-1787
870 **Lozano-Juste J, Colom-Moreno R, Leon J** (2011) In vivo protein tyrosine nitration in
871 *Arabidopsis thaliana*. J Exp Bot **62:** 3501-3517
872 **Mahalingam R, Jambunathan N, Gunjan SK, Faustin E, Weng H, Ayoubi P** (2006)
873 Analysis of oxidative signalling induced by ozone in *Arabidopsis thaliana*. Plant Cell
874 Environ **29:** 1357-1371
875 **Merl J, Ueffing M, Hauck SM, von Toerne C** (2012) Direct comparison of MS-based label-
876 free and SILAC quantitative proteome profiling strategies in primary retinal Muller cells.
877 Proteomics **12**: 1902-1911
878 **Michelet L, Zaffagnini M, Morisse S, Sparla F, Pérez-Pérez ME, Francia F, Danon A,**
879 **Marchand CH, Fermani S, Trost P, Lemaire SD** (2013) Redox regulation of the
880 Calvin-Benson cycle: something old, something new. Front Plant Sci **4:** 470
881 **Mittler R** (2002) Oxidative stress, antioxidants and stress tolerance. Trends Plant Sci 7: 405-410

882 **Moreau M, Lindermayr C, Durner J, Klessig DF** (2010) NO synthesis and signaling in plants
883 - where do we stand? Physiol Plant **138:** 372-383
884 **Neill SJ, Desikan R, Clarke A, Hancock JT** (2002) Nitric oxide is a novel component of
885 abscisic acid signaling in stomatal guard cells. Plant Physiol **128:** 13-16
886 **Noctor G, Mhamdi A, Foyer CH** (2014) The roles of reactive oxygen metabolism in drought:
887 Not so cut and dried. Plant Physiol **164:** 1636-1648
888 **Ortega-Galisteo AP, Rodriguez-Serrano M, Pazmino DM, Gupta DK, Sandalio LM,**
889 **Romero-Puertas MC** (2012) S-Nitrosylated proteins in pea (*Pisum sativum* L.) leaf
890 peroxisomes: changes under abiotic stress. J Exp Bot **63:** 2089-2103
891 **Pasqualini S, Meier S, Gehring C, Madeo L, Fornaciari M, Romano B, Ederli L** (2009)
892 Ozone and nitric oxide induce cGMP-dependent and -independent transcription of
893 defence genes in tobacco. New Phytol **181:** 860-870
894 **Peñuelas J, Llusia J, Asensio D, Munne-Bosch S** (2005) Linking isoprene with plant
895 thermotolerance, antioxidants and monoterpene emissions. Plant Cell Environ **28:** 278-
896 286
897 **Portis AR Jr** (2003) Rubisco activase - Rubisco's catalytic chaperone. Photosynth Res **75**: 11-27
898 **Quideau S, Deffieux D, Douat-Casassus C, Pouysegu L** (2011) Plant polyphenols: Chemical
899 properties, biological activities, and synthesis. Angew Chem Int Edit **50:** 586-621
900 **Rao MV, Paliyath, Ormrod, DP** (1996) Ultraviolet-B- and ozone-induced biochemical changes
901 in antioxidant enzymes of *Arabidopsis thaliana*. Plant Physiol **110:** 125-136
902 **Richet N, Tozo K, Afif D, Banvoy J, Legay S, Dizengremel P, Cabané M** (2012) The
903 response to daylight or continuous ozone of phenylpropanoid and lignin biosynthesis
904 pathways in poplar differs between leaves and wood. Planta **236:** 727-737
905 **Rizzini L, Favory J-J, Cloix C, Faggionato D, O'Hara A, Kaiserli E, Baumeister R,**
906 **Schaefer E, Nagy F, Jenkins GI, Ulm R** (2011) Perception of UV-B by the Arabidopsis
907 UVR8 Protein. Science **332:** 103-106
908 **Rodriguez-Serrano M, Romero-Puertas MC, Zabalza A, Corpas FJ, Gomez M, Del Rio**
909 **LA, Sandalio LM** (2006) Cadmium effect on oxidative metabolism of pea (*Pisum*
910 *sativum* L.) roots. Imaging of reactive oxygen species and nitric oxide accumulation *in*
911 *vivo*. Plant Cell Environ **29:** 1532-1544
912 **Sandermann H, Ernst D, Heller W, langebartels C** (1998) Ozone: an elicitor of plant defence
913 reactions. Trends Plant Sci **3:** 47-50

914 **Seifert GJ, Blaukopf C** (2010) Irritable Walls: The plant extracellular matrix and signaling.
915 Plant Physiol **153:** 467-478
916 **Sharkey TD, Singsaas EL.**(1995) Why plants emit isoprene. Nature **374:** 769-769
917 **Sharkey TD, Yeh SS** (2001) Isoprene emission from plants. Annu Rev Plant Physiol Plant Mol
918 Biol **52:** 407-436
919 **Shih MC, Heinrich P, Goodman HM** (1991) Cloning and chromosomal mapping of nuclear
920 genes encoding chloroplast and cytosolic glyceraldehyde-3-phosphate-dehydrogenase
921 from *Arabidopsis thaliana*. Gene **104**: 133-138
922 **Simontacchi M, Garcia-Mata C, Bartoli CG, Santa-Maria GE, Lamattina L** (2013) Nitric
923 oxide as a key component in hormone-regulated processes. Plant Cell Rep **32:** 853-866
924 **Singsaas EL, Lerdau M, Winter K, Sharkey TD** (1997) Isoprene increases thermotolerance of
925 isoprene-emitting species. Plant Physiol **115:** 1413-1420
926 **Singsaas EL, Sharkey TD** (2000) The effects of high temperature on isoprene synthesis in oak
927 leaves. Plant Cell Environ **23:** 751-757
928 **Siwko ME, Marrink SJ, de Vries AH, Kozubek A, Uiterkamp AJMS, Mark AE** (2007)
929 Does isoprene protect plant membranes from thermal shock? A molecular dynamics
930 study. Biochim Biophys Acta - Biomembranes **1768:** 198-206
931 **Sumiyoshi M, Nakamura A, Nakamura H, Hakata M, Ichikawa H, Hirochika H, Ishii T,**
932 **Satoh S, Iwai H** (2013) Increase in cellulose accumulation and improvement of
933 saccharification by overexpression of arabinofuranosidase in rice. Plos One **8:** e10.1371
934 **Tanaka R, Kobayashi K, Masudac T** (2011) Tetrapyrrole Metabolism in *Arabidopsis thaliana*.
935 Arabidopsis Book **9:** e0145
936 **Tanou G, Filippou P, Belghazi M, Job D, Diamantidis G, Fotopoulos V, Molassiotis A**
937 (2012) Oxidative and nitrosative-based signaling and associated post-translational
938 modifications orchestrate the acclimation of citrus plants to salinity stress. Plant J **72:**
939 585-599
940 **Thiel S, Döhring T, Köfferlein M, Kosak A, Martin P, Seidlitz HK (1996)** A phytotron for
941 plant stress research: How far can artificial lighting compare to natural sunlight? J Plant
942 Physiol **148:** 456-463
943 **Tossi V, Amenta M, Lamattina L, Cassia R** (2011) Nitric oxide enhances plant ultraviolet-B
944 protection up-regulating gene expression of the phenylpropanoid biosynthetic pathway.
945 Plant Cell Environ **34:** 909-921

946 **Vandenabeele S, Vanderauwera S, Vuylsteke M, *et al.*** (2004) Catalase deficiency drastically
947 affects gene expression induced by high light in *Arabidopsis thaliana*. Plant J **39:** 45-58
948 **Vanzo EM, Merl J, Lindermayr C, Heller H, Hauck SM, Durner J, Schnitzler JP** (2014) S-
949 nitroso-proteome in poplar leaves in response to acute ozone. PLoS One **9:** e106886
950 **Velikova V, Edreva A, Loreto F** (2004) Endogenous isoprene protects *Phragmites australis*
951 leaves against singlet oxygen. Physiol Plant **122:** 219-225
952 **Velikova V, Ghirardo A, Vanzo E, Merl J, Hauck SM, Schnitzler JP** (2014) Genetic
953 manipulation of isoprene emissions in poplar plants remodels the chloroplast proteome. J
954 Prot Res **13:** 2005-2018
955 **Velikova V, Loreto F** (2005) On the relationship between isoprene emission and
956 thermotolerance in Phragmites australis leaves exposed to high temperatures and during
957 the recovery from a heat stress. Plant Cell Environ **28:** 318-327
958 **Velikova V, Müller C, Ghirardo A, Rock TM, Aichler M, Walch A, Schmitt-Kopplin P,**
959 **Schnitzler JP** (2015) Knocking down of isoprene emission modifies the lipid matrix of
960 thylakoid membranes and influences the chloroplast ultrastructure in poplar. Plant
961 Physiol **168:** 859-870
962 **Velikova V, Fares S, Loreto F** (2008) Isoprene and nitric oxide reduce damages in leaves
963 exposed to oxidative stress. Plant Cell Environ **31:** 1882-1894
964 **Velikova V, Pinelli P, Pasqualini S, Reale L, Ferranti F, Loreto F** (2005) Isoprene decreases
965 the concentration of nitric oxide in leaves exposed to elevated ozone. New Phytol **166:**
966 419-425
967 **Velikova V, Varkonyi Z, Szabo M, Maslenkova L, Nogues I, Kovács L, Peeva V, Busheva**
968 **M, Garab G, Sharkey TD, Loreto F et al.** (2011) Increased thermostability of thylakoid
969 membranes in isoprene-emitting leaves probed with three biophysical techniques. Plant
970 Physiol **157:** 905-916
971 **Velikova V, Loreto F, Tsonev T, Brilli F, Edreva A** (2006) Isoprene prevents the negative
972 consequences of high temperature stress in *Platanus orientalis* leaves. Functional Plant
973 Biology **33:** 931-940
974 **Vickers CE, Possell M, Cojocariu CI, Velikova VB, Laothawornkitkul J, Ryan A,**
975 **Mullineaux PM, Hewitt CN** (2009a) Isoprene synthesis protects transgenic tobacco
976 plants from oxidative stress. Plant Cell Environ **32:** 520-531

977 **Vickers CE, Gershenzon J, Lerdau MT, Loreto F** (2009b) A unified mechanism of action for
978 volatile isoprenoids in plant abiotic stress. Nat Chem Biol **5:** 283-291
979 **Volkov RA, Panchuk II, Mullineaux PM, Schoffl F** (2006) Heat stress-induced H_2O_2 is
980 required for effective expression of heat shock genes in Arabidopsis. Plant Mol Biol **61:**
981 733-746
982 **Wang Y, Lin A, Loake GJ, Chu C** (2013) H_2O_2-induced leaf cell death and the crosstalk of
983 reactive nitric/oxygen species. J Integr Plant Biol **55:** 202-208
984 **Way DA, Schnitzler JP, Monson RK, Jackson RB** (2011) Enhanced isoprene-related tolerance
985 of heat- and light-stressed photosynthesis at low, but not high, CO_2 concentrations,
986 Oecologia **166:** 273-282
987 **Way DA, Ghirardo A, Kanawati B, Esperschütz J, Monson RK, Jackson RB, Schmitt-**
988 **Kopplin P, Schnitzler JP** (2013) Increasing atmospheric CO_2 reduces metabolic and
989 physiological differences between isoprene and non-isoprene-emitting poplars. New
990 Phytol **200:** 534-546
991 **Wink DA, Cook JA, Pacelli R, Liebmann J, Krishne MC, Mitchell JB** (1995) Nitric oxide
992 (NO) protects against cellular damage by reactive oxygen species. Toxicol Lett **82-83:**
993 221–226
994 **Wilson ID, Ribeiro DM, Bright J, Confraria A, Harrison J, Barros RS, Desikan R, Neill SJ,**
995 **Hancock JT** (2009) Role of nitric oxide in regulating stomatal apertures. Plant Signal
996 Behav**4**: 467-469
997 **Wisniewski JR, Zougman A, Nagaraj N, Mann M** (2009) Universal sample preparation
998 method for proteome analysis. Nat Methods **6:** 359-362
999 **Xu J, Yang J, Duan X, Jiang Y, Zhang P** (2014) Increased expression of native cytosolic
1000 Cu/Zn superoxide dismutase and ascorbate peroxidase improves tolerance to oxidative
1001 and chilling stresses in cassava (*Manihot esculenta* Crantz). BMC Plant Biol **14:** 208
1002 **Yang H, Mu J, Chen L, Feng J, hu J, Li L, Zhou J-M, Zua J (2015)** S-Nitrosylation
1003 positively regulates ascorbate peroxidase activity during plant stress responses. Plant
1004 Physiol **167:** 1604-1615
1005 **Zaffagnini M, Fermani S, Costa A, Lemaire SD, Trost P** (2013) Plant cytoplasmic GAPDH:
1006 redox post-translational modifications and moonlighting properties. Front Plant Sci **4:**
1007 450

1008 Zaffagnini M, Michelet L, Sciabolini C, Di Giacinto N, Morisse S, Marchand CH, Trost P,
1009 Fermani S, Lemaire SD (2014) High-resolution crystal structure and redox properties of
1010 chloroplastic triosephosphate isomerase from *Chlamydomonas reinhardtii*. Mol Plant **7:**
1011 101-120
1012 **Zimmermann G, Baumlein H, Mock HP, Himmelbach A, Schweizer P** (2006) The multigene
1013 family encoding germin-like proteins of barley. Regulation and function in basal host
1014 resistance. Plant Physiol **142**: 181-192
1015
1016

Figure legends

Figure 1. Whole proteome comparison of isoprene-emitting (IE, black) and non-isoprene-emitting (NE, red) gray poplar leaves. A) Volcano plot showing the magnitude of differential protein abundance in NE and IE (Log2 (fold change)) compared to the measure of the statistical significance (-Log10 (*P*-value, *t*-test)). Vertical, dashed lines indicate the log fold change of ± 1, and the horizontal line a significance value of $\alpha = 0.05$. The proteins with the highest and significant fold changes between NE and IE samples are highlighted and numbered: 1 = terpenoid cyclase, 2 = isoprene synthase, 3 = Rubisco large chain, 4 = 50S ribosomal protein, 5 = ubiquinone biosynthesis protein, 6 = chloroplast inner membrane import protein Tic22, 7 = basic pentacysteine 4, 8 = EP3-3 chitinase, 9 = eukaryotic aspartyl protease family. B) Discriminant proteins that explain the separation between IE and NE (116 in total, Supplemental Table S1) grouped according their functional category. Black bars mean up-regulated in IE, red bars indicate an up-regulation in the NE samples. Score (C) and loading (D) plots of OPLS of the whole proteome. C) Plants were divided into IE group (black circles, n = 6) and NE group (red circles, n = 6). Ellipse indicates the tolerance based on Hotelling's T^2 with a significance level of 0.05. D) Each functional group of proteins is indicated with different colors. The outer and inner ellipses indicate 100% and 75% explained variance, respectively. Each point represents an independent plant in the score plot and an individual protein in the loading plot. OPLS model fitness: $R^2(X) = 69.9\%$, $R^2(Y) = 100\%$, $r^2 = 98.6\%$, $Q^2(cum) = 79.3\%$ using 1 predictive component. RMSEE = 0.072; RMSEcv = 0.227. $P < 0.05$, cross-validated ANOVA.

Figure 2. Voronoi Treemaps showing the overall proteome changes of isoprene-emitting (IE: WT/EV) and non-isoprene-emitting (NE: Ra1/Ra2) gray poplar leaves. The Treemaps subdivide the 2D plane into subsections according to the hierarchical data structure of gene functional assignments, taken from the corresponding *Arabidopsis thaliana* L. orthologs (http://www.arabidopsis.org/tools/bulk/go/index.jsp), which were obtained via the POPGENIE (http://www.popgenie.org) database. Protein expression changes are displayed according to their functional categories: Hierarchically structured functional assignments were displayed in treemaps (A, B). C) Expression changes (log2 ratios of condition 1 vs condition 2) were color-coded. Orange codes for increased in NE (log2 ratio 4), grey means unchanged and blue codes for decreased (log2 ratio 4) expression in NE genotype.

Figure 3. Time-course curves of NO emission rates in shoots of isoprene-emitting (IE: WT/EV) and non-isoprene-emitting (NE: Ra1/Ra2) gray poplars before and after ozone fumigation (800 nL L^{-1} for 1 h) Measurements were performed at 25°C and 500 µmol m^{-2} s^{-1} PPFD. Values are means of four biological replicates ± SE. The vertical gray bar indicates the period of ozone fumigation.

Figure 4. Voronoi Treemaps showing the 63 S-nitrosylated proteins discriminant in IE and NE genotypes (see also Supplemental Table S3) and assigned to functional categories at the 1st level (A) and 3rd level (B).

Figure 5. Score (A) and loading (B) plots of the OPLS of S-nitrosylated protein abundances from control and ozone samples of isoprene emitting (IE = WT/EV) and non-isoprene-emitting (NE = Ra1/Ra2) genotypes. A) Plants were divided into ozone group (triangles, n = 12) and control group (circles, n = 12). Ellipse indicates the tolerance based on Hotelling's T^2 with a significance level of 0.05. B) Each functional group of proteins is indicated with different colors. The outer and inner ellipses indicate 100% and 75% explained variance, respectively. Each point represents an independent plant in the score plot and an individual protein in the loading plot. OPLS model fitness: $R^2(X)$ = 48.7%, $R^2(Y)$ = 100%, r^2 = 69%, $Q^2(cum)$ = 59% using 1 predictive component. RMSEE = 0.224; RMSEcv = 0.293. *P*-values of cross-validated ANOVA: NE/IE (genotype), $P < 0.05$; O/C (treatment), $P < 0.01$.

Figure 6. Voronoi Treemaps showing changes in the S-nitroso-proteome depending on (A) ozone treatment (O/C) and (B) genotype (NE/IE). Ozone-induced changes in the S-nitroso-proteome of (C) isoprene-emitting (IE = WT/EV) and (E) non-isoprene-emitting (NE = Ra1/Ra2) genotypes. Ratios of S-nitrosylation rates in NE/IE under control conditions (D) and (F) ozone treatment. S-Nitrosylated proteins were assigned to the functional categories displayed in Figure 4. Expression changes (log2 ratios of two conditions (see A, B, C, D, E, and F)) were color-coded. Orange means increased (log2 ratio -3), grey means unchanged and blue means decreased (log2 ratio 3) expression.

1080 **Figure 7**. Scheme of the possible interactions of isoprene with NO formation processes and
1081 biochemical target sites of NO in non-isoprene-emitting (NE) gray poplar (modifed after Moreau
1082 et al. 2010).

1083

1084

TABLES

Table 1. Log-fold changes of the abundances of S-nitrosylated proteins between isoprene-emitting (IE) and non-isoprene-emitting (NE) gray poplar after ozone fumigation (only ozone samples) which differ significantly between lines (VIP score). The intensities of the S-nitrosylated proteins were normalized to the corresponding global protein abundances of ozone-treated (O) leaves. Functional categorization was done according to MapMan BIN (http://ppdb.tc.cornell.edu/dbsearch/searchacc.aspx). * LC-MS/MS quantification based on one unique peptide.

Accession	VIP score	SE	Log2 NE_O/IE_O	Annotation	MapMan BIN category	*P*-value (*t*-test)
POPTR_0004s01030	1.73	0.60	0.9	Glycine cleavage T-protein family	Amino acid metabolism/degradation	0.091
POPTR_0004s01320*	1.49	0.78	0.7	Glyoxalase I homolog	Amino acid metabolism/degradation	0.075
POPTR_0001s37650*	1.61	0.58	0.5	Fasciclin-like arabinogalactan 1	Cell wall	0.115
POPTR_0016s02620*	1.36	1.07	0.8	Alpha-N-arabinofuranosidase 1 (ARA1)	Cell wall	0.023
POPTR_0006s02850*	< 1	-	0.6	Alpha-N-arabinofuranosidase (ARA)	Cell wall	0.045
POPTR_0006s12740*	1.45	1.08	1.6	Cell division protein 48 (CDC48)	Cell/division	0.065
POPTR_0001s25630*	1.92	0.74	1.0	Thiamine biosynthesis protein (ThiC)	Co-factor and vitamine metabolism	0.025
POPTR_0015s08540*	2.08	0.66	1.5	Aldehyde dehydrogenase 2B4	Fermentation	0.010
POPTR_0008s05640	1.61	0.46	1.0	Triosephosphate isomerase (TPI)	Glycolysis	0.007
POPTR_0008s08400*	< 1	-	1.1	Phosphoglycerate kinase	Glycolysis	0.013
POPTR_0006s10480	1.50	0.86	0.9	Ferretin 1	Metal handling	0.079
POPTR_0016s14950*	< 1	-	1.6	2,3-Bisphosphoglycerate mutase, putative	Metal handling/binding, chelation and storage	0.002
POPTR_0016s14310	1.54	0.74	0.4	NADPH dependent ketone reductase (AOR)	Misc	0.052
POPTR_0006s19810*	1.48	0.83	1.0	Leucyl aminopeptidase (LAP2)	Protein/degradation	0.008
POPTR_0001s35230*	1.73	0.83	1.4	Ribosomal protein L12-A	Protein/synthesis	0.008
POPTR_0001s26970*	< 1	-	1.6	Ribosomal protein	Protein/synthesis	0.009
POPTR_0004s23490*	< 1	-	1.7	Elongation factor 1 gamma 1,	Protein/synthesis	0.024

				putative		
POPTR_0002s00840	2.39	1.06	0.9	Glyceraldehyde-3-phosphate dehydrogenase, subunit B	PS/calvin cyle	0.135
POPTR_0010s20060	2.28	0.29	1.2	Sedoheptulose-1,7-bisphosphatase	PS/calvin cyle	0.000
POPTR_0010s20810	2.15	0.91	0.6	Rubisco activase	PS/calvin cyle	0.134
POPTR_0013s03700	1.79	0.59	0.5	Ribose 5-phosphate isomerase, type A protein	PS/calvin cyle	0.079
POPTR_0003s09830	1.63	0.84	0.6	Phosphoribulokinase (PRK)	PS/calvin cyle	0.009
POPTR_0001s08420*	1.55	0.94	0.9	Ferredoxin-plastoquinone reductase (PGR5-like A)	PS/lightreaction	0.001
POPTR_0008s15100*	1.14	0.48	3.1	Photosystem I subunit D-2	PS/lightreaction	0.148
POPTR_0002s01080	1.55	0.80	0.8	Catalase 2 (CAT2)	Redox	0.053
POPTR_0005s17350*	1.27	1.10	1.3	Ascorbate peroxidase (APX)	Redox	0.001
POPTR_0001s44990*	1.18	1.00	1.0	Thioredoxin-dependent peroxidase 1 (PrxII B)	Redox	0.011
POPTR_0009s02070	< 1	-	0.7	Ascorbate peroxidase (APX)	Redox	0.020
POPTR_0009s07040*	2.33	0.83	0.7	NIFS-like cysteine desulfurase, chloroplastic	S-assimilation	0.131
POPTR_0002s01990*	1.82	0.53	1.2	Cinnamyl alcohol dehydrogenase-like protein (CAD)	Secondary metabolism	0.011
POPTR_0007s04700*	1.89	1.18	1.7	UVB-resistance protein (UVR8)	Stress/abiotic	0.043
POPTR_0005s10990	2.03	1.24	0.6	Aconitase 1 (ACO1)	TCA / org.transformation	0.064
POPTR_0008s16670	1.36	1.08	1.2	Malate dehydrogenase	TCA / org.transformation	0.002

1095

1096

1097

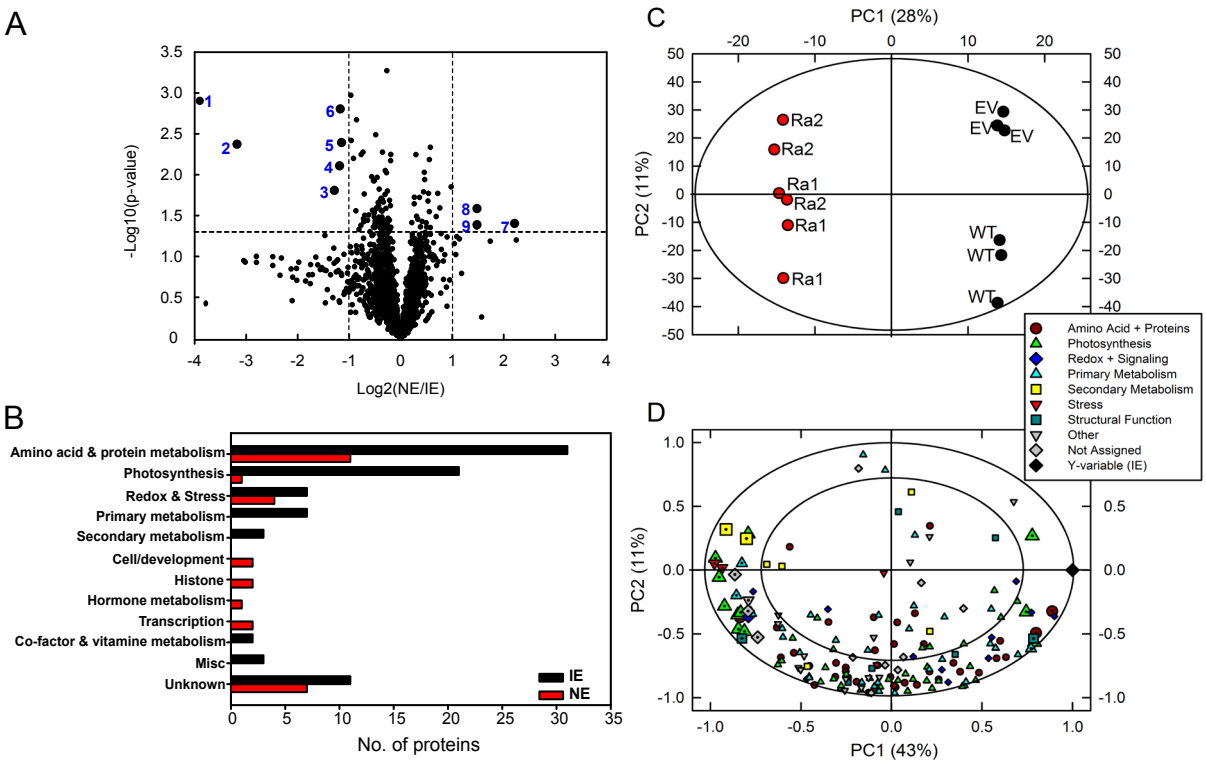

Figure 1. Whole proteome comparison of isoprene-emitting (IE, black) and non-isoprene-emitting (NE, red) gray poplar leaves. A) Volcano plot showing the magnitude of differential protein abundance in NE and IE (Log2 (fold change)) compared to the measure of the statistical significance (-Log10 (*P*-value, *t*-test)). Vertical, dashed lines indicate the log fold change of ± 1, and the horizontal line a significance value of $\alpha = 0.05$. The proteins with the highest and significant fold changes between NE and IE samples are highlighted and numbered: 1 = terpenoid cyclase, 2 = isoprene synthase, 3 = Rubisco large chain, 4 = 50S ribosomal protein, 5 = ubiquinone biosynthesis protein, 6 = chloroplast inner membrane import protein Tic22, 7 = basic pentacysteine 4, 8 = EP3-3 chitinase, 9 = eukaryotic aspartyl protease family. B) Discriminant proteins that explain the separation between IE and NE (116 in total, Supplemental Table S1) grouped according their functional category. Black bars mean up-regulated in IE, red bars indicate an up-regulation in the NE samples. Score (C) and loading (D) plots of OPLS of the whole proteome. C) Plants were divided into IE group (black circles, n = 6) and NE group (red circles, n = 6). Ellipse indicates the tolerance based on Hotelling's T^2 with a significance level of 0.05. D) Each functional group of proteins is indicated with different colors. The outer and inner ellipses indicate 100% and 75% explained variance, respectively. Each point represents an independent plant in the score plot and an individual protein in the loading plot. OPLS model fitness: $R^2(X) = 69.9\%$, $R^2(Y) = 100\%$, $r^2 = 98.6\%$, $Q^2(cum) = 79.3\%$ using 1 predictive component. RMSEE = 0.072; RMSEcv = 0.227. $P < 0.05$, cross-validated ANOVA.

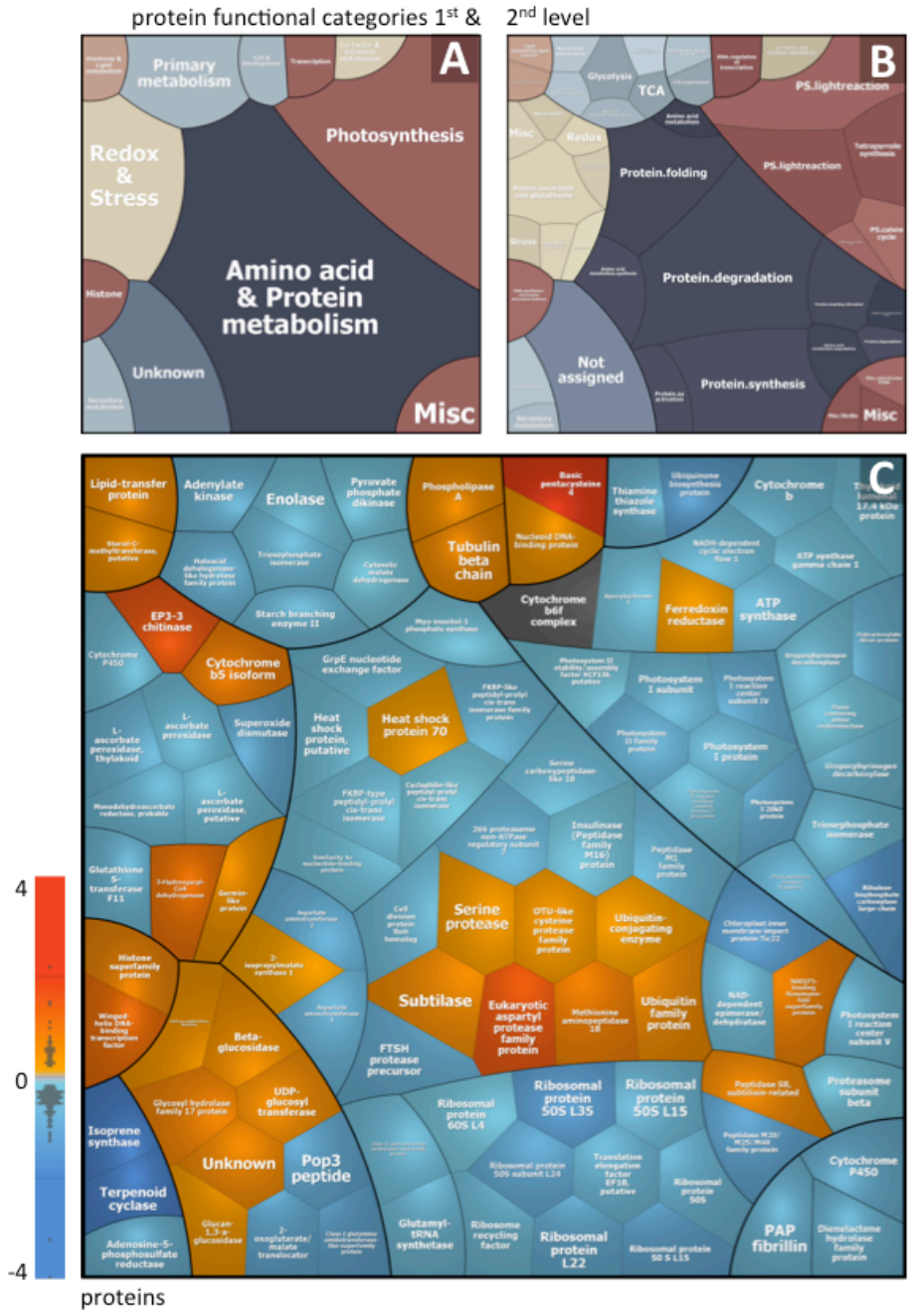

Figure 2. Voronoi Treemaps showing the overall proteome changes of isoprene-emitting (IE: WT/EV) and non-emitting (NE: Ra1/Ra2) gray poplar leaves. The Treemaps subdivide the 2D plane into subsections according to the hierarchical data structure of gene functional assignments, taken from the corresponding *Arabidopsis thaliana* L. orthologs (http://www.arabidopsis.org/tools/bulk/go/index.jsp), which were obtained via the POPGENIE (http://www.popgenie.org) database. Protein expression changes are displayed according their functional categories: Hierarchically structured functional assignments were displayed in treemaps (A, B). C) Expression changes (log2 ratios of condition 1 vs condition 2) were color-coded. Orange codes for increased in NE (log2 ratio 4), grey means unchanged and blue codes for decreased (log2 ratio 4) expression in NE genotype.

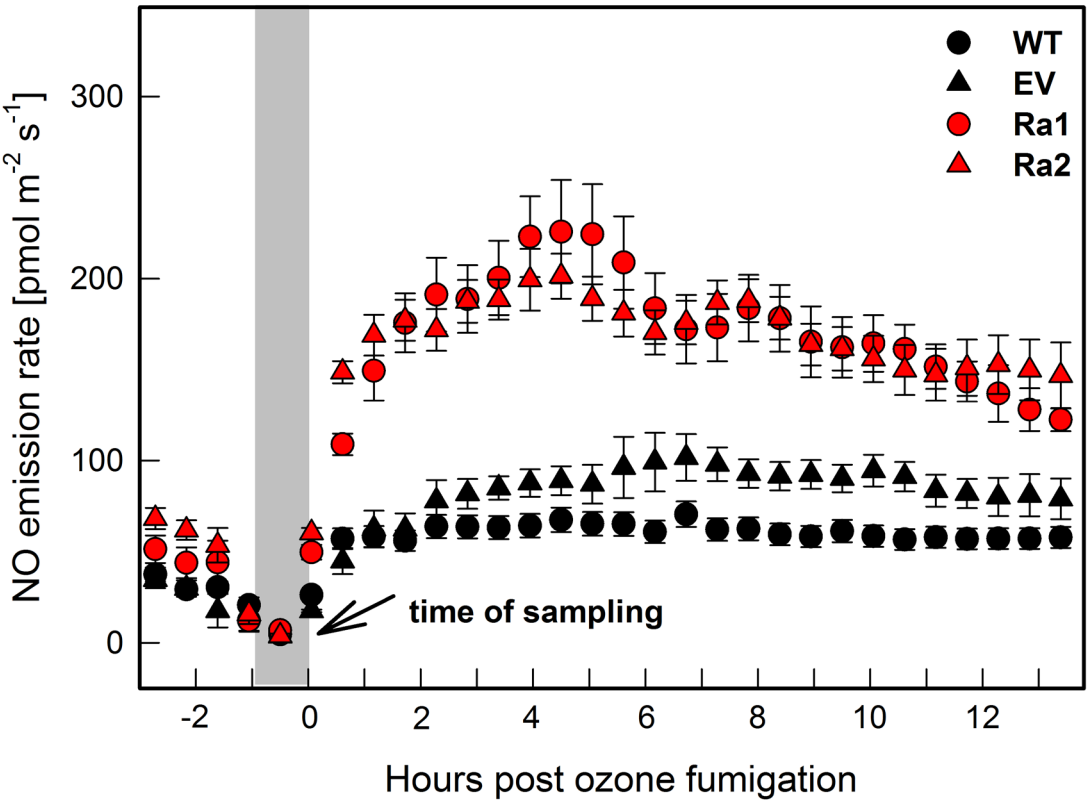

Figure 3. Time-course curves of NO emission rates in shoots of isoprene-emitting (IE: WT/EV) and non-isoprene-emitting (NE: Ra1/Ra2) gray poplars before and after ozone fumigation (800 nl L^{-1} for 1 h) Measurements were performed at 25°C and 500 µmol m^{-2} s^{-1} PPFD. Values are means of four biological replicates ± SE. The vertical gray bar indicates the period of ozone fumigation.

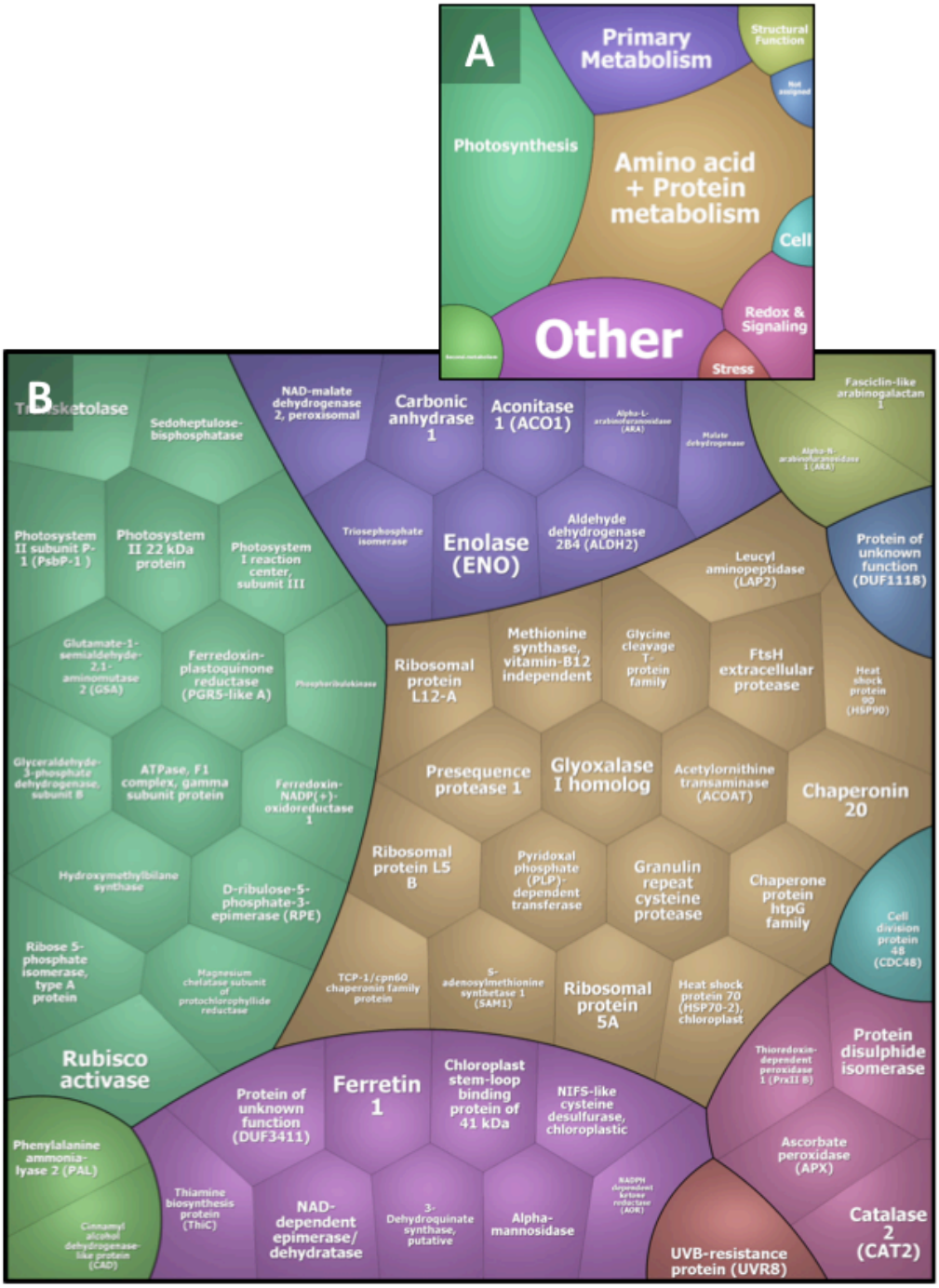

Figure 4. Voronoi Treemaps showing the 63 S-nitrosylated proteins discriminant in IE and NE genotypes (see also Supplemental Table S3) and assigned to functional categories at the 1st level (A) and 3rd level (B).

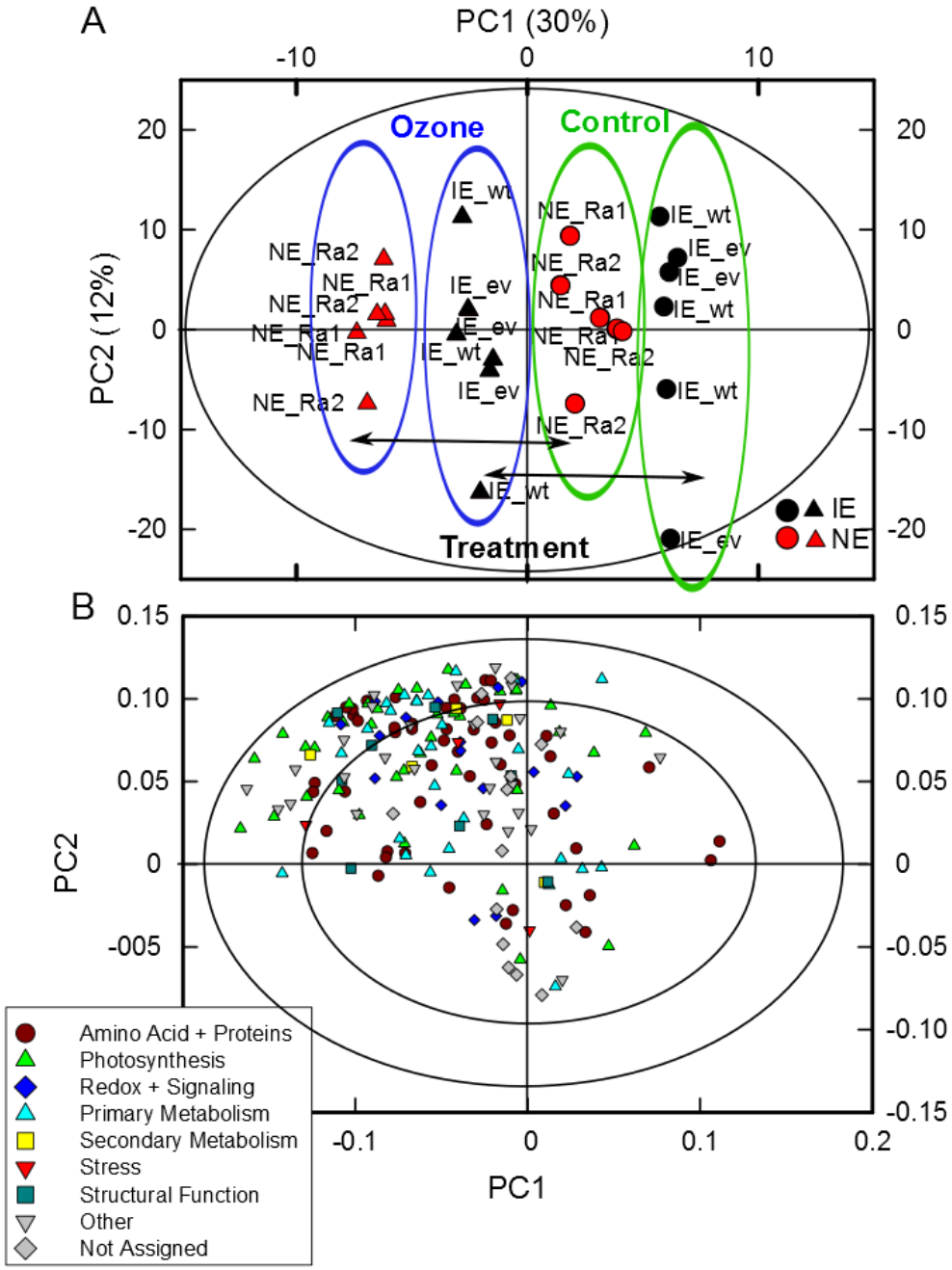

Figure 5. Score (A) and loading (B) plots of the OPLS of S-nitrosylated protein abundances from control and ozone samples of isoprene emitting (IE = WT/EV) and non-isoprene-emitting (NE = Ra1/Ra2) genotypes. A) Plants were divided into ozone group (triangles, n = 12) and control group (circles, n = 12). Ellipse indicates the tolerance based on Hotelling's T^2 with a significance level of 0.05. B) Each functional group of proteins is indicated with different colors. The outer and inner ellipses indicate 100% and 75% explained variance, respectively. Each point represents an independent plant in the score plot and an individual protein in the loading plot. OPLS model fitness: $R^2(X)$ = 48.7%, $R^2(Y)$ = 100%, r^2 = 69%, $Q^2(cum)$ = 59% using 1 predictive component. RMSEE = 0.224; RMSEcv = 0.293. *P*-values of cross-validated ANOVA: NE/IE (genotype), $P < 0.05$; O/C (treatment), $P < 0.01$.

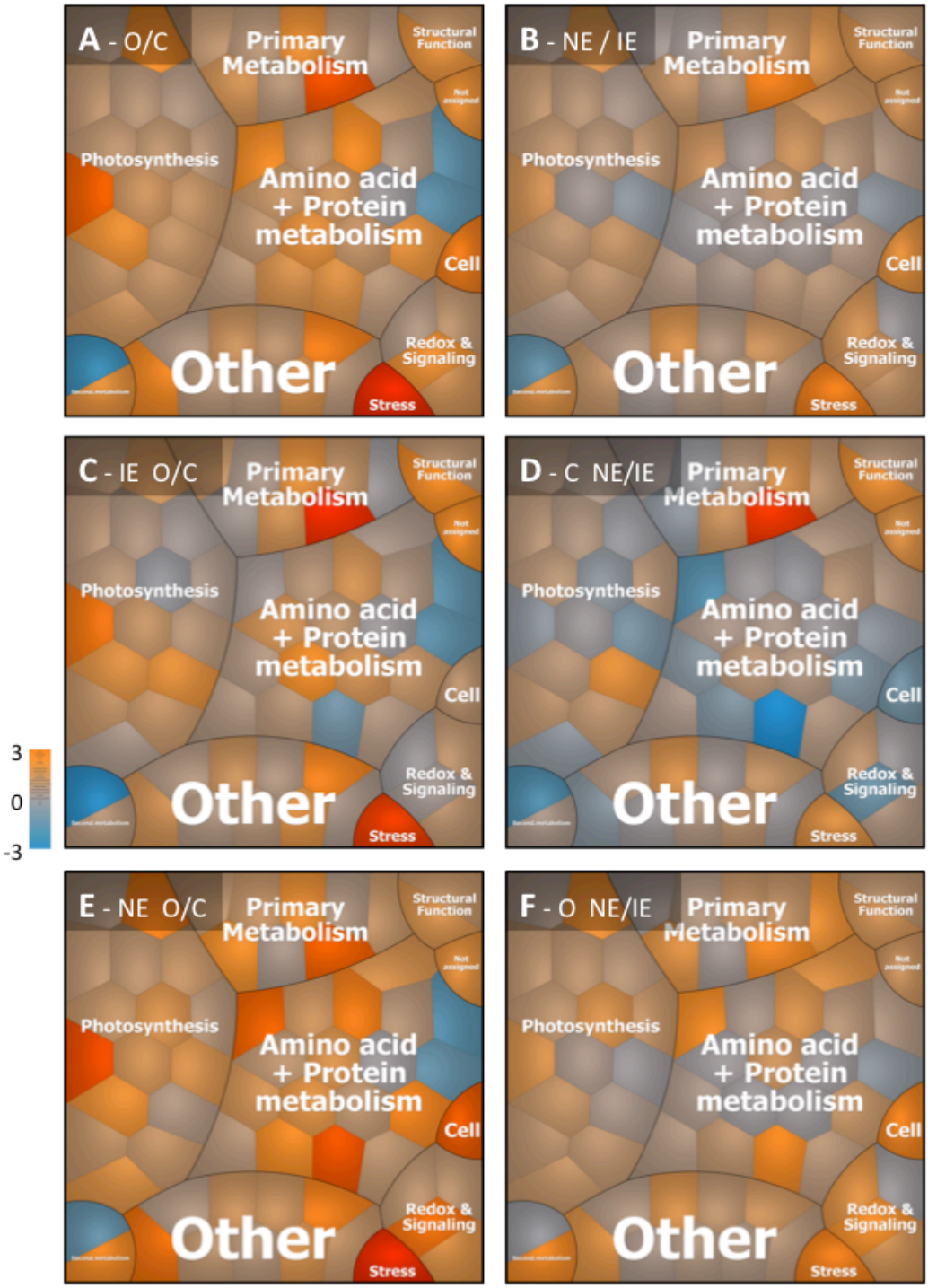

Figure 6. Voronoi Treemaps showing changes in the S-nitroso-proteome depending on (A) ozone treatment (O/C) and (B) genotype (NE/IE). Ozone-induced changes in the S-Nitroso-proteome of (C) isoprene-emitting (IE = WT/EV) and (E) non-isoprene-emitting (NE = Ra1/Ra2) genotypes. Ratios of S-nitrosylation rates in NE/IE under control conditions (D) and (F) ozone treatment. S-Nitrosylated proteins were assigned to the functional categories displayed in Figure 4. Expression changes (log2 ratios of two conditions (see A, B, C, D, E, and F)) were color-coded. Orange means increased (log2 ratio -3), grey means unchanged and blue means decreased (log2 ratio 3) expression.

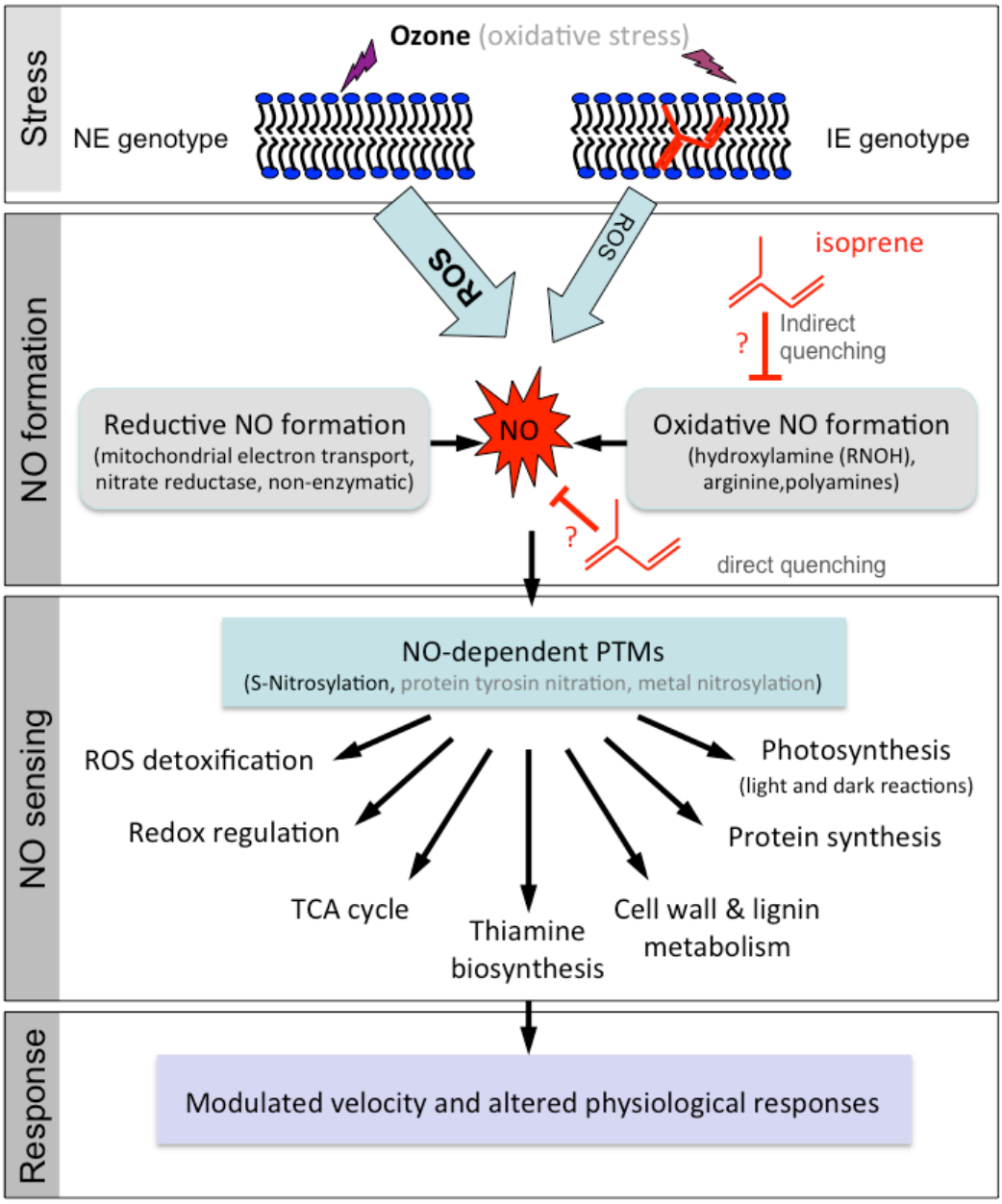

Figure 7. Scheme of the possible interactions of isoprene with NO formation processes and biochemical target sites of NO in isoprene-emitting (IE) non-isoprene-emitting (NE) gray poplars (modifed after Moreau et al. 2010).

Parsed Citations

Abat JK, Deswal R (2009) Differential modulation of S-nitrosoproteome of Brassica juncea by low temperature: change in S-nitrosylation of Rubisco is responsible for the inactivation of its carboxylase activity. Proteomics 9: 4368-4380
Pubmed: Author and Title
CrossRef: Author and Title
Google Scholar: Author Only Title Only Author and Title

Abat JK, Mattoo AK, Deswal R (2008) S-nitrosylated proteins of a medicinal CAM plant Kalanchoe pinnata- ribulose-1,5-bisphosphate carboxylase/oxygenase activity targeted for inhibition. FEBS J 275: 2862-2872
Pubmed: Author and Title
CrossRef: Author and Title
Google Scholar: Author Only Title Only Author and Title

Affek HP, Yakir D (2002) Protection by isoprene against singlet oxygen in leaves. Plant Physiol 129: 269-277
Pubmed: Author and Title
CrossRef: Author and Title
Google Scholar: Author Only Title Only Author and Title

Ahlfors R, Brosché M, Kollist H, Kangasjärvi J (2009) Nitric oxide modulates ozone-induced cell death, hormone biosynthesis and gene expression in Arabidopsis thaliana. Plant J 58: 1-12
Pubmed: Author and Title
CrossRef: Author and Title
Google Scholar: Author Only Title Only Author and Title

Alvarez C, Lozano-Juste J, Romero LC, Garcia I, Gotor C, Leon J (2011) Inhibition of Arabidopsis O-acetylserine(thiol)lyase A1 by tyrosine nitration. J Biol Chem 286: 578-586
Pubmed: Author and Title
CrossRef: Author and Title
Google Scholar: Author Only Title Only Author and Title

Apel K, Hirt H (2004) Reactive oxygen species: Metabolism, oxidative stress, and signal transduction. Annu Rev Plant Biol 55: 373-399
Pubmed: Author and Title
CrossRef: Author and Title
Google Scholar: Author Only Title Only Author and Title

Aspeborg H, Schrader J, Coutinho PM, Stam M, Kallas Å, Djerbi S, Nilsson P, Denman S, Amini B, Sterky F, Master E, Sandberg G, Mellerowicz E, Sundberg B, Henrissat B, Teeri TT (2005) Carbohydrate-active enzymes involved in the secondary cell wall biogenesis in hybrid aspen. Plant Physiol 137: 983-997
Pubmed: Author and Title
CrossRef: Author and Title
Google Scholar: Author Only Title Only Author and Title

Astier J, Kulik A, Koen E, Besson-Bard A, Bourque S, Jeandroz S, Lamotte O, Wendehenne D (2012) Protein S-nitrosylation: what's going on in plants? Free Radic Biol Med 53: 1101-1110
Pubmed: Author and Title
CrossRef: Author and Title
Google Scholar: Author Only Title Only Author and Title

Banerjee A, Wu Y, Banerjee R, Li Y, Yan HG, Sharkey TD (2013) Feedback inhibition of deoxy-D-xylulose-5-phosphate synthase regulates the methylerythritol 4-phosphate pathway. J Biol Chem 288: 16926-16936
Pubmed: Author and Title
CrossRef: Author and Title
Google Scholar: Author Only Title Only Author and Title

Behnke K, Ehlting B, Teuber M, Bauerfeind M, Louis S, Hänsch R, Polle A, Bohlmann J, Schnitzler JP (2007) Transgenic, non-isoprene emitting poplars don't like it hot. Plant J 51: 485-499
Pubmed: Author and Title
CrossRef: Author and Title
Google Scholar: Author Only Title Only Author and Title

Behnke K, Kleist E, Uerlings R, Wildt J, Rennenberg H, Schnitzler JP (2009) RNAi-mediated suppression of isoprene biosynthesis in hybrid poplar impacts ozone tolerance. Tree Physiol 29: 725-736
Pubmed: Author and Title
CrossRef: Author and Title
Google Scholar: Author Only Title Only Author and Title

Behnke K, Kaiser A, Zimmer I, Brüggemann N, Janz D, Polle A, Hampp R, Hänsch R, Popko J, Schmitt-Kopplin P, Ehlting B, Rennenberg H, Barta C, Loreto F, Schnitzler JP (2010a) RNAi-mediated suppression of isoprene emission in poplar transiently impacts phenolic metabolism under high temperature and high light intensities: a transcriptomic and metabolomic analysis. Plant Mol Biol 74: 61-75
Pubmed: Author and Title
CrossRef: Author and Title
Google Scholar: Author Only Title Only Author and Title

Behnke K, Loivamäki M, Zimmer I, Rennenberg H, Schnitzler JP, Louis S (2010b) Isoprene emission protects photosynthesis in sunfleck exposed Grey poplar. Photosynth Res 104: 5-17
Pubmed: Author and Title

CrossRef: Author and Title
Google Scholar: Author Only Title Only Author and Title

Benhar M, Forrester MT, Stamler JS (2009) Protein denitrosylation: enzymatic mechanisms and cellular functions. Nat Rev Mol Cell Biol 10: 721-732
Pubmed: Author and Title
CrossRef: Author and Title
Google Scholar: Author Only Title Only Author and Title

Bernhardt J, Funke S, Hecker M, Siebourg J (2009) Visualizing Gene Expression Data via Voronoi Treemaps. Conference paper. Sixth International Symposium on Voronoi Diagrams, ISVD 2009, Copenhagen, Denmark, June 23-26, DOI: 10.1109/ISVD.2009.33
Pubmed: Author and Title
CrossRef: Author and Title
Google Scholar: Author Only Title Only Author and Title

Bethke PC, Gubler F, Jacobsen JV, Jones RL (2004) Dormancy of Arabidopsis seeds and barley grains can be broken by nitric oxide. Planta 219: 847-855
Pubmed: Author and Title
CrossRef: Author and Title
Google Scholar: Author Only Title Only Author and Title

Booker FL, Miller JE (1998) Phenylpropanoid metabolism and phenolic composition of soybean [Glycine max (L.) Merr.] leaves following exposure to ozone. J Exp Bot 49: 1191-1202
Pubmed: Author and Title
CrossRef: Author and Title
Google Scholar: Author Only Title Only Author and Title

Brosch M, Yu L, Hubbard T, Choudhary J (2009) Accurate and sensitive peptide identification with Mascot Percolator. J Prot Res 8: 3176-3181
Pubmed: Author and Title
CrossRef: Author and Title
Google Scholar: Author Only Title Only Author and Title

Cabané M, Pireaux JC, Leger E, Weber E, Dizengremel P, Pollet B, Lapierre C (2004) Condensed lignins are synthesized in poplar leaves exposed to ozone. Plant Physiol 134: 586-594
Pubmed: Author and Title
CrossRef: Author and Title
Google Scholar: Author Only Title Only Author and Title

Cai B, Zhang A, Yang Z, Lu Q, Wen X, Lu C (2010) Characterization of photosystem II photochemistry in transgenic tobacco plants with lowered Rubisco activase content. J Plant Physiol 167: 1457-1465
Pubmed: Author and Title
CrossRef: Author and Title
Google Scholar: Author Only Title Only Author and Title

Corpas FJ, Chaki M, Leterrier M, Barroso JB (2009) Protein tyrosine nitration: a new challenge in plants. Plant Signal Behav 4: 920-923
Pubmed: Author and Title
CrossRef: Author and Title
Google Scholar: Author Only Title Only Author and Title

Corpas FJ, Leterrier M, Valderrama R, Airaki M, Chaki M, Palma JM, Barroso JB (2011) Nitric oxide imbalance provokes a nitrosative response in plants under abiotic stress. Plant Sci 181: 604-611
Pubmed: Author and Title
CrossRef: Author and Title
Google Scholar: Author Only Title Only Author and Title

Dat JF, Pellinen R, Beeckman T, Van de Cotte B, Langebartels C, Kangasjärvi J, Inze D, Van Breusegem F (2003) Changes in hydrogen peroxide homeostasis trigger an active cell death process in tobacco. Plant J 33: 621-632
Pubmed: Author and Title
CrossRef: Author and Title
Google Scholar: Author Only Title Only Author and Title

Davletova S, Rizhsky L, Liang HJ, Zhong SQ, Oliver DJ, Coutu J, Shulaev V, Schlauch K, Mittler R (2005) Cytosolic ascorbate peroxidase 1 is a central component of the reactive oxygen gene network of Arabidopsis. Plant Cell 17: 268-281
Pubmed: Author and Title
CrossRef: Author and Title
Google Scholar: Author Only Title Only Author and Title

Day CD, Lee E, Kobayashi T, Holappa LD, Albert H, Ow DW (2000) Transgene integration into the same chromosome location can produce alleles that express at a predictable level, or alleles that are differentially silenced. Genes Dev 14: 2869-2880
Pubmed: Author and Title
CrossRef: Author and Title
Google Scholar: Author Only Title Only Author and Title

de Pinto MC, Locato V, Sgobba A, Romero-Puertas MD, Gadaleta C, Delledonne M, De Gara L (2013) S-Nitrosylation of ascorbate peroxidase is part of programmed cell death signaling in tobacco Bright Yellow-2 cells. Plant Physiol 163: 1766-1775
Pubmed: Author and Title
CrossRef: Author and Title
Google Scholar: Author Only Title Only Author and Title

de Pinto MC, Paradiso A, Leonetti P, De Gara L (2006) Hydrogen peroxide, nitric oxide and cytosolic ascorbate peroxidase at the crossroad between defence and cell death. Plant J48: 784-795
Pubmed: Author and Title
CrossRef: Author and Title
Google Scholar: Author Only Title Only Author and Title

Delledonne M, Xia Y, Dixon RA, Lamb C (1998) Nitric oxide functions as a signal in plant disease resistance. Nature 394: 585-588
Pubmed: Author and Title
CrossRef: Author and Title
Google Scholar: Author Only Title Only Author and Title

Di Baccio D, Castagna A, Paoletti E, Sebastiani L, Ranier A (2008) Could the differences in O3 sensitivity between two poplar clones be related to a difference in antioxidant defense and secondary metabolic response to O3 influx? Tree Physiol 28: 1761-1772
Pubmed: Author and Title
CrossRef: Author and Title
Google Scholar: Author Only Title Only Author and Title

Durner J, Wendehenne D, Klessig DF (1998) Defense gene induction in tobacco by nitric oxide, cyclic GMP, and cyclic ADP-ribose. Proc Natl Acad Sci USA 95: 10328-10333
Pubmed: Author and Title
CrossRef: Author and Title
Google Scholar: Author Only Title Only Author and Title

Eriksson L, Johansson E, Kettaneh-Wold N, Trygg J, Wikström C, Wold S (2006) Multi- and megavariate data analysis. Part I: Basic principles and applications. Umeå, Sweden: Umetrics Academy
Pubmed: Author and Title
CrossRef: Author and Title
Google Scholar: Author Only Title Only Author and Title

Favory JJ, Stec A, Gruber H, et al. (2009) Interaction of COP1 and UVR8 regulates UV-B-induced photomorphogenesis and stress acclimation in Arabidopsis. Embo J 28: 591-60
Pubmed: Author and Title
CrossRef: Author and Title
Google Scholar: Author Only Title Only Author and Title

Foyer CH, Noctor G (2003) Redox sensing and signalling associated with reactive oxygen in chloroplasts, peroxisomes and mitochondria. Physiol Plant 119: 355-364
Pubmed: Author and Title
CrossRef: Author and Title
Google Scholar: Author Only Title Only Author and Title

Foyer CH, Noctor G (2011) Ascorbate and glutathione: the heart of the redox hub. Plant Physiol 155: 2-18
Pubmed: Author and Title
CrossRef: Author and Title
Google Scholar: Author Only Title Only Author and Title

Ghirardo A, Wright LP, Bi Z, Rosenkranz M, Pulido P, Rodríguez-Concepción M, Niinemets Ü, Brüggemann N, Gershenzon J, Schnitzler JP (2014) Metabolic flux analysis of plastidic isoprenoid biosynthesis in poplar leaves emitting and nonemitting isoprene. Plant Physiol 165: 37-51
Pubmed: Author and Title
CrossRef: Author and Title
Google Scholar: Author Only Title Only Author and Title

Goyer A (2010) Thiamine in plants: aspects of its metabolism and fucntions. Phytochem 71: 1615-1624
Pubmed: Author and Title
CrossRef: Author and Title
Google Scholar: Author Only Title Only Author and Title

Guo FQ, Crawford NM (2005) Arabidopsis nitric oxide synthase1 is targeted to mitochondria and protects against oxidative damage and dark-induced senescence. Plant Cell 17: 3436-3450
Pubmed: Author and Title
CrossRef: Author and Title
Google Scholar: Author Only Title Only Author and Title

Gupta KJ, Shah JK, Brotman Y, Jahnke K, Willmitzer L, Kaiser WM, Bauwe H, Igamberdiev AU (2012) Inhibition of aconitase by nitric oxide leads to induction of the alternative oxidase and to a shift of metabolism towards biosynthesis of amino acids. J Exp Bot 63: 1773-1784
Pubmed: Author and Title
CrossRef: Author and Title
Google Scholar: Author Only Title Only Author and Title

Hara MR, Agrawal N, Kim SF, et al. (2005) S-nitrosylated GAPDH initiates apoptotic cell death by nuclear translocation following Siah1 binding. Nat Cell Biol 7: 665-674
Pubmed: Author and Title
CrossRef: Author and Title
Google Scholar: Author Only Title Only Author and Title

Harvey CM, Li Z, Tjellsröm H, Blanchard GJ, Sharkey TD (2015) Concentration of isoprene in artificial and thylakoid membranes. J Bioenerg Biomembr DOI 10.1007/s10863-015-9625-9

Pubmed: Author and Title
CrossRef: Author and Title
Google Scholar: Author Only Title Only Author and Title

Hauck SM, Dietter J, Kramer RL, Hofmaier F, Zipplies JK, et al. (2010) Deciphering membrane-associated molecular processes in target tissue of autoimmune uveitis by label-free quantitative mass spectrometry. Mol Cell Prot 9: 2292-2305
Pubmed: Author and Title
CrossRef: Author and Title
Google Scholar: Author Only Title Only Author and Title

He Y, Tang RH, Hao Y, Stevens RD, Cook CW, Ahn SM, Jing L, Yang Z, Chen L, Guo F, Fiorani F, Jackson RB, Crawford NM, Pei ZM (2004) Nitric oxide represses the Arabidopsis floral transition. Science 305: 1968-1971
Pubmed: Author and Title
CrossRef: Author and Title
Google Scholar: Author Only Title Only Author and Title

Heijde M, Ulm R (2012) UV-B photoreceptor-mediated signalling in plants. Trends Plant Sci 17: 230-237
Pubmed: Author and Title
CrossRef: Author and Title
Google Scholar: Author Only Title Only Author and Title

Holtgrefe S, Gohlke J, Starmann J, Druce S, Klocke S, Altmann B, Wojtera J, Lindermayr C, Scheibe R (2008) Regulation of plant cytosolic glyceraldehyde 3-phosphate dehydrogenase isoforms by thiol modifications. Physiol Plant 133: 211-228
Pubmed: Author and Title
CrossRef: Author and Title
Google Scholar: Author Only Title Only Author and Title

Hu J, Huang X, Chen L, Sun X, Lu C, Zhang L, Wang Y, Zuo J (2015) Site-specific nitrosoproteomic identification of endogenously S-nitrosylated proteins in Arabidopsis. Plant Physiol 167: 1731-46
Pubmed: Author and Title
CrossRef: Author and Title
Google Scholar: Author Only Title Only Author and Title

Huang D, Zhang X, Chen ZM, Zhao Y, Shen XL (2011) The kinetics and mechanism of an aqueous phase isoprene reaction with hydroxyl radical. Atmos Chem Phys 11: 7399-7415
Pubmed: Author and Title
CrossRef: Author and Title
Google Scholar: Author Only Title Only Author and Title

Janz D, Behnke K, Schnitzler JP, Kanawati B, Schmitt-Kopplin P, Polle A (2010) Pathway analysis of the transcriptome and metabolome of salt sensitive and tolerant poplar species reveals evolutionary adaption of stress tolerance mechanisms. BMC Plant Biol 10: 150
Pubmed: Author and Title
CrossRef: Author and Title
Google Scholar: Author Only Title Only Author and Title

Jasid S, Simontacchi M, Bartoli CG, Puntarulo S (2006) Chloroplasts as a nitric oxide cellular source. Effect of reactive nitrogen species on chloroplastic lipids and proteins Plant Physiol 142: 1246-1255
Pubmed: Author and Title
CrossRef: Author and Title
Google Scholar: Author Only Title Only Author and Title

Johnson KL, Jones BJ, Bacic A, Schultz CJ (2003) The fasciclin-like arabinogalactan proteins of arabidopsis. A multigene family of putative cell adhesion molecules. Plant Physiol 133: 1911-1925
Pubmed: Author and Title
CrossRef: Author and Title
Google Scholar: Author Only Title Only Author and Title

Kaling M, Kanawati B, Ghirardo A, Albert A, Winkler JB, Heller W, Barta C, Loreto F, Schmitt-Kopplin P, Schnitzler JP (2015) UV-B mediated metabolic rearrangements in poplar revealed by non-targeted metabolomics. Plant Cell Environ 38: 892-904
Pubmed: Author and Title
CrossRef: Author and Title
Google Scholar: Author Only Title Only Author and Title

Kasprzewska A (2003) Plant chitinases--regulation and function. Cell Mol Biol Lett 8: 809-824
Pubmed: Author and Title
CrossRef: Author and Title
Google Scholar: Author Only Title Only Author and Title

Kotak S, Larkindale J, Lee U, von Koskull-Doring P, Vierling E, Scharf KD (2007) Complexity of the heat stress response in plants. Curr Opin Plant Biol 10: 310-316
Pubmed: Author and Title
CrossRef: Author and Title
Google Scholar: Author Only Title Only Author and Title

Lane BG (2002) Oxalate, germins, and higher-plant pathogens. IUBMB Life 53: 67-75
Pubmed: Author and Title
CrossRef: Author and Title
Google Scholar: Author Only Title Only Author and Title

Latham JR, Wilson AK, Steinbrecher RA (2006) The mutational consequences of plant transformation. J Biomed Biotechnol 25376:

1-7
Pubmed: Author and Title
CrossRef: Author and Title
Google Scholar: Author Only Title Only Author and Title

Lindermayr C, Durner J (2015) Interplay of reactive oxygen species and nitric oxide: nitric oxide coordinates reactive oxygen species homeostasis. Plant Physiol 167: 1209-1210
Pubmed: Author and Title
CrossRef: Author and Title
Google Scholar: Author Only Title Only Author and Title

Lindermayr C, Durner J (2009) S-Nitrosylation in plants: Pattern and function. J Proteomics 73: 1-9
Pubmed: Author and Title
CrossRef: Author and Title
Google Scholar: Author Only Title Only Author and Title

Lindermayr C, Saalbach G, Durner J (2005) Proteomic identification of S-nitrosylated proteins in Arabidopsis. Plant Physiol 137: 921-930
Pubmed: Author and Title
CrossRef: Author and Title
Google Scholar: Author Only Title Only Author and Title

Loreto F, Mannozzi M, Maris C, Nascetti P, Ferranti F, Pasqualini S (2001) Ozone quenching properties of isoprene and its antioxidant role in leaves. Plant Physiol 126: 993-1000
Pubmed: Author and Title
CrossRef: Author and Title
Google Scholar: Author Only Title Only Author and Title

Loreto F, Schnitzler JP (2010) Abiotic stresses and induced BVOCs. Trends Plant Sci 15: 154-166
Pubmed: Author and Title
CrossRef: Author and Title
Google Scholar: Author Only Title Only Author and Title

Loreto F, Velikova V (2001) Isoprene produced by leaves protects the photosynthetic apparatus against ozone damage, quenches ozone products, and reduces lipid peroxidation of cellular membranes. Plant Physiol 127: 1781-1787
Pubmed: Author and Title
CrossRef: Author and Title
Google Scholar: Author Only Title Only Author and Title

Lozano-Juste J, Colom-Moreno R, Leon J (2011) In vivo protein tyrosine nitration in Arabidopsis thaliana. J Exp Bot 62: 3501-3517
Pubmed: Author and Title
CrossRef: Author and Title
Google Scholar: Author Only Title Only Author and Title

Mahalingam R, Jambunathan N, Gunjan SK, Faustin E, Weng H, Ayoubi P (2006) Analysis of oxidative signalling induced by ozone in Arabidopsis thaliana. Plant Cell Environ 29: 1357-1371
Pubmed: Author and Title
CrossRef: Author and Title
Google Scholar: Author Only Title Only Author and Title

Merl J, Ueffing M, Hauck SM, von Toerne C (2012) Direct comparison of MS-based label-free and SILAC quantitative proteome profiling strategies in primary retinal Muller cells. Proteomics 12: 1902-1911
Pubmed: Author and Title
CrossRef: Author and Title
Google Scholar: Author Only Title Only Author and Title

Michelet L, Zaffagnini M, Morisse S, Sparla F, Pérez-Pérez ME, Francia F, Danon A, Marchand CH, Fermani S, Trost P, Lemaire SD (2013) Redox regulation of the Calvin-Benson cycle: something old, something new. Front Plant Sci 4: 470
Pubmed: Author and Title
CrossRef: Author and Title
Google Scholar: Author Only Title Only Author and Title

Mittler R (2002) Oxidative stress, antioxidants and stress tolerance. Trends Plant Sci 7: 405-410
Pubmed: Author and Title
CrossRef: Author and Title
Google Scholar: Author Only Title Only Author and Title

Moreau M, Lindermayr C, Durner J, Klessig DF (2010) NO synthesis and signaling in plants - where do we stand? Physiol Plant 138: 372-383
Pubmed: Author and Title
CrossRef: Author and Title
Google Scholar: Author Only Title Only Author and Title

Neill SJ, Desikan R, Clarke A, Hancock JT (2002) Nitric oxide is a novel component of abscisic acid signaling in stomatal guard cells. Plant Physiol 128: 13-16
Pubmed: Author and Title
CrossRef: Author and Title
Google Scholar: Author Only Title Only Author and Title

Noctor G, Mhamdi A, Foyer CH (2014) The roles of reactive oxygen metabolism in drought: Not so cut and dried. Plant Physiol 164: 1636-1648

Pubmed: Author and Title
CrossRef: Author and Title
Google Scholar: Author Only Title Only Author and Title

Ortega-Galisteo AP, Rodriguez-Serrano M, Pazmino DM, Gupta DK, Sandalio LM, Romero-Puertas MC (2012) S-Nitrosylated proteins in pea (Pisum sativum L.) leaf peroxisomes: changes under abiotic stress. J Exp Bot 63: 2089-2103
Pubmed: Author and Title
CrossRef: Author and Title
Google Scholar: Author Only Title Only Author and Title

Pasqualini S, Meier S, Gehring C, Madeo L, Fornaciari M, Romano B, Ederli L (2009) Ozone and nitric oxide induce cGMP-dependent and -independent transcription of defence genes in tobacco. New Phytol 181: 860-870
Pubmed: Author and Title
CrossRef: Author and Title
Google Scholar: Author Only Title Only Author and Title

Peñuelas J, Llusia J, Asensio D, Munne-Bosch S (2005) Linking isoprene with plant thermotolerance, antioxidants and monoterpene emissions. Plant Cell Environ 28: 278-286
Pubmed: Author and Title
CrossRef: Author and Title
Google Scholar: Author Only Title Only Author and Title

Portis AR Jr (2003) Rubisco activase - Rubisco's catalytic chaperone. Photosynth Res 75: 11-27
Pubmed: Author and Title
CrossRef: Author and Title
Google Scholar: Author Only Title Only Author and Title

Quideau S, Deffieux D, Douat-Casassus C, Pouysegu L (2011) Plant polyphenols: Chemical properties, biological activities, and synthesis. Angew Chem Int Edit 50: 586-621
Pubmed: Author and Title
CrossRef: Author and Title
Google Scholar: Author Only Title Only Author and Title

Rao MV, Paliyath, Ormrod, DP (1996) Ultraviolet-B- and ozone-induced biochemical changes in antioxidant enzymes of Arabidopsis thaliana. Plant Physiol 110: 125-136
Pubmed: Author and Title
CrossRef: Author and Title
Google Scholar: Author Only Title Only Author and Title

Richet N, Tozo K, Afif D, Banvoy J, Legay S, Dizengremel P, Cabané M (2012) The response to daylight or continuous ozone of phenylpropanoid and lignin biosynthesis pathways in poplar differs between leaves and wood. Planta 236: 727-737
Pubmed: Author and Title
CrossRef: Author and Title
Google Scholar: Author Only Title Only Author and Title

Rizzini L, Favory J-J, Cloix C, Faggionato D, O'Hara A, Kaiserli E, Baumeister R, Schaefer E, Nagy F, Jenkins GI, Ulm R (2011) Perception of UV-B by the Arabidopsis UVR8 Protein. Science 332: 103-106
Pubmed: Author and Title
CrossRef: Author and Title
Google Scholar: Author Only Title Only Author and Title

Rodriguez-Serrano M, Romero-Puertas MC, Zabalza A, Corpas FJ, Gomez M, Del Rio LA, Sandalio LM (2006) Cadmium effect on oxidative metabolism of pea (Pisum sativum L.) roots. Imaging of reactive oxygen species and nitric oxide accumulation in vivo. Plant Cell Environ 29: 1532-1544
Pubmed: Author and Title
CrossRef: Author and Title
Google Scholar: Author Only Title Only Author and Title

Sandermann H, Ernst D, Heller W, langebartels C (1998) Ozone: an elicitor of plant defence reactions. Trends Plant Sci 3: 47-50
Pubmed: Author and Title
CrossRef: Author and Title
Google Scholar: Author Only Title Only Author and Title

Seifert GJ, Blaukopf C (2010) Irritable Walls: The plant extracellular matrix and signaling. Plant Physiol 153: 467-478
Pubmed: Author and Title
CrossRef: Author and Title
Google Scholar: Author Only Title Only Author and Title

Sharkey TD, Singsaas EL.(1995) Why plants emit isoprene. Nature 374: 769-769
Pubmed: Author and Title
CrossRef: Author and Title
Google Scholar: Author Only Title Only Author and Title

Sharkey TD, Yeh SS (2001) Isoprene emission from plants. Annu Rev Plant Physiol Plant Mol Biol 52: 407-436
Pubmed: Author and Title
CrossRef: Author and Title
Google Scholar: Author Only Title Only Author and Title

Shih MC, Heinrich P, Goodman HM (1991) Cloning and chromosomal mapping of nuclear genes encoding chloroplast and cytosolic glyceraldehyde-3-phosphate-dehydrogenase from Arabidopsis thaliana. Gene 104: 133-138
Pubmed: Author and Title

CrossRef: Author and Title
Google Scholar: Author Only Title Only Author and Title

Simontacchi M, Garcia-Mata C, Bartoli CG, Santa-Maria GE, Lamattina L (2013) Nitric oxide as a key component in hormone-regulated processes. Plant Cell Rep 32: 853-866
Pubmed: Author and Title
CrossRef: Author and Title
Google Scholar: Author Only Title Only Author and Title

Singsaas EL, Lerdau M, Winter K, Sharkey TD (1997) Isoprene increases thermotolerance of isoprene-emitting species. Plant Physiol 115: 1413-1420
Pubmed: Author and Title
CrossRef: Author and Title
Google Scholar: Author Only Title Only Author and Title

Singsaas EL, Sharkey TD (2000) The effects of high temperature on isoprene synthesis in oak leaves. Plant Cell Environ 23: 751-757
Pubmed: Author and Title
CrossRef: Author and Title
Google Scholar: Author Only Title Only Author and Title

Siwko ME, Marrink SJ, de Vries AH, Kozubek A, Uiterkamp AJMS, Mark AE (2007) Does isoprene protect plant membranes from thermal shock? A molecular dynamics study. Biochim Biophys Acta - Biomembranes 1768: 198-206
Pubmed: Author and Title
CrossRef: Author and Title
Google Scholar: Author Only Title Only Author and Title

Sumiyoshi M, Nakamura A, Nakamura H, Hakata M, Ichikawa H, Hirochika H, Ishii T, Satoh S, Iwai H (2013) Increase in cellulose accumulation and improvement of saccharification by overexpression of arabinofuranosidase in rice. Plos One 8: e10.1371
Pubmed: Author and Title
CrossRef: Author and Title
Google Scholar: Author Only Title Only Author and Title

Tanaka R, Kobayashi K, Masudac T (2011) Tetrapyrrole Metabolism in Arabidopsis thaliana. Arabidopsis Book 9: e0145
Pubmed: Author and Title
CrossRef: Author and Title
Google Scholar: Author Only Title Only Author and Title

Tanou G, Filippou P, Belghazi M, Job D, Diamantidis G, Fotopoulos V, Molassiotis A (2012) Oxidative and nitrosative-based signaling and associated post-translational modifications orchestrate the acclimation of citrus plants to salinity stress. Plant J 72: 585-599
Pubmed: Author and Title
CrossRef: Author and Title
Google Scholar: Author Only Title Only Author and Title

Thiel S, Döhring T, Köfferlein M, Kosak A, Martin P, Seidlitz HK (1996) A phytotron for plant stress research: How far can artificial lighting compare to natural sunlight? J Plant Physiol 148: 456-463
Pubmed: Author and Title
CrossRef: Author and Title
Google Scholar: Author Only Title Only Author and Title

Tossi V, Amenta M, Lamattina L, Cassia R (2011) Nitric oxide enhances plant ultraviolet-B protection up-regulating gene expression of the phenylpropanoid biosynthetic pathway. Plant Cell Environ 34: 909-921
Pubmed: Author and Title
CrossRef: Author and Title
Google Scholar: Author Only Title Only Author and Title

Vandenabeele S, Vanderauwera S, Vuylsteke M, et al. (2004) Catalase deficiency drastically affects gene expression induced by high light in Arabidopsis thaliana. Plant J 39: 45-58
Pubmed: Author and Title
CrossRef: Author and Title
Google Scholar: Author Only Title Only Author and Title

Vanzo EM, Merl J, Lindermayr C, Heller H, Hauck SM, Durner J, Schnitzler JP (2014) S-nitroso-proteome in poplar leaves in response to acute ozone. PLoS One 9: e106886
Pubmed: Author and Title
CrossRef: Author and Title
Google Scholar: Author Only Title Only Author and Title

Velikova V, Edreva A, Loreto F (2004) Endogenous isoprene protects Phragmites australis leaves against singlet oxygen. Physiol Plant 122: 219-225
Pubmed: Author and Title
CrossRef: Author and Title
Google Scholar: Author Only Title Only Author and Title

Velikova V, Ghirardo A, Vanzo E, Merl J, Hauck SM, Schnitzler JP (2014) Genetic manipulation of isoprene emissions in poplar plants remodels the chloroplast proteome. J Prot Res 13: 2005-2018
Pubmed: Author and Title
CrossRef: Author and Title
Google Scholar: Author Only Title Only Author and Title

Velikova V, Loreto F (2005) On the relationship between isoprene emission and thermotolerance in Phragmites australis leaves exposed to high temperatures and during the recovery from a heat stress. Plant Cell Environ 28: 318-327
Pubmed: Author and Title
CrossRef: Author and Title
Google Scholar: Author Only Title Only Author and Title

Velikova V, Müller C, Ghirardo A, Rock TM, Aichler M, Walch A, Schmitt-Kopplin P, Schnitzler JP (2015) Knocking down of isoprene emission modifies the lipid matrix of thylakoid membranes and influences the chloroplast ultrastructure in poplar. Plant Physiol 168: 859-870
Pubmed: Author and Title
CrossRef: Author and Title
Google Scholar: Author Only Title Only Author and Title

Velikova V, Fares S, Loreto F (2008) Isoprene and nitric oxide reduce damages in leaves exposed to oxidative stress. Plant Cell Environ 31: 1882-1894
Pubmed: Author and Title
CrossRef: Author and Title
Google Scholar: Author Only Title Only Author and Title

Velikova V, Pinelli P, Pasqualini S, Reale L, Ferranti F, Loreto F (2005) Isoprene decreases the concentration of nitric oxide in leaves exposed to elevated ozone. New Phytol 166: 419-425
Pubmed: Author and Title
CrossRef: Author and Title
Google Scholar: Author Only Title Only Author and Title

Velikova V, Varkonyi Z, Szabo M, Maslenkova L, Nogues I, Kovács L, Peeva V, Busheva M, Garab G, Sharkey TD, Loreto F et al. (2011) Increased thermostability of thylakoid membranes in isoprene-emitting leaves probed with three biophysical techniques. Plant Physiol 157: 905-916
Pubmed: Author and Title
CrossRef: Author and Title
Google Scholar: Author Only Title Only Author and Title

Velikova V, Loreto F, Tsonev T, Brilli F, Edreva A (2006) Isoprene prevents the negative consequences of high temperature stress in Platanus orientalis leaves. Functional Plant Biology 33: 931-940
Pubmed: Author and Title
CrossRef: Author and Title
Google Scholar: Author Only Title Only Author and Title

Vickers CE, Possell M, Cojocariu CI, Velikova VB, Laothawornkitkul J, Ryan A, Mullineaux PM, Hewitt CN (2009a) Isoprene synthesis protects transgenic tobacco plants from oxidative stress. Plant Cell Environ 32: 520-531
Pubmed: Author and Title
CrossRef: Author and Title
Google Scholar: Author Only Title Only Author and Title

Vickers CE, Gershenzon J, Lerdau MT, Loreto F (2009b) A unified mechanism of action for volatile isoprenoids in plant abiotic stress. Nat Chem Biol 5: 283-291
Pubmed: Author and Title
CrossRef: Author and Title
Google Scholar: Author Only Title Only Author and Title

Volkov RA, Panchuk II, Mullineaux PM, Schoffl F (2006) Heat stress-induced H2O2 is required for effective expression of heat shock genes in Arabidopsis. Plant Mol Biol 61: 733-746
Pubmed: Author and Title
CrossRef: Author and Title
Google Scholar: Author Only Title Only Author and Title

Wang Y, Lin A, Loake GJ, Chu C (2013) H2O2-induced leaf cell death and the crosstalk of reactive nitric/oxygen species. J Integr Plant Biol 55: 202-208
Pubmed: Author and Title
CrossRef: Author and Title
Google Scholar: Author Only Title Only Author and Title

Way DA, Schnitzler JP, Monson RK, Jackson RB (2011) Enhanced isoprene-related tolerance of heat- and light-stressed photosynthesis at low, but not high, CO2 concentrations, Oecologia 166: 273-282
Pubmed: Author and Title
CrossRef: Author and Title
Google Scholar: Author Only Title Only Author and Title

Way DA, Ghirardo A, Kanawati B, Esperschütz J, Monson RK, Jackson RB, Schmitt-Kopplin P, Schnitzler JP (2013) Increasing atmospheric CO2 reduces metabolic and physiological differences between isoprene and non-isoprene-emitting poplars. New Phytol 200: 534-546
Pubmed: Author and Title
CrossRef: Author and Title
Google Scholar: Author Only Title Only Author and Title

Wink DA, Cook JA, Pacelli R, Liebmann J, Krishne MC, Mitchell JB (1995) Nitric oxide (NO) protects against cellular damage by reactive oxygen species. Toxicol Lett 82-83: 221-226
Pubmed: Author and Title
CrossRef: Author and Title
Google Scholar: Author Only Title Only Author and Title

Wilson ID, Ribeiro DM, Bright J, Confraria A, Harrison J, Barros RS, Desikan R, Neill SJ, Hancock JT (2009) Role of nitric oxide in regulating stomatal apertures. Plant Signal Behav4: 467-469
Pubmed: Author and Title
CrossRef: Author and Title
Google Scholar: Author Only Title Only Author and Title

Wisniewski JR, Zougman A, Nagaraj N, Mann M (2009) Universal sample preparation method for proteome analysis. Nat Methods 6: 359-362
Pubmed: Author and Title
CrossRef: Author and Title
Google Scholar: Author Only Title Only Author and Title

Xu J, Yang J, Duan X, Jiang Y, Zhang P (2014) Increased expression of native cytosolic Cu/Zn superoxide dismutase and ascorbate peroxidase improves tolerance to oxidative and chilling stresses in cassava (Manihot esculenta Crantz). BMC Plant Biol 14: 208
Pubmed: Author and Title
CrossRef: Author and Title
Google Scholar: Author Only Title Only Author and Title

Yang H, Mu J, Chen L, Feng J, hu J, Li L, Zhou J-M, Zua J (2015) S-Nitrosylation positively regulates ascorbate peroxidase activity during plant stress responses. Plant Physiol 167: 1604-1615
Pubmed: Author and Title
CrossRef: Author and Title
Google Scholar: Author Only Title Only Author and Title

Zaffagnini M, Fermani S, Costa A, Lemaire SD, Trost P (2013) Plant cytoplasmic GAPDH: redox post-translational modifications and moonlighting properties. Front Plant Sci 4: 450
Pubmed: Author and Title
CrossRef: Author and Title
Google Scholar: Author Only Title Only Author and Title

Zaffagnini M, Michelet L, Sciabolini C, Di Giacinto N, Morisse S, Marchand CH, Trost P, Fermani S, Lemaire SD (2014) High-resolution crystal structure and redox properties of chloroplastic triosephosphate isomerase from Chlamydomonas reinhardtii. Mol Plant 7: 101-120
Pubmed: Author and Title
CrossRef: Author and Title
Google Scholar: Author Only Title Only Author and Title

Zimmermann G, Baumlein H, Mock HP, Himmelbach A, Schweizer P (2006) The multigene family encoding germin-like proteins of barley. Regulation and function in basal host resistance. Plant Physiol 142: 181-192
Pubmed: Author and Title
CrossRef: Author and Title
Google Scholar: Author Only Title Only Author and Title

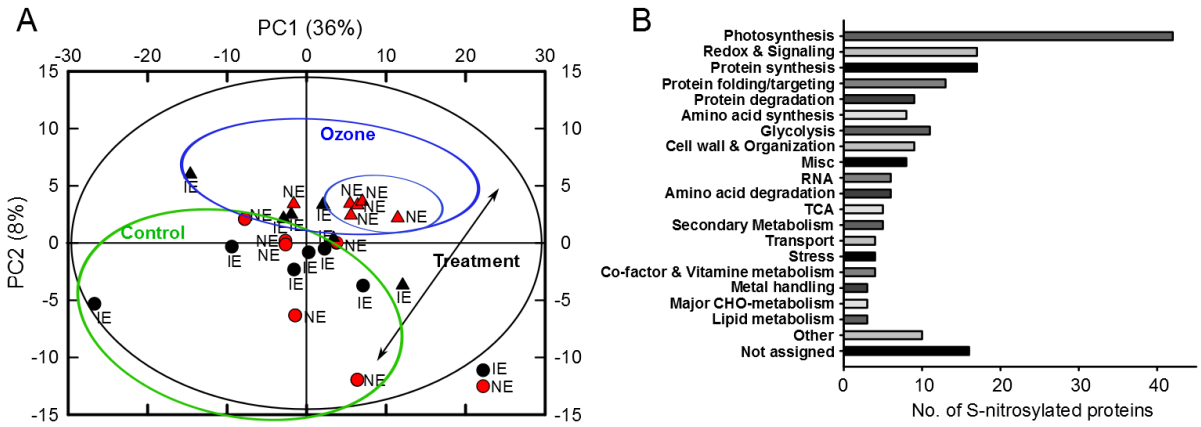

Supplemental Figure S1. S-nitrosylated proteins detected in the control and ozone samples of the isoprene emitting (IE, black) and non-isoprene emitting (NE, red) genotypes. S-nitroso-proteins from IE and NE leaf extracts were detected by the Biotin switch assay, purified via affinity chromatography und identified by LC-MS/MS. A) PCA score plot based on protein abundances of S-nitrosylated proteins in IE and NE samples (control and ozone). The green square highlights the control samples (circles, n = 12), the blue square the ozone samples (triangles, n = 12). Within the ozone samples, the clustering of the NE samples is highlighted. B) Functional categorization of the 203 identified S-nitrosylated proteins in IE and NE poplar (control and ozone). The category 'Other' comprises C1-metabolism (1 protein), fermentation (1), gluconeogenesis (1), hormone metabolism (1), mitochondrial electron transport (1), nucleotide metabolism (1), N-metabolism (2), and S-assimilation (2).

Supplemental Figure S2

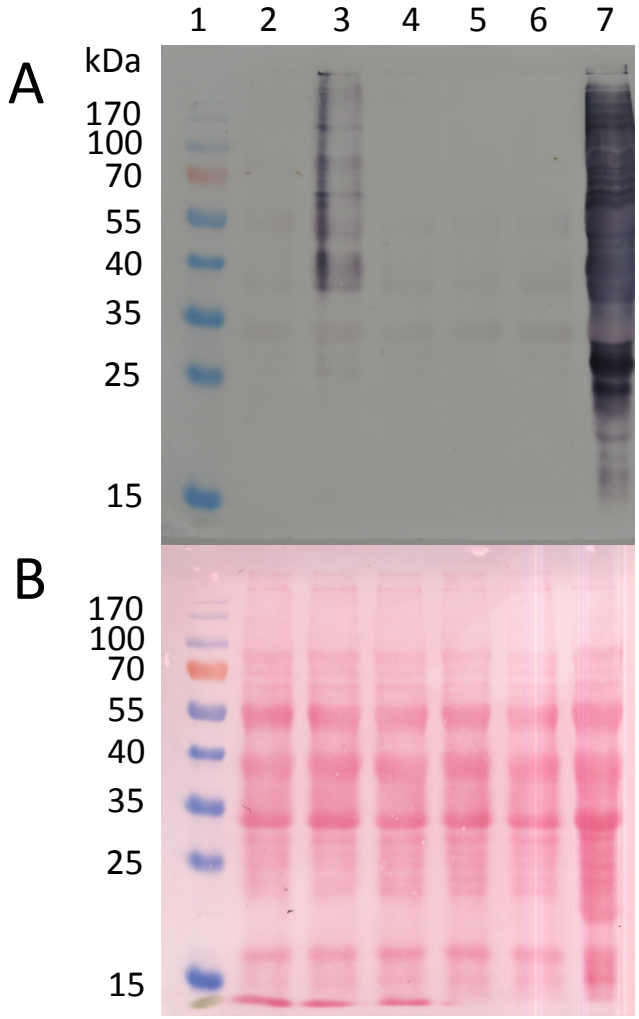

1) Protein ladder
2) NE control
3) NE ozone
4) NE (control) false positive endogen
5) NE (control) without biotin
6) NE (control) without sinapinic acid
7) NE (control) without blocking (NEM)

Supplemental Figure S2. Detection of endogenously S-nitrosylated proteins in non-isoprene-emitting (NE) gray poplar. (A) Western blot showing *in vivo* S-nitrosylated proteins including controls for false-positives (FP) (line 4: FP endogen (reduced with 3 mM sinapinic acid and blocked with 30 mM NEM simultaneously); line 5: without 1 mM biotin; line 6: without 3 mM sinapinic acid; line 7: without 30 mM NEM). Biotinylated (=S-nitrosylated) proteins were detected by an anti-biotin antibody (for details see Material and methods and Vanzo et al. *2014*). (B) Ponceau S staining of total protein.

Supplemental Table S1. Proteins, that discriminately separate non–isoprene-emitting (NE) from isoprene emitting (IE) gray poplar samples in the OPLS model of the whole proteome. Proteins with a VIP score > 1 and uncertainty bars of jack-knifing method smaller than the respective VIP value are considered discriminant. Additionally, proteins with VIP scores < 1 were added to the list when they showed a significant difference between IE and NE in the *t*-test ($P < 0.05$). OPLS analysis was performed on LC-MS/MS protein abundances obtained from whole leaf extracts from two IE (WT/EV, n = 6 biological replicates per line) and two NE (Ra1/Ra2, n = 6 biological replicates per line) genotypes. Log2 ratios between NE and IE are given to show different amounts of the proteins. SE = standard error of jack-knifing method. Annotation and functional classification was achieved by several databases (Phytozome, PopGenIE, MapMan BIN). Proteins highlighted in bold are discussed in the text. * Identified and quantified by only one unique peptide.

	VIP score	SE	Log2 (NE/IE)	Description	MapMan BIN category
UP in NE					
Amino acid & Protein metabolism					
POPTR_0005s08480	1.822	1.377	0.22	2-isopropylmalate synthase 1	Amino acid metabolism.synthesis
POPTR_0009s16390*	2.050	1.231	1.47	Eukaryotic aspartyl protease family protein	Protein.degradation
POPTR_0009s11450	2.099	0.595	0.72	NAD(P)-binding Rossmann-fold superfamily protein	Protein.targeting.chloroplast
POPTR_0010s21270	1.895	1.131	0.23	Heat shock protein 70	Protein.folding
POPTR_0008s11610*	1.821	1.045	0.78	Methionine aminopeptidase 1B	Protein.degradation
POPTR_0011s14290*	1.832	1.415	0.33	OTU-like cysteine protease family protein	Protein.degradation
POPTR_0002s12610*	< 1	-	0.58	Peptidase S8, subtilisin-related	Amino acid metabolism.degradation
POPTR_0012s14320*	1.941	1.682	0.31	**Serine protease**	Protein.degradation
POPTR_0014s02650	2.252	0.570	0.56	**Subtilase**	Protein.degradation
POPTR_0009s13560	2.016	0.638	0.53	**Ubiquitin family protein**	Protein.degradation
POPTR_0006s22210	2.043	1.103	0.27	**Ubiquitin-conjugating enzyme**	Protein.degradation
Cell & Development					
POPTR_0011s16520	1.899	1.208	0.56	Tubulin beta chain	Cell.organisation
POPTR_0007s11360*	1.842	1.082	0.50	Phospholipase A	Development.storage proteins
Histone					
POPTR_0013s04000*	1.928	1.124	1.09	**Winged-helix DNA-binding transcription factor**	DNA.synthesis/chromatin structure.histone
POPTR_0010s22080	2.059	1.287	0.64	**Histone superfamily protein**	DNA.synthesis/chromatin structure.histone

Hormone & Lipid metabolism					
POPTR_0002s01780	2.018	1.224	0.45	Sterol-C-methyltransferase, putative	Hormone metabolism.brassinosteroide
POPTR_0001s21750*	< 1	-	0.51	Lipid-transfer protein	Lipid metabolism.lipid transfer
Photosynthesis					
POPTR_0005s11500	1.936	1.782	0.26	**Ferredoxin reductase**	PS.lightreaction
Redox & Stress					
POPTR_0001s40920*	2.191	0.733	0.98	3-Hydroxyacyl-CoA dehydrogenase	Biodegradation of Xenobiotic
POPTR_0002s24400*	1.881	0.872	0.76	Cytochrome b5 isoform	Redox
POPTR_0019s12360	2.030	1.313	1.48	**EP3-3 chitinase**	Stress.biotic
POPTR_0003s06370	1.907	1.776	0.42	**Germin-like protein**	Stress.abiotic
Transcription					
POPTR_0002s02820*	1.829	0.903	2.20	Basic pentacysteine 4	RNA.regulation of transcription
POPTR_0018s02960	2.004	1.253	0.37	Nucleoid DNA-binding protein	RNA.regulation of transcription
Unknown					
POPTR_0009s11830*	1.899	0.789	0.69	Glycosyl hydrolase family 17 protein	Not assigned
POPTR_0016s05780	2.484	1.397	0.58	Unknown	Not assigned
Potri.011G061000*	2.199	0.534	0.54	UDP-glucosyl transferase	Not assigned
POPTR_0006s26630	2.057	0.975	0.47	Unknown	Not assigned
POPTR_0003s01730	2.261	0.830	0.46	Beta-glucosidase	Not assigned
Potri.T099600*	1.873	0.698	0.38	Hydroxyacylglutathione hydrolase	Not assigned
POPTR_0007s04720	2.215	0.885	0.30	Glucan-1,3-α-glucosidase	Not assigned
DOWN in NE					
Amino acid & Protein metabolism					
POPTR_0014s10800*	1.997	0.712	-0.38	Class II aaRS and biotin synthetases superfamily protein	Protein.aa activation
POPTR_0001s41530	2.128	1.566	-0.19	Cyclophilin-like peptidyl-prolyl cis-trans isomerase	Protein.folding
POPTR_0016s10970	2.120	0.888	-0.51	FKBP-like peptidyl-prolyl cis-trans isomerase family protein	Protein.folding
POPTR_0010s04610	2.016	1.179	-0.20	Insulinase (Peptidase family M16) protein	Protein.degradation
POPTR_0002s08590*	2.542	1.727	-0.97	Peptidase M20/M25/M40 family protein	Amino acid metabolism.degradation
POPTR_0022s00410	2.389	0.762	-0.48	Translation elongation factor EF1B, putative	Protein.synthesis
POPTR_0010s19960*	1.931	1.024	-0.55	26S proteasome non-ATPase regulatory subunit 7	Protein.degradation
POPTR_0014s14010	1.889	0.941	-0.64	Aspartate aminotransferase 1	Amino acid metabolism.synthesis
POPTR_0018s02250	1.842	0.616	-0.72	Aspartate aminotransferase 2	Amino acid metabolism.synthesis
POPTR_0002s01320	2.129	0.792	-0.39	Cell division protein ftsH homolog	Protein.degradation

POPTR_0002s23710*	2.436	1.732	-1.15	Chloroplast inner membrane import protein Tic22	Protein.targeting.chloroplast
POPTR_0014s13560	1.922	0.910	-0.71	FTSH protease precursor	Protein.degradation
POPTR_0009s17070*	< 1	-	-0.42	Glutamyl-tRNA synthetase	Protein.aa activation
POPTR_0013s06430	1.968	1.647	-0.36	GrpE nucleotide exchange factor	Protein.folding
POPTR_0014s16280	< 1	-	-0.26	Heat shock protein, putative	Protein.folding
POPTR_0001s12920	< 1	-	-0.30	FKBP-type peptidyl-prolyl cis-trans isomerase	Protein.folding
POPTR_0005s08050	< 1	-	-0.21	Myo-inositol-1 phosphate synthase	Amino acid metabolism
POPTR_0001s01960	< 1	-	-0.37	NAD-dependent epimerase/dehydratase	Protein.targeting.chloroplast
POPTR_0003s12960	1.999	0.604	-0.51	Peptidase M1 family protein	Protein.degradation
POPTR_0011s17170*	< 1	-	-0.41	Photosystem I reaction center subunit V	PS.lightreaction.photosystem I.PSI
POPTR_0008s17700	< 1	-	-0.22	Proteasome subunit beta	Protein.degradation
POPTR_0010s13410*	2.233	1.263	-0.92	**Ribosomal protein 50 S L15**	Protein.synthesis
POPTR_0271s00220	1.882	1.552	-0.51	**Ribosomal protein 50S**	Protein.synthesis
POPTR_0008s12000*	< 1	-	-0.46	**Ribosomal protein 50S L15**	Protein.synthesis
POPTR_0018s11170	2.383	1.293	-1.19	**Ribosomal protein 50S L35**	Protein.synthesis
POPTR_0001s44110	2.272	1.548	-0.86	**Ribosomal protein 50S subunit L24**	Protein.synthesis
Potri.013G136600	2.472	0.679	-0.76	**Ribosomal protein L22**	Protein.synthesis
POPTR_0006s13480	< 1	-	-0.22	**Ribosomal protein 60S L4**	Protein.synthesis
POPTR_0002s05330	1.829	0.623	-0.41	**Ribosome recycling factor**	Protein.synthesis
POPTR_0001s29870*	1.915	1.449	-0.36	Serine carboxypeptidase-like 18	Protein.degradation
POPTR_0018s06210	2.240	1.167	-0.28	Similarity to nucleotide-binding protein	Protein.folding
Co-factor & Vitamine metabolism					
POPTR_0011s00500	2.171	0.849	-0.46	Thiamine thiazole synthase	Co-factor and vitamine metabolism
POPTR_0006s14200*	2.632	1.211	-1.11	Ubiquinone biosynthesis protein	Co-factor and vitamine metabolism
Misc					
POPTR_0008s20590	1.880	1.611	-0.51	Dienelactone hydrolase family protein	Misc
POPTR_0014s05740*	< 1	-	-0.49	PAP fibrillin	Misc.fibrillin
POPTR_0001s40780*	< 1	-	-0.59	Cytochrome P450	Misc.cytochrome P450
Photosynthesis					
POPTR_0002s18740	2.091	1.611	-0.21	**Flavin containing amine oxidoreductase**	Tetrapyrrole synthesis
POPTR_0019s04970	1.951	0.633	-0.38	**NADH-dependent cyclic electron flow 1**	PS.lightreaction
POPTR_0001s40130	2.288	1.331	-0.35	**Uroporphyrinogen decarboxylase**	Tetrapyrrole synthesis
Potri.T058600	< 1	-	-0.27	**Apocytochrome f**	PS.lightreaction
Potri.T171800	1.887	1.294	-0.40	**ATP synthase**	PS.lightreaction

POPTR_0004s01470	2.089	1.611	-0.26	**ATP synthase gamma chain 1**	PS.lightreaction
Potri.011G113500*	1.830	0.757	-0.37	**Cytochrome b**	PS.lightreaction
Potri.T058600	2.513	1.318	-0.27	**Cytochrome b6f complex**	PS.lightreaction
POPTR_0016s02570	1.845	0.662	-0.53	**Didicarboxylate diiron protein**	Tetrapyrrole synthesis
POPTR_0013s14520	1.907	0.931	-0.51	**Photosynthetic electron transfer C**	PS.lightreaction.cytochrome b6/f
POPTR_0003s05110	2.083	1.832	-0.42	**Photosystem I protein**	PS.lightreaction
POPTR_0008s15100	2.176	0.512	-0.71	**Photosystem I 20kD protein**	PS.lightreaction
POPTR_0002s25510	2.016	0.617	-0.70	**Photosystem I reaction center subunit IV**	PS.lightreaction
POPTR_0007s04160	2.034	1.176	-0.47	**Photosystem I subunit**	PS.lightreaction
POPTR_0005s22780*	1.974	1.120	-0.62	**Photosystem II family protein**	PS.lightreaction
POPTR_0005s22830	1.877	0.539	-0.29	**Photosystem II oxygen-evolving complex protein 2 precursor**	PS.lightreaction
POPTR_0007s07780	< 1	-	-0.19	**Photosystem II stability/assembly factor HCF136, putative**	PS.lightreaction
Potri.T006000	2.132	1.368	-1.28	**Ribulose bisphosphate carboxylase large chain**	PS.calvin cycle
POPTR_0012s02510	< 1	-	-0.29	**Thylakoid lumenal 17.4 kDa protein**	PS.lightreaction
POPTR_0004s17530	1.846	0.799	-0.36	**Triosephosphate isomerase**	PS.calvin cycle
Potri.T071000	1.916	1.193	-0.26	**Uroporphyrinogen decarboxylase**	Tetrapyrrole synthesis
Primary metabolism					
POPTR_0015s14380	2.184	0.910	-0.30	Enolase	Glycolysis
POPTR_0010s05400	1.866	0.526	-0.24	Pyruvate phosphate dikinase	Major CHO metabolism.degradation
POPTR_0012s09720	2.063	1.063	-0.53	Adenylate kinase	Nucleotide metabolism
POPTR_0008s16670	2.273	1.166	-0.19	Cytosolic malate dehydrogenase	TCA
POPTR_0013s00930	2.221	0.678	-0.56	Haloacid dehalogenase-like hydrolase family protein	Minor CHO metabolism.trehalose
POPTR_0006s11620	1.974	0.866	-0.43	Starch branching enzyme II	Major CHO metabolism.synthesis.starch
POPTR_0009s13210	1.994	1.080	-0.40	Triosephosphate isomerase	Glycolysis
Redox & Stress					
POPTR_0015s12190	< 1	-	-0.77	**Superoxide dismutase**	Redox.dismutases and catalases
POPTR_0006s00800	1.872	1.710	-0.29	**Cytochrome P450**	Misc
POPTR_0002s01650	1.903	1.588	-0.45	**Glutathione S-transferase F11**	Stress
POPTR_0009s13650	2.156	0.630	-0.36	**L-ascorbate peroxidase**	Redox.ascorbate and glutathione
POPTR_0005s17350	1.951	1.432	-0.33	**L-ascorbate peroxidase, putative**	Redox.ascorbate and glutathione
POPTR_0005s20140	1.821	0.609	-0.50	**L-ascorbate peroxidase, thylakoid**	Redox.ascorbate and glutathione
POPTR_0001s35220	2.007	0.734	-0.44	**Monodehydroascorbate reductase, probable**	Redox.ascorbate and glutathione
Secondary metabolism					
Potri.T104400	1.910	1.281	-0.53	Adenosine-5-phosphosulfate reductase	Secondary metabolism

Potri.007G118400*	< 1	-	-3.25	**Isoprene synthase**	Secondary metabolism.isoprenoids
POPTR_0017s06920	2.884	1.165	-4.01	**Terpenoid cyclase**	Secondary metabolism.isoprenoids
Unknown					
POPTR_0002s22560	< 1	-	-0.26	Unknown	Not assigned
Potri.013G138001	1.951	1.343	-0.30	Unknown	Not assigned
POPTR_0001s19130*	< 1	-	-0.33	Unknown	Not assigned
POPTR_0003s19210*	1.830	1.236	-0.35	Unknown	Not assigned
POPTR_0015s04810*	< 1	-	-0.50	Unknown	Not assigned
POPTR_0009s06450*	1.865	1.324	-0.53	Unknown	Not assigned
POPTR_0014s11390*	2.004	0.858	-0.72	Unknown	Not assigned
Potri.013G049700*	2.141	0.907	-0.73	Unknown	Not assigned
Potri.009G053800*	1.894	0.561	-0.81	2-oxoglutarate/malate translocator	Not assigned
POPTR_0010s16030	2.175	1.164	-0.87	Pop3 peptide	Not assigned
POPTR_0017s01540*	2.380	1.049	-0.96	Class I glutamine amidotransferase-like superfamily protein	Not assigned

Supplemental Table S2. Complete list of LC-MS/MS identified S-nitrosylated proteins in isoprene-emitting (IE) and non-isoprene-emitting (NE) gray poplar leaves (control and ozone). Proteins were extracted from IE and NE leaf samples, subjected to the Biotin switch assay, purified by affinity chromatography and identified by LC-MS/MS. The functional categorization of S-nitrosylated proteins was done according to MapMan BIN (http://ppdb.tc.cornell.edu/dbsearch/mapman.aspx). The protein identification is based on the unique peptide count given in the right column. The prediction of the putative S-nitrosylated cysteine (Cys) within the primary amino acid sequence was performed with the software GPS-SNO 1.0 (Xue et al., 2010).

Accession	Functional category	Annotation	Mascot ion score	Unique peptide count	Predicted S-nitrosylation site (Cys-NO)
POPTR_0005s09860	Amino acid synthesis	Acetylornithine aminotransferase	175.4	4	
POPTR_0017s08060	Amino acid synthesis	HOPW1-1-interacting 1	51.6	1	91, 443
POPTR_0010s05530	Amino acid synthesis	Alanine aminotransferase	211.9	4	226, 417
POPTR_0017s12240	Amino acid synthesis	Pyridoxal phosphate-dependent transferase	291.0	5	6, 8, 19, 240, 334
POPTR_0010s16330	Amino acid synthesis	S-adenosylmethionine synthetase 1	98.5	2	
POPTR_0002s19000	Amino acid synthesis	S-adenosylmethionine synthetase 2	118.0	2	20
POPTR_0013s13150	Amino acid synthesis	O-acetylserine(thiol)lyase	181.3	4	68
POPTR_0001s07870	Amino acid synthesis	Primary amine oxidase	35.6	1	
POPTR_0004s20220	Amino acid degradation	Methionine synthase, vitamin-B12 independent	108.9	2	116
POPTR_0009s07200	Amino acid degradation	Dihydropyrimidinase	111.7	2	
POPTR_0006s25630	Amino acid degradation	Glyoxalase	34.6	1	125
POPTR_0004s01320	Amino acid degradation	Glyoxalase I homolog	52.3	1	
POPTR_0017s08610	Amino acid degradation	S-adenosyl-L-homocysteine hydrolase	88.1	2	42
POPTR_0004s01030	Amino acid degradation	Glycine cleavage T-protein family	119.2	3	
POPTR_0001s26970	Protein synthesis	Ribosomal protein	40.8	1	6
POPTR_0001s06260	Protein synthesis	Ribosomal protein	59.2	1	121
POPTR_0001s35230	Protein synthesis	Ribosomal protein	51.0	1	
POPTR_0019s11310	Protein synthesis	Ribosomal protein	46.9	1	13
POPTR_0001s22620	Protein synthesis	Ribosomal protein	31.6	1	
POPTR_0001s16430	Protein synthesis	Ribosomal protein 40S	36.4	1	38
POPTR_0006s21210	Protein synthesis	Ribosomal protein	49.5	1	

POPTR_0002s09970	Protein synthesis	Ribosomal protein	36.1	1	12
POPTR_0002s06680	Protein synthesis	Ribosomal protein	44.1	1	
POPTR_0001s45810	Protein synthesis	Ribosomal protein 60S	32.6	1	
POPTR_0013s13220	Protein synthesis	Ribosomal protein	39.6	1	229
POPTR_0001s20480	Protein synthesis	Eukaryotic translation initiation factor 4A1	132.5	3	
POPTR_0004s23490	Protein synthesis	Elongation factor 1-gamma 1, putative	43.8	1	
POPTR_0006s13310	Protein synthesis	Elongation factor Tu family protein	110.1	2	
POPTR_0001s08770	Protein synthesis	RAB GTPase homolog E1B	359.2	5	
POPTR_0007s08390	Protein synthesis	Ribosomal protein	129.2	3	131
POPTR_0003s11300	Protein synthesis	Translation elongation factor	78.1	2	635
POPTR_0006s12560	Protein targeting	Plastid transcriptionally active 4	35.1	1	
POPTR_0006s10930	Protein targeting	Vacuolar sorting receptor homolog 1	36.9	1	321
POPTR_0006s19810	Protein degradation	Cytosol aminopeptidase	42.2	1	
POPTR_0018s11600	Protein degradation	Cytosol aminopeptidase	141.1	3	
POPTR_0002s02010	Protein degradation	Subtilisin-like serine endopeptidase family protein	129.4	3	390, 655
POPTR_0001s40300	Protein degradation	Ubiquitin-conjugating enzyme 36	39.2	1	
POPTR_0001s40780	Protein degradation	F-box family protein	34.3	1	30
POPTR_0014s02410	Protein degradation	Granulin repeat cysteine protease family protein	143.2	2	161, 200
POPTR_0012s10770	Protein degradation	CLPC homologue 1	157.0	4	58, 405
POPTR_0002s01320	Protein degradation	FTSH protease 1	129.4	3	
POPTR_0004s14960	Protein degradation	Presequence protease 1	89.8	2	760
POPTR_0018s14840	Protein folding	Activator of Hsp90	31.5	1	93
POPTR_0010s14660	Protein folding	Chaperone protein htpG family	148.5	3	67, 170
POPTR_0018s07410	Protein folding	Chaperonin	77.0	2	
POPTR_0009s01470	Protein folding	Chaperonin	278.1	6	14
POPTR_0008s05470	Protein folding	Heat shock protein 70	254.8	5	319, 326, 609
POPTR_0010s21270	Protein folding	Heat shock protein 70	201.7	4	319, 326, 609
POPTR_0004s23310	Protein folding	Heat shock protein 70, chloroplast	335.5	7	
POPTR_0001s47020	Protein folding	Heat shock protein 90	243.3	5	190
POPTR_0001s03980	Protein folding	TCP-1/cpn60 chaperonin family protein	460.9	7	
POPTR_0003s20870	Protein folding	TCP-1/cpn60 chaperonin family protein	519.8	8	
POPTR_0007s07780	Protein folding	Photosystem II stability/assembly factor	31.7	1	15
POPTR_0008s00350	C1-metabolism	Serine transhydroxymethyltransferase 1	204.1	4	129, 367
POPTR_0016s02620	Cell wall & Organization	Alpha-L-arabinofuranosidase	37.8	1	8

POPTR_0006s02850	Cell wall & Organization	Alpha-L-arabinofuranosidase	68.8	1	
POPTR_0006s12740	Cell wall & Organization	Cell division protein 48 (CDC48)	50.7	1	428
POPTR_0001s37650	Cell wall & Organization	Fasciclin-like arabinogalactan 1	35.5	1	
POPTR_0001s09910	Cell wall & Organization	Glycosyl hydrolase	32.6	1	
POPTR_0013s01500	Cell wall & Organization	Plant invertase/pectin methylesterase inhibitor superfamily	32.2	1	75
POPTR_0004s11700	Cell wall & Organization	Reversibly glycosylated polypeptide 2	33.4	1	
POPTR_0001s09180	Cell wall & Organization	Tubulin, beta chain	32.3	1	12
POPTR_0001s29670	Cell wall & Organization	Tubulin/FtsZ family protein	108.8	2	20, 347
POPTR_0001s25630	Co-factor & Vitamine metabolism	ThiaminC	71.9	1	
POPTR_0004s01990	Co-factor & Vitamine metabolism	Thiazole biosynthetic enzyme	335.9	5	101
POPTR_0005s11300	Co-factor & Vitamine metabolism	3-Dehydroquinate synthase, putative	30.8	1	303
POPTR_0008s07710	Co-factor & Vitamine metabolism	4-Nitrophenylphosphatase, putative	58.5	1	
POPTR_0015s08540	Fermentation	Aldehyde dehydrogenase	32.6	1	181, 274
POPTR_0009s08520	Gluconeogenesis	NAD-malate dehydrogenase, peroxisomal	76.1	2	150
POPTR_0010s16120	Glycolysis	Dihydrolipamide dehydrogenase	603.7	9	
POPTR_0008s10020	Glycolysis	Dihydrolipoamide dehydrogenase	1184.4	17	
POPTR_0006s11800	Glycolysis	Enolase	87.9	2	409
POPTR_0015s14380	Glycolysis	Enolase	85.6	2	409
POPTR_0008s08340	Glycolysis	Glyceraldehyde-3-phosphate dehydrogenase	31.3	1	236, 240
POPTR_0012s09570	Glycolysis	Glyceraldehyde-3-phosphate dehydrogenase	170.0	2	154
POPTR_0002s22600	Glycolysis	Glyceraldehyde-3-phosphate dehydrogenase	369.1	7	344
POPTR_0008s08400	Glycolysis	Phosphoglycerate kinase	138.8	3	
POPTR_0008s05640	Glycolysis	Triosephosphate isomerase	103.1	2	13, 127
POPTR_0004s07280	Glycolysis	UDP-glucose pyrophosphorylase 2	91.0	2	
POPTR_0017s01390	Glycolysis	UDP-glucose pyrophosphorylase 2	120.2	2	
POPTR_0012s06940	Hormone metabolism	Leucine-rich repeat protein kinase family protein	36.7	1	598, 1026
POPTR_0004s10240	Lipid metabolism	Allene oxide cyclase	39.2	1	64
POPTR_0001s32660	Lipid metabolism	Acyl-transferase family protein	36.7	1	4
POPTR_0002s09330	Lipid metabolism	Acetyl-CoA carboxylase 1	43.3	1	340, 1176, 2071
POPTR_0018s11820	Major CHO-metabolism	Aldehyde dehydrogenase	192.2	4	
POPTR_0014s07940	Major CHO-metabolism	Beta-amylase, putative	44.8	1	285, 326
POPTR_0008s19960	Major CHO-metabolism	ADP glucose pyrophosphorylase large subunit 1	35.1	1	
POPTR_0006s10480	Metal handling	Ferretin 1	144.0	3	100
POPTR_0016s13260	Metal handling	Ferritin	85.1	2	87

POPTR_0016s14950	Metal handling	2,3-Bisphosphoglycerate-independent phosphoglycerate mutase, putative	50.5	1	357
POPTR_0001s23310	Misc	Beta-glucosidase	536.8	8	
POPTR_0005s25160	Misc	Cytochrome P450	62.3	2	81
POPTR_0003s12920	Misc	Cytochrome P450	32.0	1	
POPTR_0012s10830	Misc	Glycosyl hydrolase	117.5	3	69, 444, 472
POPTR_0016s14310	Misc	Oxidoreductase, zinc-binding dehydrogenase	140.9	3	
POPTR_0005s25480	Misc	Purple acid phosphatase 12	95.6	2	
POPTR_0019s10280	Misc	Rieske (2Fe-2S) domain-containing protein	54.9	1	
POPTR_0002s17040	Misc	Thylakoid rhodanese-like protein	45.4	1	16, 52
POPTR_0008s12550	Mit. electron transport	ATP synthase alpha/beta	139.0	3	
POPTR_0006s03660	N-metabolism	Glutamate synthase 1	1381.6	22	
POPTR_0016s03630	N-metabolism	Glutamate synthase 1	971.7	16	
POPTR_0008s03800	Nucleotide metabolism	Adenosine kinase 2	73.9	2	
POPTR_0001s26020	Photosynthesis	Alanine glyoxylate aminotransferase	453.5	8	
POPTR_0002s08280	Photosynthesis	Aldolase superfamily protein	34.2	1	44, 71, 404
POPTR_0011s11390	Photosynthesis	Aldolase-type TIM barrel family protein	273.6	5	
POPTR_0006s28990	Photosynthesis	ATPase	70.0	2	33, 332, 440
POPTR_0005s24670	Photosynthesis	ATPase	30.5	1	
POPTR_0004s01470	Photosynthesis	ATPase, F1 complex, gamma subunit	185.0	3	3
POPTR_0015s07330	Photosynthesis	D-ribulose-5-phosphate-3-epimerase	73.9	1	12
POPTR_0005s11500	Photosynthesis	Ferredoxin-NADP(+)-oxidoreductase 1	368.1	6	163
POPTR_0007s09630	Photosynthesis	Ferredoxin-NADP(+)-oxidoreductase 2	249.6	4	163
POPTR_0004s16920	Photosynthesis	Fructose-bisphosphate aldolase 2	482.3	7	34, 275
POPTR_0015s11320	Photosynthesis	Glutamate-1-semialdehyde-2,1-aminomutase 2	76.8	2	
POPTR_0002s00840	Photosynthesis	Glyceraldehyde-3-phosphate dehydrogenase	314.1	7	17, 70, 265
POPTR_0006s24570	Photosynthesis	Glycine decarboxylase complex, P subunit	65.9	1	266
POPTR_0006s09550	Photosynthesis	High cyclic electron flow 1	95.1	2	
POPTR_0007s07680	Photosynthesis	Hydroxymethylbilane synthase	52.5	1	8, 24
POPTR_0004s18190	Photosynthesis	Hydroxypyruvate reductase	114.8	3	
POPTR_0006s10040	Photosynthesis	Light harvesting complex photosystem II	49.7	1	
POPTR_0008s06720	Photosynthesis	Light harvesting complex photosystem II	54.7	1	
POPTR_0001s21740	Photosynthesis	Light harvesting complex photosystem II	56.4	1	
POPTR_0001s08420	Photosynthesis	PGR5-like A	49.3	1	306
POPTR_0008s08410	Photosynthesis	Phosphoglycerate kinase	426.3	9	

POPTR_0010s17860	Photosynthesis	Phosphoglycerate kinase	392.2	8	
POPTR_0001s01630	Photosynthesis	Phosphoribulokinase	185.9	3	53
POPTR_0003s09830	Photosynthesis	Phosphoribulokinase	343.7	6	
POPTR_0016s11450	Photosynthesis	Photosynthetic electron transfer A	105.1	2	280
POPTR_0001s11600	Photosynthesis	Photosystem I reaction center, subunit III	40.4	1	
POPTR_0008s15100	Photosynthesis	Photosystem I subunit D-2	32.1	1	
POPTR_0002s08410	Photosynthesis	Photosystem II 22 kDa protein	66.4	1	
POPTR_0005s22830	Photosynthesis	Photosystem II subunit P-1	95.9	2	
POPTR_0019s14050	Photosynthesis	Photosystem II, assembly	102.6	2	60, 287
POPTR_0002s01740	Photosynthesis	Plastocyanin 1	47.1	1	
POPTR_0004s05270	Photosynthesis	Protochlorophyllide reductase	46.6	1	352
POPTR_0005s13860	Photosynthesis	PS II oxygen-evolving complex 1	254.5	5	
POPTR_0007s12070	Photosynthesis	PS II oxygen-evolving complex 1	309.9	6	
POPTR_0013s03700	Photosynthesis	Ribose 5-phosphate isomerase, type A protein	99.1	2	
POPTR_2555s00200	Photosynthesis	Ribulose bisphosphate carboxylase large chain	135.8	2	
POPTR_0008s05870	Photosynthesis	RuBisCO activase	341.3	7	454
POPTR_0010s20810	Photosynthesis	RuBisCO activase	1158.0	19	453
POPTR_0010s20060	Photosynthesis	Sedoheptulose-1,7-bisphosphatase	89.8	2	96, 151
POPTR_0005s04090	Photosynthesis	Thylakoid lumen 18.3 kDa protein	54.6	1	
POPTR_0002s14730	Photosynthesis	Transketolase	230.7	6	
POPTR_0004s17530	Photosynthesis	Triosephosphate isomerase	97.8	2	184
POPTR_0005s17350	Redox	Ascorbate peroxidase	36.5	1	43
POPTR_0009s02070	Redox	Ascorbate peroxidase	74.6	2	32
POPTR_0002s01080	Redox	Catalase	104.7	2	
POPTR_0011s14410	Redox	Glutathione S-transferase	34.1	1	66
POPTR_0006s11570	Redox	Monodehydroascorbate reductase	96.2	2	
POPTR_0006s13980	Redox	Peroxiredoxin	31.1	1	
POPTR_0006s22130	Redox	Peroxiredoxin B	95.7	2	3, 116
POPTR_0002s08260	Redox	Protein disulphide isomerase	75.6	2	10, 58, 61, 403, 406
POPTR_0009s01920	Redox	Thioredoxin	44.5	1	131, 134, 470, 473
POPTR_0013s10250	Redox	Thioredoxin	134.9	3	104
POPTR_0001s44990	Redox	Thioredoxin-dependent peroxidase 1	36.4	1	
POPTR_0012s09200	RNA	31-kDa RNA binding protein	152.3	3	73
POPTR_0015s09810	RNA	31-kDa RNA binding protein	32.6	1	

POPTR_0005s23110	RNA	Chloroplast stem-loop binding protein of 41 kDa	82.9	2	16, 92
POPTR_0005s01370	RNA	RNA binding, chloroplast	136.5	2	
POPTR_0013s00760	RNA	RNA binding, chloroplast	235.0	4	
POPTR_0001s12570	RNA	U2 small nuclear ribonucleoprotein A	33.4	1	
POPTR_0009s07040	S-assimilation	Chloroplast NIFS-like cysteine desulfurase	67.2	1	
POPTR_0004s01220	S-assimilation	APS reductase 3	31.6	1	
POPTR_0009s01900	Secondary Metabolism	4-Hydroxy-3-methylbut-2-en-1-yl diphosphate synthase	37.2	1	180
POPTR_0002s01990	Secondary metabolism	Cinnamyl alcohol dehydrogenase-like protein	47.9	1	
POPTR_0006s12870	Secondary Metabolism	Phenylalanine-amino lyase	104.2	2	18, 560, 691
POPTR_0001s39630	Secondary Metabolism	Polyphenol oxidase	156.1	3	
POPTR_0001s39950	Secondary Metabolism	Polyphenol oxidase	131.0	2	
POPTR_0015s06230	Signaling	Calcium sensing receptor, extracellular	54.6	1	
POPTR_0001s22980	Signaling	Calmodulin	36.1	1	
POPTR_0005s01850	Signaling	Calreticulin	53.4	1	166
POPTR_0002s10000	Signaling	General regulatory factor	171.2	3	103
POPTR_0004s10120	Signaling	General regulatory factor	114.2	2	90
POPTR_0010s10790	Signaling	Phytosulfokin receptor 1	31.2	1	70, 399
POPTR_0019s12370	Stress	EP3 chitinase	54.0	1	171
POPTR_0001s29350	Stress	Heat shock protein 80	225.1	5	
POPTR_0019s13000	Stress	Tir-nbs-lrr resistance protein	33.3	1	116
POPTR_0007s04700	Stress	UVB-resistance protein (UVR8)	40.3	1	
POPTR_0005s10990	TCA	Aconitase 1	73.6	2	102
POPTR_0001s34950	TCA	Carbonic anhydrase	62.6	2	171, 278
POPTR_0001s38560	TCA	Lactate/malate dehydrogenase family protein	32.1	1	
POPTR_0008s16670	TCA	Lactate/malate dehydrogenase family protein	77.5	2	
POPTR_0008s03160	TCA	Malate dehydrogenase	35.3	1	418
POPTR_0012s03440	Transport	Organic cation/carnitine transporter	37.2	1	
POPTR_0001s26960	Transport	Unknown	36.4	1	239
POPTR_0005s01840	Transport	Vacuolar H+-translocating inorganic pyrophosphatase	45.8	1	123
POPTR_0008s07920	Transport	Vps51/Vps67 family (components of vesicular transport) protein	36.5	1	348, 56, 883
POPTR_0002s25620	Not assigned	Alcohol dehydrogenase	52.5	1	10, 271
POPTR_0015s09990	Not assigned	Haloacid dehalogenase-like hydrolase (HAD)	40.5	1	
POPTR_0004s04730	Not assigned	MAC/Perforin domain-containing protein	32.9	1	
POPTR_0001s40580	Not assigned	PIF1 helicase	30.6	1	381

POPTR_0004s07900	Not assigned	Ran GTPase binding protein	33.7	1	344, 462, 471
POPTR_0015s06950	Not assigned	Unknown	33.8	1	
POPTR_0008s07430	Not assigned	Unknown	31.1	1	
POPTR_0017s06680	Not assigned	Unknown	33.2	1	
POPTR_0015s06140	Not assigned	Unknown	30.6	1	14, 174, 478
POPTR_0010s20020	Not assigned	Unknown	42.6	1	159
POPTR_0003s18370	Not assigned	Unknown	117.6	2	11
POPTR_0003s02860	Not assigned	Unknown	45.2	1	
POPTR_0011s01315	Not assigned	Unknown	67.6	2	17, 90, 438, 534, 558
POPTR_0011s15110	Not assigned	Unknown	168.3	3	12
POPTR_0259s00200	Not assigned	Unknown	53.7	1	744, 857, 914
POPTR_0010s24370	Not assigned	Vacuolar sorting-associated protein	35.0	1	59, 342

Supplemental Table S3. Proteins, that discriminately separate non–isoprene-emitting (NE) from isoprene-emitting (IE) gray poplar samples (n = 6 biological replicates per individual line: WT, EV, Ra1, Ra2) in the control (C) and ozone (O) treatment in the OPLS of the S-nitroso proteome (*P* = 0.0028; CV-ANOVA). Proteins showing VIP (Variable Importance in the Projection) scores > 1 and uncertainty bars of jackknifing method (SE) smaller than the respective VIP value were defined as discriminant proteins. Additionally, log2 fold changes and *P*-values (*t*-test) are given for the main treatment effect (IE and NE combined), for the main genotype effect (C and O combined), for the treatment effects within the IE genotype or within the NE genotype, and for the genotype effect within C or within O. Significant *P*-values are highlighted in bold (*t*-test, $P \leq 0.05$). * LC-MS/MS quantification based on one unique peptide.

					***P*- value (*t*-test)**						**Log fold change**					
						IE	**NE**		**C**	**O**	**Main treat. effect**	**IE**	**NE**	**Main genotype effect**	**C**	**O**
Accession	**VIP score**	**SE**	**Annotation**	**Functional category**	**Main treat. effect**	**O vs. C**	**O vs. C**	**Main geno. effect**	**IE vs. NE**	**IE vs. NE**	**Log2 O/C**	**Log2 O_{IE}/C_{IE}**	**Log2 O_{NE}/C_{NE}**	**Log2 NE/IE**	**Log2 NE_C/IE_C**	**Log2 NE_O/IE_O**
POPTR_0017s08060*	1.21	0.99	Acetylornithine transaminase (ACOAT)	Amino acid + Protein metabolism	1.000	1.000	1.000	1.000	1.000	1.000	0.0	0.0	0.0	0.0	0.0	0.0
POPTR_0010s14660	1.17	1.16	Chaperone protein htpG family	Amino acid + Protein metabolism	**0.004**	0.250	**0.002**	0.392	0.603	0.092	1.1	0.6	1.6	0.3	-0.4	0.6
POPTR_0018s07410	1.66	0.87	Chaperonin 20	Amino acid + Protein metabolism	**0.006**	**0.026**	0.061	0.428	0.445	0.719	-0.9	-0.9	-0.8	-0.2	-0.2	-0.2
POPTR_0002s01320	1.16	0.96	FtsH extracellular protease	Amino acid + Protein metabolism	0.142	0.416	0.199	0.079	0.301	0.134	0.3	0.3	0.4	0.4	0.4	0.4
POPTR_0004s01030	1.73	0.60	Glycine cleavage T-protein family	Amino acid + Protein metabolism	**0.002**	0.260	**0.001**	0.098	0.950	**0.021**	1.4	0.8	1.8	0.7	-0.1	0.9
POPTR_0004s01320*	1.49	0.78	Glyoxalase I homolog	Amino acid + Protein metabolism	**0.010**	0.285	**0.008**	0.059	0.630	**0.030**	0.7	0.5	0.9	0.5	0.2	0.7
POPTR_0014s02410	1.66	1.22	Granulin repeat cysteine protease	Amino acid + Protein metabolism	**0.003**	**0.013**	0.064	0.444	0.358	0.870	0.6	0.8	0.5	0.1	0.3	0.0
POPTR_0004s23310	1.37	0.67	Heat shock protein 70 (HSP70-2), chloroplast	Amino acid + Protein metabolism	**0.049**	0.312	0.068	0.061	0.350	0.079	0.4	0.3	0.5	0.4	0.3	0.4
POPTR_0001s47020*	1.50	1.14	Heat shock protein 90 (HSP90)	Amino acid +	**0.020**	0.139	0.056	0.407	0.408	0.728	-0.9	-0.9	-1.0	0.3	0.3	0.3

				Protein metabolism													
POPTR_0006s19810*	1.48	0.83	Leucyl aminopeptidase (LAP2)	Amino acid + Protein metabolism	**0.009**	0.681	**0.001**	**0.004**	0.491	**0.001**	0.6	0.2	0.9	0.7	0.3	1.0
POPTR_0004s20220	1.63	0.62	Methionine synthase, vitamin-B12 independent	Amino acid + Protein metabolism	**0.006**	0.129	**0.012**	0.446	0.967	0.267	0.5	0.4	0.7	0.1	0.0	0.2
POPTR_0004s14960	1.47	0.56	Presequence protease 1	Amino acid + Protein metabolism	**0.007**	**0.020**	0.096	0.697	0.512	0.915	0.6	0.8	0.5	0.1	0.2	0.0
POPTR_0017s12240	1.84	1.67	Pyridoxal phosphate (PLP)-dependent transferase	Amino acid + Protein metabolism	**0.002**	**0.011**	**0.029**	0.685	0.604	0.956	1.1	1.3	1.0	0.1	0.4	0.0
POPTR_0006s21210*	1.03	0.61	Ribosomal protein 5A	Amino acid + Protein metabolism	0.157	0.620	**0.018**	0.576	0.267	0.066	1.0	-0.6	2.9	0.4	-1.9	1.5
POPTR_0001s35230*	1.73	0.83	Ribosomal protein L12-A	Amino acid + Protein metabolism	**0.001**	0.898	**0.000**	0.062	0.252	**0.001**	1.4	0.1	2.5	0.7	-1.0	1.4
POPTR_0013s13220*	1.07	0.78	Ribosomal protein L5 B	Amino acid + Protein metabolism	0.112	0.556	0.095	0.926	0.615	0.528	0.5	0.3	0.8	0.0	-0.3	0.2
POPTR_0010s16330*	1.38	0.84	S-adenosylmethionine synthetase 1 (SAM1)	Amino acid + Protein metabolism	**0.004**	0.336	**0.002**	0.513	0.418	0.092	0.9	0.4	1.4	0.2	-0.4	0.5
POPTR_0003s20870	1.38	0.61	TCP-1/cpn60 chaperonin family protein	Amino acid + Protein metabolism	**0.047**	0.261	**0.081**	0.125	0.440	0.156	0.4	0.3	0.4	0.3	0.2	0.3
POPTR_0006s12740*	1.45	1.08	Cell division protein 48 (CDC48)	Cell	**0.013**	0.708	**0.002**	0.096	0.754	**0.011**	1.8	0.5	2.7	1.1	-0.6	1.6
POPTR_0004s01470	1.90	0.53	ATPase, F1 complex, gamma subunit protein	Photosynthesis	**0.001**	**0.032**	**0.004**	0.427	0.929	0.303	0.7	0.6	0.8	0.1	0.0	0.2
POPTR_0015s07330*	1.79	0.27	D-ribulose-5-phosphate-3-epimerase (RPE)	Photosynthesis	0.067	0.056	0.487	0.078	0.063	0.521	0.6	1.1	0.3	0.6	1.1	0.2
POPTR_0005s11500	1.41	0.67	Ferredoxin-NADP(+)-oxidoreductase 1	Photosynthesis	**0.002**	0.115	**0.003**	0.330	0.133	0.878	0.6	0.4	0.9	-0.2	-0.5	0.0
POPTR_0001s08420*	1.55	0.94	Ferredoxin-plastoquinone reductase (PGR5-like A)	Photosynthesis	**0.037**	0.673	**0.002**	0.052	0.587	**0.002**	0.5	-0.1	0.9	0.4	-0.2	0.9
POPTR_0015s11320	1.55	0.96	Glutamate-1-semialdehyde-2,1-aminomutase 2 (GSA)	Photosynthesis	**0.042**	0.302	0.057	**0.050**	0.331	0.064	0.5	0.4	0.6	0.5	0.4	0.5
POPTR_0002s00840	2.39	1.06	Glyceraldehyde-3-phosphate dehydrogenase, subunit B	Photosynthesis	**0.000**	0.078	**0.000**	0.131	0.938	**0.032**	2.6	2.0	3.1	0.8	-0.2	0.9
POPTR_0007s07680*	2.05	0.52	Hydroxymethylbilane synthase	Photosynthesis	**0.001**	0.063	**0.003**	0.086	0.571	0.062	1.2	1.0	1.2	0.5	0.4	0.6
POPTR_0004s05270*	1.32	0.79	Magnesium chelatase subunit of protochlorophyllide reductase	Photosynthesis	0.065	0.258	0.127	0.091	0.311	0.157	0.6	0.6	0.6	0.5	0.5	0.5
POPTR_0003s09830	1.63	0.84	Phosphoribulokinase	Photosynthesis	**0.023**	0.358	**0.019**	**0.002**	0.108	**0.004**	0.4	0.2	0.4	0.5	0.4	0.6
POPTR_0001s11600*	1.08	0.67	Photosystem I reaction center, subunit III	Photosynthesis	0.166	0.815	0.088	0.479	0.791	0.212	0.3	0.1	0.6	0.2	-0.1	0.4

POPTR_0002s08410*	1.27	1.20	Photosystem II 22 kDa protein	Photosynthesis	0.079	0.465	0.075	0.064	0.422	0.065	0.4	0.3	0.5	0.4	0.3	0.5
POPTR_0005s22830	1.04	0.89	Photosystem II subunit P-1 (PsbP-1)	Photosynthesis	0.293	0.601	0.331	0.287	0.594	0.326	0.5	0.4	0.5	0.5	0.4	0.5
POPTR_0013s03700	1.79	0.59	Ribose 5-phosphate isomerase, type A protein	Photosynthesis	**0.008**	0.115	**0.021**	**0.025**	0.217	**0.045**	0.6	0.6	0.6	0.5	0.5	0.5
POPTR_0008s05870	1.30	1.12	Rubisco activase	Photosynthesis	**0.043**	0.651	**0.017**	0.356	0.690	0.097	0.7	0.2	1.0	0.3	-0.2	0.6
POPTR_0010s20810	2.15	0.91	Rubisco activase	Photosynthesis	**0.000**	**0.005**	**0.012**	**0.004**	**0.022**	**0.047**	1.1	1.7	0.8	0.8	1.5	0.6
POPTR_0010s20060	2.28	0.29	Sedoheptulose-bisphosphatase	Photosynthesis	**0.000**	0.060	**0.000**	**0.000**	0.666	**0.000**	1.3	0.7	1.7	0.9	0.2	1.2
POPTR_0002s14730	1.47	0.85	Transketolase	Photosynthesis	0.052	0.133	0.188	0.128	0.235	0.319	0.3	0.4	0.3	0.2	0.3	0.2
POPTR_0005s10990	2.03	1.24	Aconitase 1 (ACO1)	Primary Metabolism	**0.000**	**0.027**	**0.001**	**0.044**	0.478	**0.031**	1.2	1.1	1.2	0.5	0.4	0.6
POPTR_0015s08540*	2.08	0.66	Aldehyde dehydrogenase 2B4 (ALDH2)	Primary Metabolism	**0.000**	**0.041**	**0.000**	**0.002**	0.352	**0.000**	3.0	4.8	2.6	1.7	3.7	1.5
POPTR_0006s02850*	1.53	0.70	Alpha-L-arabinofuranosidase (ARA)	Primary Metabolism	0.140	0.264	0.319	**0.019**	0.076	0.096	0.4	0.6	0.3	0.7	0.9	0.6
POPTR_0001s34950	1.51	0.66	Carbonic anhydrase 1	Primary Metabolism	**0.013**	0.351	**0.009**	0.447	0.681	0.145	0.4	0.2	0.6	0.1	-0.1	0.3
POPTR_0015s14380*	1.19	1.09	Enolase (ENO)	Primary Metabolism	0.152	0.118	0.642	0.272	0.183	0.828	0.4	0.8	0.2	0.3	0.7	0.1
POPTR_0008s16670	1.36	1.08	Malate dehydrogenase	Primary Metabolism	0.240	0.936	0.088	**0.008**	0.258	**0.006**	0.3	0.0	0.6	0.9	0.5	1.2
POPTR_0009s08520	1.17	0.98	NAD-malate dehydrogenase 2, peroxisomal	Primary Metabolism	0.137	0.262	0.313	0.795	0.808	0.900	0.5	0.6	0.5	0.1	0.1	0.1
POPTR_0008s05640	1.61	0.46	Triosephosphate isomerase	Primary Metabolism	**0.005**	0.883	**0.000**	**0.029**	0.699	**0.001**	0.8	0.1	1.3	0.6	-0.2	1.0
POPTR_0005s17350*	1.27	1.10	Ascorbate peroxidase (APX)	Redox & Signaling	**0.000**	0.910	**0.000**	**0.014**	0.242	**0.000**	1.2	0.1	2.1	0.7	-0.7	1.3
POPTR_0002s01080	1.55	0.80	Catalase 2 (CAT2)	Redox & Signaling	**0.012**	0.358	**0.007**	**0.031**	0.545	**0.015**	0.8	0.5	1.0	0.6	0.3	0.8
POPTR_0002s08260	1.22	0.32	Protein disulphide isomerase	Redox & Signaling	0.057	0.154	0.185	0.958	0.928	0.987	0.5	0.5	0.5	0.0	0.0	0.0
POPTR_0001s44990*	1.18	1.00	Thioredoxin-dependent peroxidase 1 (PrxII B)	Redox & Signaling	0.229	0.978	0.090	**0.010**	0.286	**0.009**	0.3	0.0	0.5	0.8	0.5	1.0
POPTR_0002s01990*	1.82	0.53	Cinnamyl alcohol dehydrogenase-like protein (CAD)	Second.metabolism	**0.002**	0.463	**0.000**	**0.010**	0.817	**0.001**	1.1	0.4	1.5	1.0	0.2	1.5
POPTR_0008s03810	1.14	0.48	Phenylalanine ammonia-lyase 2 (PAL)	Second.metabolism	**0.040**	**0.030**	0.320	0.158	0.536	0.331	-1.4	-1.7	-0.8	-0.8	-1.1	-0.1

POPTR_0007s04700*	1.89	1.18	UVB-resistance protein (UVR8)	Stress	**0.001**	0.200	**0.000**	**0.025**	0.903	**0.003**	4.1	3.5	4.3	1.7	1.0	1.7
POPTR_0016s02620*	1.36	1.07	Alpha-N-arabinofuranosidase 1 (ARA)	Structural Function	**0.001**	**0.020**	**0.003**	**0.002**	**0.043**	**0.008**	1.1	1.4	0.9	0.9	1.2	0.8
POPTR_0001s37650*	1.61	0.58	Fasciclin-like arabinogalactan 1	Structural Function	**0.010**	0.120	**0.026**	**0.026**	0.206	**0.050**	0.6	0.5	0.6	0.5	0.4	0.5
POPTR_0015s06950*	1.18	1.04	Protein of unknown function (DUF1118)	Not assigned	**0.002**	**0.047**	**0.010**	**0.036**	0.237	0.064	1.2	1.4	1.1	0.8	1.0	0.7
POPTR_0005s11300*	1.33	1.08	3-Dehydroquinate synthase, putative	Other	0.064	0.233	0.137	0.195	0.440	0.281	0.4	0.4	0.4	0.3	0.3	0.3
POPTR_0012s10830	2.09	1.06	Alpha-mannosidase	Other	**0.000**	**0.007**	**0.003**	0.066	0.247	0.135	0.9	1.0	0.9	0.4	0.5	0.3
POPTR_0005s23110	1.50	0.50	Chloroplast stem-loop binding protein of 41 kDa	Other	**0.033**	0.399	**0.028**	0.182	0.826	0.099	0.5	0.3	0.7	0.3	0.1	0.5
POPTR_0006s10480	1.50	0.86	Ferretin 1	Other	0.057	0.315	0.082	**0.017**	0.167	**0.037**	0.7	0.7	0.7	0.9	0.9	0.9
POPTR_0005s01370*	1.21	0.55	NAD-dependent epimerase/dehydratase	Other	**0.048**	0.373	0.052	0.508	0.920	0.304	0.4	0.3	0.5	0.1	0.0	0.2
POPTR_0016s14310	1.54	0.74	NADPH dependent ketone reductase (AOR)	Other	**0.013**	0.384	**0.008**	0.106	0.871	**0.037**	0.4	0.2	0.6	0.3	0.0	0.4
POPTR_0009s07040*	2.33	0.83	NIFS-like cysteine desulfurase, chloroplastic	Other	**0.000**	**0.029**	**0.001**	0.061	0.570	**0.037**	1.7	1.6	1.7	0.7	0.6	0.7
POPTR_0001s26960*	1.04	0.85	Protein of unknown function (DUF3411)	Other	0.180	0.411	0.273	0.246	0.491	0.335	0.3	0.3	0.3	0.3	0.3	0.3
POPTR_0001s25630*	1.92	0.74	Thiamine biosynthesis protein (ThiC)	Other	**0.000**	0.179	**0.000**	0.061	0.735	**0.005**	1.5	0.8	2.1	0.6	-0.3	1.0

Supplemental Table S4. Constitutively S-nitrosylated proteins, which are differentially abundant in isoprene-emitting (IE: WT/EV, n = 6 biological replicates per line) and non-emitting (NE: Ra1/Ra2, n = 6 biological replicates per line) gray poplar under steady-state conditions (only control samples). Functional categorization was done according to MapMan BIN (http://ppdb.tc.cornell.edu/dbsearch/searchacc.aspx). *LC-MS/MS quantification based on one unique peptide.

Accession	VIP score	SE	Log2 NE_C/IE_C	Annotation	MapMan BIN category	*P*-value (*t*-test)
POPTR_0010s20810	2.15	0.91	1.5	RuBisCO activase	PS/calvin cyle	0.004
POPTR_0016s02620*	1.36	1.07	1.2	Alpha-N-arabinofuranosidase	Cell wall	0.050
POPTR_0001s01630*	< 1	-	1.3	Phosphoribulokinase	PS/calvin cyle	0.004
POPTR_0010s21270*	< 1	-	1.0	Heat shock protein 70	Protein folding	0.023
POPTR_0013s13150	< 1	-	0.8	O-acetylserine(thiol)lyase	Amino acid metabolism	0.004
POPTR_0019s14050	< 1	-	-0.6	Photosystem II, assembly protein	PS/lightreaction	0.003

Supplermental Table S5. S-nitrosylated proteins, which are differentially abundant in ozone and control treatments of (A) isoprene-emitting (IE: WT/EV, n = 6 biological replicates per line) and (B) non-isoprene-emitting (NE: Ra1/Ra2, n = 6 biological replicates per line) gray poplar samples. Functional categorization was done according to MapManBIN (http://ppdb.tc.cornell.edu/dbsearch/searchacc.aspx). *LC-MS/MS quantification based on one unique peptide.

Table S5A IE genotypes

Accession	VIP score	SE	Log2 O_{IE}/C_{IE}	Annotation	MapMan BIN category	*P*-value (*t*-test)
POPTR_0005s10990	2.03	1.24	1.1	Aconitase 1 (ACO1)	TCA / org.transformation	0.035
POPTR_0017s12240	1.84	1.67	1.3	Pyridoxal phosphate-dependent transferases superfamily protein	Amino acid metabolism/synthesis	0.009
POPTR_0016s02620*	1.36	1.07	1.4	Alpha-N-arabinofuranosidase 1	Cell wall	0.037
POPTR_0015s08540*	2.08	0.66	4.8	Aldehyde dehydrogenase 2B4 (ALDH2)	Fermentation	0.023
POPTR_0012s10830	2.09	1.06	1.0	Alpha-mannosidase	Misc/gluco-, galacto- and mannosidases	0.003
POPTR_0015s06950*	1.18	1.04	1.4	Protein of unknown function (DUF1118)	Not assigned/unknown	0.098
POPTR_0014s02410	1.66	1.22	0.8	Granulin repeat cysteine protease family protein	Protein/degradation	0.016
POPTR_0004s14960	1.47	0.56	0.8	Presequence protease 1	Protein/degradation	0.071
POPTR_0018s07410	1.66	0.87	-0.9	Chaperonin 20	Protein/folding	0.072
POPTR_0001s47020*	< 1	-	-0.9	Heat shock protein 90	Protein/folding	0.006
POPTR_0008s05470*	< 1	-	1.3	Heat shock protein 70	Protein/folding	0.028
POPTR_0010s20810	2.15	0.91	1.7	RuBisCO activase	PS/calvin cyle	0.002
POPTR_0015s07330*	< 1	-	1.1	D-ribulose-5-phosphate-3-epimerase	PS/calvin cyle	0.016
POPTR_0004s01470	1.90	0.53	0.6	ATPase, F1 complex, gamma subunit protein	PS/lightreaction	0.072
POPTR_0009s07040*	2.33	0.83	1.6	NIFS-like cysteine desulfurase, chloroplastidic	S-assimilation	0.078
POPTR_0008s03810	1.14	0.48	-1.7	Phenylalanine ammonia-lyase 2 (PAL)	Secondary metabolism	0.027

Table S5B NE genotypes

Accession	VIP score	SE	Log2 O_{NE}/C_{NE}	Annotation	MapMan BIN category	*P*-value (*t*-test)
POPTR_0004s01030	1.730	0.600	1.8	Glycine cleavage T-protein family	Amino acid metabolism/degradation	0.009
POPTR_0004s01320*	1.490	0.782	0.9	Glyoxalase I homolog	Amino acid metabolism/degradation	0.015
POPTR_0010s16330*	1.380	0.836	1.4	S-adenosylmethionine synthetase 1 (SAM1)	Amino acid metabolism/synthesis	0.001
POPTR_0004s20220	1.633	0.624	0.7	Methionine synthase, vitamin-B12 independent	Amino acid metabolism/synthesis	0.011
POPTR_0017s12240	1.841	1.672	1.0	Pyridoxal phosphate-dependent transferases superfamily protein	Amino acid metabolism/synthesis	0.069

POPTR_0008s00350	< 1	-	0.9	Serine transhydroxymethyltransferase 1	C1-metabolism	0.020
POPTR_0016s02620*	1.359	1.067	0.9	Alpha-N-arabinofuranosidase 1	Cell wall	0.011
POPTR_0001s37650*	1.615	0.578	0.6	Fasciclin-like arabinogalactan 1	Cell wall	0.033
POPTR_0006s12740*	1.447	1.084	2.7	Cell division protein 48 (CDC48)	Cell division	0.028
POPTR_0001s25630*	1.917	0.736	2.1	Thiamine biosynthesis protein (ThiC)	Co-factor and vitamine metabolism	0.003
POPTR_0015s08540*	2.083	0.659	2.6	Aldehyde dehydrogenase 2B4 (ALDH2)	Fermentation	0.002
POPTR_0008s05640	1.605	0.456	1.3	Triosephosphate isomerase	Glycolysis	0.002
POPTR_0008s08400*	< 1	-	1.1	Phosphoglycerate kinase	Glycolysis	0.024
POPTR_0017s01390*	< 1	-	0.4	UDP-glucose pyrophosphorylase 2	Glycolysis	0.050
POPTR_0012s10830	2.090	1.057	0.9	Alpha-mannosidase	Misc.gluco-, galacto- and mannosidases	0.019
POPTR_0016s14310	1.537	0.739	0.6	NADPH dependent ketone reductase (AOR)	Misc.oxidases - copper, flavone etc.	0.011
POPTR_0015s06950*	1.180	1.042	1.1	Protein of unknown function (DUF1118)	Not assigned	0.008
POPTR_0007s07780*	< 1	-	1.0	Photosystem II stability/assembly factor	Protein assembly and cofactor ligation	0.024
POPTR_0004s14960	< 1	-	0.5	Presequence protease 1	Protein degradation	0.040
POPTR_0001s08770	< 1	-	0.8	RAB GTPase homolog E1B	Protein synthesis	0.013
POPTR_0004s23490*	< 1	-	1.5	Elongation factor 1-gamma 1, putative	Protein synthesis	0.026
POPTR_0001s26970*	< 1	-	1.2	Ribosomal protein	Protein synthesis	0.034
POPTR_0006s19810*	1.482	0.826	0.9	Leucyl aminopeptidase (LAP2)	Protein degradation	0.002
POPTR_0008s05470*	< 1	-	0.9	Heat shock protein 70	Protein folding	0.001
POPTR_0010s14660	1.167	1.158	1.6	Chaperone protein htpG family protein	Protein folding	0.004
POPTR_0001s35230*	1.727	0.829	2.5	Ribosomal protein L12-A	Protein synthesis	0.002
POPTR_0006s21210*	1.029	0.607	2.9	Ribosomal protein 5A	Protein synthesis	0.040
POPTR_0010s20060	2.280	0.285	1.7	Sedoheptulose-1,7-bisphosphatase	PS/calvin cyle	0.000
POPTR_0008s05870	1.295	1.117	1.0	RuBisCO activase	PS/calvin cyle	0.004
POPTR_0002s00840	2.390	1.062	3.1	Glyceraldehyde-3-phosphate dehydrogenase, subunit B	PS/calvin cyle	0.014
POPTR_0003s09830	1.630	0.839	0.4	Phosphoribulokinase	PS/calvin cyle	0.015
POPTR_0013s03700	1.787	0.588	0.6	Ribose 5-phosphate isomerase, type A protein	PS/calvin cyle	0.030
POPTR_0010s20810	2.152	0.906	0.8	RuBisCO activase	PS/calvin cyle	0.059
POPTR_0001s08420*	1.552	0.940	0.9	Ferredoxin-plastoquinone reductase (PGR5-like A)	PS/lightreaction	0.001
POPTR_0005s11500	1.407	0.672	0.9	Ferredoxin-NADP(+)-oxidoreductase 1	PS/lightreaction	0.001
POPTR_0004s01470	1.901	0.535	0.8	ATPase, F1 complex, gamma subunit protein	PS/lightreaction	0.004
POPTR_0008s15100*	1.144	0.477	3.0	Photosystem I subunit D-2	PS/lightreaction	0.151
POPTR_0001s11600*	< 1	-	0.6	Photosystem I reaction center, subunit III	PS/lightreaction	0.036

POPTR_0019s14050	< 1	-	0.8	Photosystem II, assembly	PS/lightreaction	0.000
POPTR_0005s17350*	1.275	1.095	2.1	Ascorbate peroxidase	Redox	0.000
POPTR_0009s02070	< 1	-	0.5	Ascorbate peroxidase	Redox	0.008
POPTR_0002s01080	1.549	0.800	1.0	Catalase 2 (CAT2)	Redox	0.025
POPTR_0002s08260	< 1	-	0.5	Protein disulphide isomerase	Redox	0.038
POPTR_0005s01370*	< 1	-	0.5	RNA binding, chloroplast	RNA/regulation of transcription	0.008
POPTR_0013s00760	< 1	-	-0.7	RNA binding, chloroplast	RNA/regulation of transcription	0.027
POPTR_0005s23110	1.501	0.499	0.7	Chloroplast stem-loop binding protein of 41 kDa	RNA/regulation of transcription	0.004
POPTR_0009s07040*	2.333	0.827	1.7	NIFS-like cysteine desulfurase, chloroplastidic	S-assimilation	0.004
POPTR_0002s01990*	1.822	0.532	1.5	Cinnamyl alcohol dehydrogenase-like protein	Secondary metabolism	0.005
POPTR_0015s06230*	< 1	-	0.4	Calcium sensing receptor, extracellular	Signaling	0.048
POPTR_0007s04700*	1.888	1.176	4.3	UVB-resistance protein (UVR8)	Stress/abiotic	0.011
POPTR_0001s34950	1.505	0.658	0.6	Carbonic anhydrase 1	TCA / org.transformation	0.000
POPTR_0005s10990	2.033	1.239	1.2	Aconitase 1 (ACO1)	TCA / org.transformation	0.004
POPTR_0007s07680*	2.048	0.520	1.2	Hydroxymethylbilane synthase	Tetrapyrrole synthesis	0.006
POPTR_0015s11320	< 1	-	0.6	Glutamate-1-semialdehyde-2,1-aminomutase 2	Tetrapyrrole synthesis	0.046